# Molecular characterization of a chromosome 1;22 translocation in a patient with a phenotype resembling Costello syndrome

A Dissertation in the Partial Fulfillment of the Requirements
for the Degree of Doctor of Natural Science
at University of Hamburg

by

**Markéta Šutajová**

Hamburg, 2004

# Table of Contents

# List of Figures

# List of Tables

# Abbreviations

| | |
|---|---|
| $A_{260}$ | absorbance at 260 nm |
| *ABCC6* | gene encoding ATP-binding cassette transporter, subfamily C, member 6 |
| Amp | ampicillin |
| AN | acanthosis nigricans |
| *ANGPTL1* | gene encoding angiopoietin-like 1 precursor |
| APS | ammonium persulfate |
| *ARHGEF6* | gene encoding Rac/Cdc42 guanine nucleotide exchange factor 6 |
| BDT | Big Dye Terminator |
| bp | base pairs |
| BSA | bovine serum albumin |
| CCFDN | congenital cataracts, facial dysmorphism neuropathy |
| cDNA | complementary deoxyribonucleic acid |
| CFC | cardiofaciocutaneous |
| CHO | chinese hamster ovary |
| Cm | chloramphenicol |
| *COL7A1* | gene encoding collagen type VII alpha 1 |
| CS | Costello syndrome |
| *CTDP1* | gene encoding CTD (carboxy-terminal domain, RNA polymerase II, polypeptide A) phosphatase, subunit 1 |
| C-terminus | carboxy-terminus |
| DAPI | 4',6-diamidino-2-phenylindole |
| dbSNP | Database of Single Nucleotide Polymorphisms |
| $ddH_2O$ | double distilled water |
| DEB | dystrophic epidermolysis bullosa |
| der | derivative |
| DFN3 | deafness type 3 |
| D-MEM | Dulbecco's Modified Eagle Medium |
| DMSO | dimethyl sulfoxide |
| DNA | deoxyribonucleic acid |
| dNTP | 2'-desoxyribonucleotide-5'-triphosphate |
| EBP | elastin-binding protein |
| ECL | enhanced chemiluminescence |
| ECM | extracellular matrix |
| *E.coli* | *Escherichia coli* |
| EDTA | ethylendiamintetraacetic acid |
| EGFP | enhanced green fluorescent protein |
| *EGFR* | gene encoding epidermal growth factor receptor |
| *ELN* | gene encoding elastin |
| EST | expressed sequence tag |
| FCS | fetal calf serum |
| *FGFR2* | gene encoding fibroblast growth factor receptor 2 |
| *FGFR3* | gene encoding fibroblast growth factor receptor 3 |
| Fig. | figure |
| FISH | fluorescence *in situ* hybridization |
| FITC | fluorescein isothiocyanate |

| | |
|---|---|
| *FLJ10244* | gene encoding Ral-A exchange factor RalGPS2 |
| *FOXO1A* | gene encoding forkhead box O1A |
| GAG | glycosaminoglycan |
| GFP | green fluorescent protein |
| *GLI3* | gene encoding GLI-Kruppel family member GLI3 |
| h | hour |
| Ham | F-12 Nutrient Mixture |
| HGPS | Hutchinson-Gilford progeria syndrome |
| HPLC | high pressure liquid chromatography |
| IGF1R | insulin-like growth factor 1 receptor |
| IF | immunofluorescence |
| JEB | junctional epidermolysis bullosa |
| kb | kilobase pairs |
| kDa | kilodalton |
| Km | kanamycin sulfate |
| *lacZα* | gene encoding N-terminal part of β-galactosidase |
| *LAMB3* | gene encoding β3 subunit of laminin 5 |
| LB | Luria Broth |
| *LMNA* | gene encoding lamin A/C |
| m | milli |
| µ | micro |
| M | molar (mol/l) |
| MAPK | mitogen-activated protein kinase |
| MCA | multiple congenital anomalies |
| min | minute |
| MOPS | 3-(N-morpholino) propanesulfonic acid |
| mRNA | messenger ribonucleic acid |
| n | nano |
| NCBI | National Center for Biotechnology Information |
| Neo | neomycin |
| NF2 | neurofibromatosis type 2 |
| NS | Noonan syndrome |
| N-terminus | amino-terminus |
| $OD_{550}$ | optical density at 550 nm |
| OMIM | Online Mendelian Inheritance in Man |
| ON | over night |
| p | pico |
| PAA | polyacrylamide |
| PAC | phague artificial chromosome |
| PAGE | polyacrylamide gel electrophoresis |
| *PAX3* | paired box gene 3 |
| *PAX6* | paired box gene 6 |
| *PAX7* | paired box gene 7 |
| PBS | phosphate buffered saline |
| PCR | polymerase chain reaction |
| *PDGFA* | gene encoding platelet-derived growth factor alpha |
| PDGF-$A_L$ | platelet-derived growth factor A; long isoform |

| | |
|---|---|
| PDGF-$A_S$ | platelet-derived growth factor A; short isoform |
| *PDGFB* | gene encoding platelet-derived growth factor beta |
| *PDGFC* | gene encoding platelet-derived growth factor C |
| *PDGFD* | gene encoding platelet-derived growth factor D |
| *PDGFRA* | gene encoding platelet-derived growth factor receptor alpha |
| *PDGFRB* | gene encoding platelet-derived growth factor receptor beta |
| *PITX2* | gene encoding paired-like homeodomain transcription factor 2 |
| PlGF | placental growth factor |
| PMSF | phenylmethyl sulphonyl fluoride (protease inhibitor) |
| *POU3F4* | gene encoding POU domain, class 3, transcription factor 4 |
| P/S | penicillin-streptomycin |
| *PTPN11* | gene encoding protein tyrosine phosphatase, non-receptor type 11 |
| PVDF | polyvinylendifluoride |
| PXE | pseudoxanthoma elasticum |
| RACE- | rapid amplification of cDNA ends- |
| RMS | rhabdomyosarcoma |
| RNA | ribonucleic acid |
| RNase | ribonuclease |
| rpm | rounds per minute |
| RT | room temperature |
| RT-PCR | reverse transcriptase polymerase chain reaction |
| s | second |
| SDS | sodium dodecyl sulfate |
| SHP2 | protein tyrosine phosphatase, non-receptor type 11 |
| *SLC22A1L* | gene encoding solute carrier family 22 (organic cation transporter) member 1-like |
| SPARC | secreted protein, rich in cysteine (also named osteonectin) |
| SSC | standard saline citrate buffer |
| SSCP | single strand conformation polymorphism |
| *STIM1* | gene encoding stromal interaction molecule 1 precursor |
| t | translocation |
| Tab. | table |
| TBE | Tris-borate-EDTA buffer |
| TBST | Tris-buffered saline + Tween 20 |
| Tc | tetracycline |
| TE | Tris-EDTA |
| TEMED | N,N,N',N'-tetramethylethylenediamine |
| *TGFB1* | gene encoding transforming growth factor beta 1 |
| *TWIST1* | gene encoding basic helix-loop-helix (bHLH) transcription factor |
| U | unit (enzymatic) |
| UTR | untranslated region |
| UV | ultraviolet |
| V | volt |
| VEGF | vascular endothelial growth factor |
| v/v | volume percent (volume per volume) |
| W | watt |
| WB | western blotting |
| w/v | weight percent (weight per volume) |

| | |
|---|---|
| X-gal | 5-bromo-4-chloro-3-indolyl-beta-D-galactopyranoside |
| YAC | yeast artificial chromosome |

Single- and three- letter amino acid code

| | | | | | |
|---|---|---|---|---|---|
| A | Ala | alanine | M | Met | methionine |
| C | Cys | cysteine | N | Asn | asparagine |
| D | Asp | aspartic acid | P | Pro | proline |
| E | Glu | glutamic acid | Q | Gln | glutamine |
| F | Phe | phenylalanine | R | Arg | arginine |
| G | Gly | glycine | S | Ser | serine |
| H | His | histidine | T | Thr | threonine |
| I | Ile | isoleucine | V | Val | valine |
| K | Lys | lysine | W | Trp | tryptophan |
| L | Leu | leucine | Y | Tyr | tyrosine |

# I. Introduction

## 1. Costello syndrome

Costello syndrome [Faciocutaneoskeletal syndrome (OMIM 218040)] was initially reported in 1971 and 1977 (Costello, 1971 and 1977; for a recent review see Hennekam, 2003). It is a distinct syndrome with multiple congenital anomalies (MCA) characterized by increased prenatal growth, followed by postnatal growth deficiency, coarse face, loose skin, mental retardation, and cardiac abnormalities. Costello syndrome (CS) is likely to be very rare, Hennekam refers to 115 cases described to date. Nonetheless, it has been suggested that the syndrome is underdiagnosed (Say et al., 1993). The genetic cause of the syndrome has not yet been defined and the diagnosis is made based on the clinical phenotype.

### 1.1 Clinical features

In about 60% of the patients, pregnancy was complicated by polyhydramnios (Hennekam, 2003). At birth, patients with Costello syndrome have normal or relatively high weight and normal length followed by a severe early postnatal growth retardation. All children have severe feeding problems and occasionally swallowing difficulties were reported (reviewed in van Eeghen et al., 1999). The major facial signs are absolute or relative macrocephaly, curly and sparse hair, thick eyebrows, epicanthal folds, strabismus, low set ears, depressed nasal bridge and bulbous nose, full cheeks, and thick lips. In total, the face gives a coarse impression (Fig. 1A). Patients with Costello syndrome have short neck and loose skin of hands and feet with deep creases (Fig. 1B). The skin is thickened, soft and velvety in feel, and has a darker (olive) color.

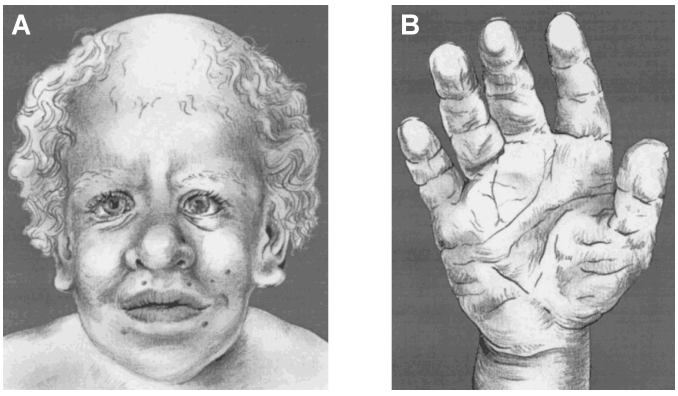


**Fig. 1: Drawing of face and palm of a patient with Costello syndrome**

**(A)** Coarse face. **(B)** Palm of hand with redundant, thickened skin with deep creases and persistent fetal pads. Figures were taken from Hennekam (2003).

The IQ of patients with CS is ranging from less than 25 to 85, usually it is between 25 and 50 (Hennekam, 2003). Most of the patients have a warm social personality. Ventricular dilatation is observed in more than 40% of cases. Other reported CNS anomalies are brain atrophy, Chiary malformation, and syringomyelia (Delrue et al., 2003). Lin and colleagues (2002) reviewed the cardiovascular abnormalities present in 63% of patients with Costello syndrome including cardiac malformation (typically pulmonary stenosis), hypertrophic cardiomyopathy, and rhythm disturbances (usually atrial tachycardia). The cardiomyopathy may already be present at birth or develop at later age (Hennekam, 2003). Children with CS tend to develop benign tumors of ectodermal origin such as papillomata that may occur at various ages in nasal, perioral, and anal areas (Kerr et al., 1998). Recently, malignant tumors have also been described in a significant number of patients with CS: seventeen cases with solid tumors [10 rhabdomyosarcomas (RMSs), 3 neuroblastomas, 2 bladder carcinomas, 1 vestibular schwanoma, and 1 epithelioma] were reported by surveying about 100 patients with Costello syndrome. Thus, the tumor frequency in Costello syndrome could be as high as 17% (Gripp et al., 2002). Recently, a patient with Costello syndrome, prolactinoma, and parathyroid adenoma was described (Cakir et al., 2004). A patient with CS and growth hormone deficiency was also reported. After supplementation with recombinant growth hormone he developed osteofibrous dysplasia of the tibia, a benign lesion consisting of fibrous tissue with woven bone formation (Kamoda et al., 2003). Because of the coarse facial appearance of the patients, it has been speculated that Costello syndrome is a metabolic disease, e.g. a lysosomal storage disorder. Di Rocco and colleagues (1993) reported two patients with CS and sialuria. In Salla disease and infantile sialic storage disease, sialic acid is increased in urine and in fibroblasts due to a defect in lysosomal transport (Gahl et al., 1989; Mancini, 1991). Several patients with Costello syndrome and hypoglycaemia have also been reported, but an enzyme defect has not been found. In 2002, Kaji and colleagues reported a case with CS and hypoglycaemia due to glycogen storage disease type III. Nevertheless, no other case of Costello syndrome and a storage disease-like disorder has been reported.

The typical clinical signs and symptoms seen in patients with Costello syndrome are listed in Table 1.

| Typical clinical findings in patients with Costello syndrome | %[a] |
|---|---|
| coarse face with full cheeks, depressed nasal bridge, and low set ears | ~97 |
| loose and wrinkled skin | 99 |
| skin is thickened, soft, and velvety in feel | ~99 |
| short neck | 88 |
| thick lips | 97 |
| sparse and curly hair | 82 |
| macrocephaly | 84 |
| high birth weight | 89 |
| failure to thrive | 96 |
| moderate to severe mental retardation | 100 |
| congenital heart defect | 63[b] |

**Tab. 1: Main characteristics of patients with Costello syndrome and their prevalence**

[a] Values were taken from Hennekam (2003).

[b] Taken from Lin et al. (2002).

## 1.2 Differential diagnosis

There is a phenotypic overlap between Costello syndrome, Noonan syndrome [NS (OMIM 163950)] and cardiofaciocutaneous (CFC) syndrome (OMIM 115150). However, in patients with CS typical phenotypic features exist that help to distinguish Costello syndrome from these two syndromes including papillomata, a history of poor feeding, redundant olive-colored skin that is thickened and soft, and full lips. Although myocardial diseases are seen both in Noonan and CFC syndromes, tachyarrhythmias are not that may help to consider Costello syndrome (Siwik et al., 1998). Some of the clinical symptoms of Costello syndrome are similar to those of cutis laxa (e.g. OMIM 219200), such as loose skin, dysmorphic face, herniae, growth retardation, and psychomotor delay. However, different distribution of loose skin and the disease specific patterns of destruction of elastic fibers suggest that the two conditions represent distinct disorders (Mori et al., 1996). Numerous other diagnoses including Donohue and Leprechaun syndromes, Berardinelli-type lipodystrophy (Zampino et al., 1993), and ectodermal dysplasias (van Eeghen et al., 1999) have been initially considered for patients showing the clinical features of Costello syndrome.

## 1.3 Mode of inheritance

The genetic cause of Costello syndrome has not yet been identified. Most of the patients with CS are sporadic providing no indication of the pattern of inheritance. Nevertheless, Ioan and Fryns (2002) described two siblings both presenting numerous main clinical signs and symptoms of Costello syndrome. The mother of the patients, too, showed mild to moderate mental retardation, short stature, full cheeks, macrostomia, thick lips, and a hyperlaxed and dark colored skin. It has been suggested that the observation of three affected members in a family provides evidence for an autosomal dominant inheritance with variable expression of the disease. In line with this assumption, Bodkin and colleagues (1999) described a father of a Costello patient who presented with many features of the disorder in an asymmetric pattern suggesting that he was a mosaic for Costello syndrome, probably as the result of a post-zygotic mutation. Similarly, Lurie (1994) concluded that affected sib pairs might result from germline mosaicism in one of the parents. A significantly higher mean paternal age (38 years) and paternal-maternal age difference (7.36 years) also suggest that autosomal dominant *de novo* mutations may be the likely cause for Costello syndrome. Yet, genetic heterogenity with a small proportion of recessively inherited cases can not be excluded either.

## 1.4 Pathogenesis and candidate genes

To date, the causative gene for Costello syndrome has not been yet identified although numerous candidate genes were analysed for mutations in patients with CS. To gain insights into the pathogenesis of Costello syndrome, autopsy tissues of two patients were examined. The major pathological findings were thin, disrupted, and loosely constructed elastic fibers indicating that pathology of elastic fibers might be involved in the pathogenesis of CS (Mori et al., 1996). Destruction of elastic fibers has also been reported in cutis laxa where it is widely distributed, while affected elastic fibers in Costello syndrome were found in the skin, tongue, pharynx, and larynx (Mori et al., 1996). While Mori and colleagues (1996) found no difference in elastin mRNA levels in Costello patients, elastin expression was decreased in fibroblasts of patients with cutis laxa (Olsen et al., 1988; Sephel et al., 1989; Hatamochi et al., 1991). In 2000, Hatamochi and colleagues also found a reduced amount of elastin fibers in a Costello patient, though the level of elastin mRNA also reduced to 1/5. These contradictory findings can be due to different severity of the skin lesion where biopsies were taken from. Considering the involvement of elastin in the cutis laxa pathogenesis, the elastin (*ELN*) gene

was good candidate for Costello syndrome. By mutation analysis of *ELN* in four patients with CS, no causative mutation was identified (Tandoi et al., 2001). These data implied that a later step of elastogenesis might be altered. In a more comprehensive study, Hinek and colleagues (2000) showed that cultured skin fibroblasts of patients with Costello syndrome did not assemble elastic fibers although they produce normal levels of tropoelastin and deposit properly the microfibrillar scaffold. They also found that impaired production of elastic fibers by these fibroblasts is associated with a functional deficiency of the 67-kDa elastin-binding protein (EBP) that may be due to an abnormal accumulation of chondroitin sulfate-bearing proteoglycans. It has been speculated that cell-surface chondroitin sulfate moieties may be responsible for shedding EBP from fibroblasts of patients with CS (Hinek et al., 2000). Remarkably, Costello syndrome, Hurler disease, Morquio B disease, and GM1-gangliosidosis, all show deficiencies in EBP-mediated transport of tropoelastin that might impair elastogenesis. These disorders belong to a growing list of human elastic-fiber diseases in which the pathomechanism lies probably in the transport mechanisms secondary to fiber assembly (Urbán and Boyd, 2000).

Four other candidate genes have been analysed for mutations in patients with CS. In five selected exons of the fibroblast growth factor receptor 3 (*FGFR3*) gene, no mutation was found in four patients with CS (Mancini et al., 2003). Somatic mutations in *FGFR3* were frequently found in bladder carcinoma (Cappellen et al., 1999; Billerey et al., 2001; Kimura et al., 2001) that was present in two patients with Costello syndrome. Moreover, a recent study excluded the protein tyrosine phosphatase, non-receptor type 11 (*PTPN11*) gene, mutated in about 50% of patients with Noonan syndrome, as the major causative gene for Costello syndrome (Tartaglia et al., 2003; Tröger et al., 2003). In addition, no mutation was found in the *PTPN11* gene in patients with CFC syndrome indicating that these three syndromes are distinct entities (Ion et al., 2002).

Kerr and colleagues (2003) proposed that the increasing number of reports of childhood malignancies in patients with CS suggest an involvement of a tumor suppressor gene in the molecular etiology of this syndrome. Loss of heterozygozity at 11p15.5 was shown to be present in embryonal rhabdomyosarcoma tumor samples of five patients with Costello syndrome. A constitutional deletion or uniparental disomy at 11p15.5 was excluded by analysis of this region in a cohort of Costello patients. Subsequently, the solute carrier family 22 (organic cation transporter) member 1-like (*SLC22A1L*) gene and the stromal interaction molecule 1 (*STIM1*) gene located at 11p15.5 were screened for mutations in three patients with CS and no mutation was identified. So far, the hypothesis that a germline

mutation in a tumor suppressor gene (first hit) leading to Costello syndrome and an alteration of the second copy of the tumor suppressor gene in somatic tissue (second hit) leading to malignant tumors in patient with Costello syndrome has not been proven (Kerr et al., 2003).

In 1995, a girl with presumed Costello syndrome and an apparently balanced *de novo* translocation, t(1;22)(q25;q11), was described providing a first possible hint for the chromosomal location of the gene (Czeizel and Tímár, 1995) (Fig. 2). Moreover, the presence of a translocation in a patient with CS is consistent with the proposed autosomal dominant inheritance.

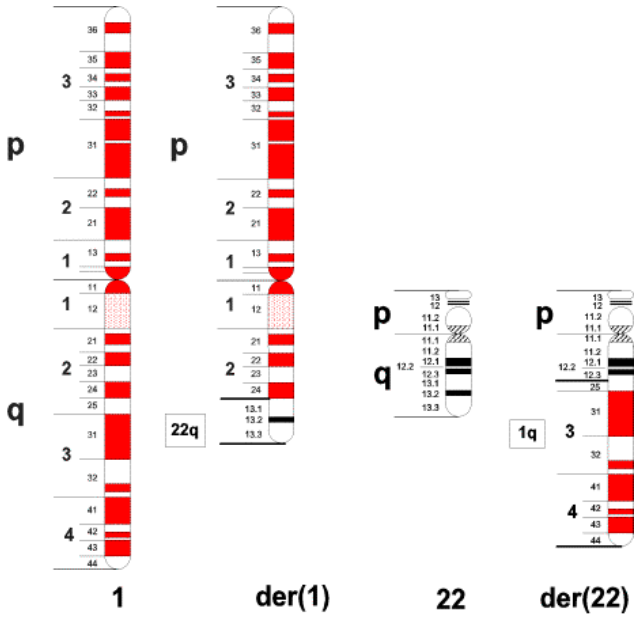


**Fig. 2: Ideogram of the chromosomes involved in the translocation t(1;22)(q25;q13.1) in a patient with presumed Costello syndrome**

From left to right are shown wild-type chromosome 1, derivative chromosome 1, wild-type chromosome 22 and derivative chromosome 22. Material from chromosome 1 is shown in red/white and material from chromosome 22 in black/white. The rearranged chromosomal segments 22q13.1-qter and 1q25-qter are indicated (22q and 1q) and highlighted by thick lines.

In an attempt to identify the gene for Costello syndrome, both breakpoint regions of the 1;22 translocation were delineated by fluorescence *in situ* hybridization and thereby, the breakpoint on chromosome 22 was refined to q13.1. A cosmid clone that overlaps the breakpoint on chromosome 22 was identified and analysis of the DNA sequence deposited at the NCBI database revealed that the gene encoding the platelet-derived growth factor beta *(PDGFB)* is located on the insert of the cosmid (Maróti et al., 2002). Support for the assumption that the gene for Costello syndrome is located on the long arm of chromosome 22 was provided by a report of Suri and Garrett (1998) describing a patient with Costello syndrome, vestibular schwannoma, and cataract. These latter are features of neurofibromatosis type 2 [NF2 (OMIM 101000)] mapped to 22q12.2 opening the possibility that a single chromosomal rearrangement in the patient is responsible for both traits.

In summary, the identification of *PDGFB* in one breakpoint region of the 1;22 translocation in a patient with presumed Costello syndrome suggested that *PDGFB* could be considered a good candidate gene for Costello syndrome.

# 2. Platelet-derived growth factor

## 2.1 Platelet-derived growth factor isoforms and receptors

Platelet-derived growth factor (PDGF) is a major mitogen for fibroblasts, smooth muscle cells, and other cells of mesenchymal origin that was originally purified from human platelets (Heldin and Westermark, 1999). PDGF is a dimeric molecule consisting of disulfide-bonded, structurally similar A- and B-polypeptide chains (PDGFA and PDGFB), which combine to homo- and heterodimers. Recently, two novel members of the PDGF family, PDGFC and -D, have been identified (Li et al., 2000; Bergsten et al., 2001; LaRochelle et al., 2001). The biological effects of PDGFs are initiated via two related receptor tyrosine kinases, the α- and β-PDGF receptors (Fig. 3).

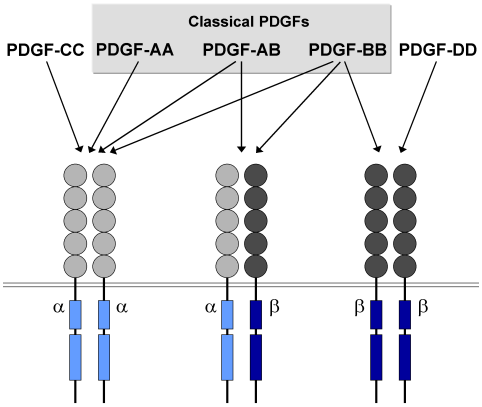


**Fig. 3: Specificities of the PDGF ligand-receptors**

Different PDGF isoforms (PDGF-AA, BB, AB, CC, and DD) bind to α- and β-PDGF receptors with different specificities that are indicated by arrows. Receptors are drawn schematically to illustrate that their extracellular part consists of five Ig-like domains whereas the intracellular part contains the tyrosine kinase domains. The figure was modified after that of Betsholtz et al. (2001).

The human *PDGFA*, *PDGFB*, *PDGFC*, and *PDGFD* genes are located on chromosome 7p22, 22q13.1, 4q32, and 11q22.3, respectively. *PDGFRA* and *PDGFRB* are located on chromosome 4q12 and 5q33.1, respectively. Two PDGFB isoforms (241 aa and 227 aa) are generated by alternative splicing of exon 1. Similarly, there are two biologically active forms of the A-chain, the long (PDGF-$A_L$; 211 aa) and the short isoforms (PDGF-$A_S$; 196 aa), that are produced by alternative splicing of exon 6 (Raines and Ross, 1992). Proteins of the PDGF family are synthesized as precursor molecules that undergo proteolytic processing before they can act on their target cells. Thus the A- and B-chain precursors are cleaved at their N-terminus whereas the B-chain is cleaved at its C-terminus as well (Östman and Heldin, 2001).

## 2.2 *In vivo* function of platelet-derived growth factor

Genetic analyses in mice revealed that PDGFs and PDGFRs have important roles during embryonic and postnatal development. *PDGFB*- or *PDGFRB*-deficient mice die during late gestation due to cardiovascular complications. Histological findings include abnormal kidney glomeruli, capillary microaneurysms, cardiac muscle hypotrophy, and placenta defects (Levéen et al., 1994; Soriano, 1994; Lindahl et al., 1997 and 1998; Hellström et al., 1999; Ohlsson et al., 1999). Similarly, both *PDGFA* and *PDGFRA* knock-out animals are embryonic or early after birth lethal (Boström et al., 1996; Soriano, 1997). It is of interest to note that while homozygous deletions of either *PDGFRB* or *PDGFB* in mice result in similar phenotypes, the phenotypes of mice lacking *PDGFA* or *PDGFRA* are different. This can be explained by the fact that PDGF receptors α and β bind the PDGFA and -B ligands with different affinities (Fig. 3). Thus, whereas PDGFR signaling is completely interrupted in the receptor knock-out mice, PDGFB ligand can still activate the α-receptor in *PDGFA* null mice and may therefore partially compensate for the lack of the A chain. In contrast, deletion of the *PDGFB* gene can not be compensated by PDGFA since the A chain is unable to bind to the β receptor (reviewed in Rosenkranz and Kazlauskas, 1999). PDGF has an important function during embryogenesis, in particular for the development of kidneys, blood vessels, lungs, and the CNS. The role of PDGF in the formation of connective tissue is also important during wound healing in adults (Heldin and Westermark, 1999).

## 2.3 Platelet-derived growth factor in disease

Overactivity of PDGF has been implicated in the pathogenesis of a number of diseases including cancer as well as disorders characterized by excessive cell growth such as atherosclerosis and various fibrotic conditions (Östman and Heldin, 2001). In human tumorigenesis, PDGF autocrine loops have been implicated in the development of mesenchymal tumors such as sarcomas and gliomas. In addition, PDGF is also involved in paracrine stimulation of stroma cells in solid tumors, e.g. mammary carcinoma, colorectal cancer, and small cell lung carcinoma (Heldin and Westermark, 1999; Östman and Heldin, 2001). Analysis of *PDGFB* expression in human soft tissue tumors showed that 60 and 82% of the tumors had demonstrable amounts of *PDGFB* mRNA and protein, respectively. Additionally, strong correlation was found between *PDGFB* expression and increasing malignant tumor grade (Wang et al., 1994).

## 2.4 Attachment of platelet-derived growth factor to the extracellular matrix

The extracellular matrix (ECM) is a network of proteins surrounding the cells and providing mechanical support for them. It also influences embryonic development, cellular migration, and sequesters important growth factors. Three major classes of molecules are located in the ECM: structural proteins (e.g. collagen, elastin), adhesive glycoproteins (e.g. fibrillin, fibronectin, and laminin), and proteoglycans. Proteoglycans contain a protein core to which a long chain of repeating disaccharide units (glycosaminoglycans) is attached. Various glycosaminoglycans are known such as hyaluronan, chondroitin, dermatan, and keratan sulfate, as well as heparin and heparan sulfate that vary in their disaccharide content (Pollard and Earnshaw, 2002).

The majority of the PDGFB and PDGF-$A_L$ molecules is associated with the cell (Östman et al., 1988; Östman et al., 1992). The domain responsible for this association was located to the carboxyl terminus of both PDGF proteins. Retention of the growth factor is necessary for its action on the same or adjacent cells or it may possibly function as migratory anchor for cells expressing the appropriate receptors (LaRochelle et al., 1991; Östman et al., 1991; Pollock and Richardson, 1992; Raines and Ross, 1992; Kelly et al., 1993). In both the PDGFA and PDGFB proteins, there is a stretch of basic amino acid residues, encoded by exon 6, that mediates the interaction with components of the extracellular matrix, mainly with negatively charged groups in the heparan sulfate proteoglycan (Raines and Ross, 1992) (Fig. 4).

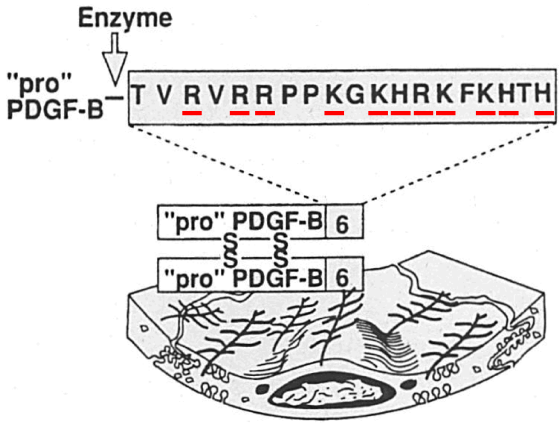


**Fig. 4: Proposed model of compartmentalization of PDGFB**

Exon 6 of *PDGFB* encodes a stretch of amino acids known as retention domain (upper box). Basic amino acids, arginine (R), lysine (K), and histidine (H), are underlined in red. A potential proteolytic cleavage site is shown by the arrow. Attachment of PDGFB to heparan sulfate proteoglycans of the extracellular matrix mediated by the retention motif is shown schematically. The figure was modified after Raines and Ross (1992).

Three research teams mapped the retention motif of PDGFB and ended up with minor differences in the region covering this domain. LaRochelle and colleagues (1991) localized the retention properties to residues 212-226, Östman and colleagues (1991) between amino acids 219-229, and Raines and Ross (1992) to 212-230 (Fig. 5A). A structural motif similar to the retention motif of PDGFA and -B was also identified in the longer splice variants of vascular endothelial growth factor (VEGF) and placental growth factor (PlGF) that are structurally related to PDGF and potent mitogens for endothelial cells (Fig. 5B; references in Andersson et al., 1994).

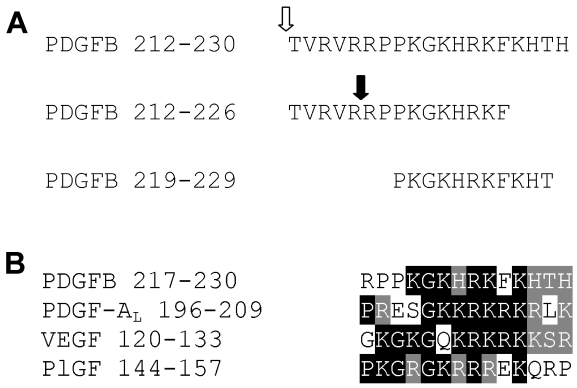


**Fig. 5: Presumed retention motifs of various growth factors**

**(A)** Alignment of the carboxyl-terminal sequences of PDGFB described by Raines and Ross (1992; first line), LaRochelle and colleagues (1991; second line) and Östman and colleagues (1991; third line). The arrows indicate potential proteolytic cleavage sites. **(B)** Alignment of the homologous sequences of the carboxyl terminus of PDGFB, the long variant of PDGF-$A_L$, VEGF, and PlGF. Identical amino acids are shaded in black whereas similar amino acids are shaded in grey. The alignment was made using programs ClustalW and BOXSHADE.

In summary, the precursor molecule of PDGFB may be retained at the surface of the cell. After maturation, when the retention motif has been cleaved off, the molecule becomes diffusible. Thus, proper matrix association of the platelet-derived growth factor beta is required for its regulated action on receptors (Raines and Ross, 1992; Kelly et al., 1993; Field et al., 1996).

## 3. Balanced chromosomal translocations as tools for disease gene identification

Balanced chromosomal rearrangements associated with a Mendelian disorder that truncate, delete, or otherwise inactivate genes are powerful tools for mapping novel disease genes (Bugge et al., 2000). Various chromosomal translocations segregating in a family with an autosomal dominantly inherited trait have been described. For example, mapping the gene for Rieger syndrome (*PITX2*), an autosomal dominant disorder characterized by malformation of the anterior eye chamber and teeth, or aniridia (*PAX6*), the bilateral complete or partial absence of the iris, was significantly facilitated by molecular characterization of translocation breakpoints (Gessler et al., 1989; Datson et al., 1996). Similarly, in the case of Greig syndrome, an autosomal dominant disorder affecting limb and craniofacial development, analysis of two balanced translocations in different families showed disruption of the *GLI3* gene (Vortkamp et al., 1991). In all cases, a single gene is expected to be disrupted in its integrity or expression and therefore leading to a disease phenotype.

An autosomal dominant disorder can be caused either by a gain-of-function mutation on one of the alleles or by loss-of-function on one homologue (haploinsufficiency). Chromosomal rearrangements associated with an autosomal dominant disorder are usually expected to cause haploinsufficiency since disruption of the coding region of a gene may lead to a functional null-allele (Vortkamp et al., 1991; Fahsold et al., 1995).

In the majority of cases, chromosomal aberrations occur sporadically and do not segregate within a family. As described above, one can assume that the phenotype of a patient with a *de novo* chromosomal rearrangement is due to the chromosome aberration. If a gene is located in the breakpoint region that is disrupted, it can be considered a candidate gene for the disease observed in the patient. Mutation screening of this candidate gene can be performed in patients presenting with the same disorder and having a normal karyotype. The identification of mutations in the gene will prove that mutations in this gene are causative for this particular disease. For example, Kutsche and colleagues (2000) characterized an X;21 translocation in a patient with severe mental retardation. The *ARHGEF6* gene in Xq26 was found to be directly disrupted by the rearrangement. Mutation analysis of 119 patients with nonspecific mental retardation revealed a second mutation in the *ARHGEF6* gene in all affected members of a large family (Kutsche et al., 2000).

# 4. Aim of the study

Chromosomal rearrangements associated with a Mendelian disorder provide a powerful tool for identification of novel disease genes. Molecular analyses of the breakpoint regions may help to identify the gene(s) that is/are interrupted and find a possible correlation between genotype and phenotype of the patient. Moreover, DNA sequence analysis of the breakpoints may shed light on the putative molecular mechanism by which various rearrangements occurred.

As a primary aim, an apparently balanced *de novo* chromosome 1;22 translocation, detected in a patient with a phenotype resembling Costello syndrome, should be analysed to identify the gene(s) affected by the rearrangement. By fluorescence *in situ* hybridization (FISH), both breakpoint regions should be delineated. Subsequent database searches using the DNA sequence of clones containing the breakpoints may reveal known or putative gene(s) located in or near the critical regions. Mutation screening of such candidate gene(s) in patients with Costello syndrome and normal karyotype will show whether mutations of any of the genes are causative for the syndrome.

In order to define the translocation breakpoints at the nucleotide level, various PCR techniques, like RACE-, RT-, and genomic PCR, should be applied. It is possible that two genes originally located on different chromosomes are now fused by the 1;22 translocation. If this is indeed the case, overexpression of the corresponding fusion protein in eukaryotic cells may allow investigating the potential functional consequences/effects of this novel protein on subcellular localization, cell proliferation, migration etc.

In an alternative approach, functional candidate genes for Costello syndrome should be investigated for the presence of pathogenic mutations in patients with no chromosomal aberrations to identify the genetic cause of this malformation syndrome.

# II. Material and Methods

## 1. Subjects

The karyotype and early phenotype of the patient with the translocation were described previously (Selypes et al., 1992; Czeizel and Tímár, 1995). She was born at 38 weeks of gestation with a birth weight of 3100 g. Head circumference was 32 cm at birth (3rd percentile) and 47 cm (-3 SD) at the age of 6 years. At age 12, she showed normal body height (-1 SD), while weight was >97th percentile.
We collected DNA or blood samples from 18 patients clinically diagnosed as Costello syndrome. Clinical data of these patients were described previously (Tröger et al., 2003).

## 2. DNA isolation

### 2.1 Isolation of genomic DNA from blood

Genomic DNA was isolated from 200 µl or 2 ml of whole blood by QIAamp DNA Blood Mini or Midi Kit (Qiagen, Hilden) according to the manufacturer's protocol. In case of Midi Kit, 2 ml of blood was mixed with 200 µl Proteinase K (20 mg/ml), then 2.4 ml Buffer AL (lysis buffer) was added and the sample was mixed thoroughly by vortexing. Blood cells were lysed for 10 min at 70°C. After addition of 2 ml 100% (v/v) ethanol, the sample was vortexed and half of the sample was transferred onto QIAamp Midi column and centrifuged at 3.000 rpm for 3 min. This step was repeated with the other half of the sample. After addition of 2 ml Buffer AW1 to the QIAamp Midi column, DNA was washed through centrifugation [4.000 rpm, 5 min (when not stated differently, all centrifugation steps were performed at room temperature)]. In the next step, the column was washed with Buffer AW2 by centrifugation at 4.000 rpm for 25 min. After adding 300 µl Buffer AE to the column and incubation at room temperature (RT) for 5 min, DNA was eluted during centrifugation at 4.000 rpm for 8 min. For maximum DNA yield, fresh 300 µl Buffer AE was added to the column and the previous step was repeated. All solutions were reduced accordingly for isolation of genomic DNA from smaller amounts of blood. DNA concentration was determined by UV spectrophotometry (II.4.7) and quantitative analysis on agarose gel (II.4.2). Genomic DNA was stored at 4°C.

### 2.2 Isolation of plasmid and cosmid DNA in small scale

For isolation of plasmid and cosmid DNA, the mini-preparation method of Birnboim and Doly (1979) was used that is based on alkaline lysis. One single colony was inoculated in 2 ml LB-medium containing the appropriate selective antibiotic and incubated over night (ON) at 37°C with constant agitation (220 rpm). The culture was transferred into a 1.5 ml Eppendorf tube and the cells were

pelleted by centrifugation (8.000 rpm, 4 min). The pellet was resuspended in 100 µl Solution I by vortexing. Then, 200 µl Solution II was added and the sample was mixed by inverting and incubated for 3-5 min at RT to lyse the bacterial cells and denature genomic DNA. 300 µl Solution III was added to precipitate genomic DNA and most of the proteins. The suspension was mixed again by inverting and incubated for 5-10 min on ice. Afterwards the sample was centrifuged at 13.000 rpm for 5 min. The plasmid/cosmid DNA that is contained in the supernatant was precipitated by adding 350 µl isopropanol and subsequent centrifugation (13.000 rpm, 5 min). RNA was removed by digestion with 100 µl 1 × TE-buffer containing 100 µg/ml RNase for 20 min at 37°C. The plasmid/cosmid DNA was precipitated by adding 120 µl 88% (v/v) isopropanol / 0.2 M potassium acetate and incubation of the sample for 10 min at RT. After a final centrifugation step at 13.000 rpm for 5 min, the pellet was resuspended in 50 µl HPLC water and plasmid DNA was kept at -20°C.

### 2.3 Isolation of plasmid and cosmid DNA in large scale

Large and pure amounts of plasmid and cosmid DNA used for either transfection of eukaryotic cells or fluorescence *in situ* hybridization (FISH) were isolated by using the QIAGEN Plasmid Midi- or Maxi-Kit (Qiagen, Hilden) according to the manufacturer's instructions. The protocol is based on the modified alkaline lysis procedure, followed by binding of plasmid/cosmid DNA to a column under appropriate conditions. RNA, proteins etc. were removed by medium-salt wash. Plasmid DNA was eluted in high-salt buffer and then concentrated and desalted by isopropanol precipitation. The DNA pellet was redissolved in HPLC water and DNA was stored at -20°C. The concentration of DNA was determined by UV spectrophotometry (II.4.7).

## 3. RNA isolation from blood

Total RNA from peripheral blood cells was isolated by High Pure RNA Isolation Kit (Roche, Mannheim) according to the supplier's instructions. The quality of RNA was controlled on agarose gel (II. 4.2) and the concentration was determined by spectrophotometry (II.4.7). RNA was kept at -80°C.

## 4. DNA and RNA standard methods

### 4.1 Restriction of DNA by restriction endonucleases

Plasmid/cosmid DNA and PCR products were incubated with 0.5-1 U of restriction enzymes and in appropriate buffers (Promega, Mannheim) in the presence of 1 x BSA (bovine serum albumin) according to the manufacturer's protocol. When necessary, restriction was terminated by heat

inactivation at 65°C for 20 min or by freezing the sample at -20°C. The DNA restriction was examined by electrophoretic separation on agarose gel.

## 4.2 Agarose gel electrophoresis

The separation of DNA fragments was performed on non-denaturing agarose gels in a horizontal chamber (BioRad, München). Agarose gel was prepared by heating 0.8-2.5% (w/v) agarose (Invitrogen, Karlsruhe) in 1 x TBE buffer, depending on the size of DNA fragments to be separated. 5 µl DNA-loading buffer I was mixed with the probe and the gel was run at constant voltage between 100-120 Volts (V). Afterwards, the agarose gel was stained in an ethidium bromide solution (Merck, Darmstadt; 1 ml/2 l water) for 5 min and washed in water for 10 min. Finally, the gel was documented under UV-light using Herolab UVT-28M Videosystem (Wiesloch). For determination of the size of DNA fragments, 100 bp and 1 Kb DNA Ladder (Invitrogen, Karlsruhe) were used. Low and High DNA Mass Ladder (Invitrogen, Karlsruhe) were used to estimate the quantity of DNA samples. The separation of RNA molecules was also done by non-denaturing horizontal agarose gel electrophoresis in 0.8-1% (w/v) agarose gel. The equipment used for electrophoresis of RNA was treated with RNase ERASE (ICN Biomedicals, USA) to render it ribonuclease-free.

## 4.3 Polyacrylamide gel electrophoresis

Non-denaturing polyacrylamide gels (PAA-gel) were used for separation of DNA fragments during single strand conformation analysis (SSCP). PCR products (5-10 µl) were mixed with 5 µl SSCP-loading buffer, denatured at 95°C for 10 min, placed on ice, and loaded on PAA-gel. Two different types of PAA-gels were used (Tab. 2). Polyacrylamide gel electrophoresis (PAGE) was performed in 1 x TBE buffer ON at 5-8 Watts (W) for 8% PAA-gels, or at ~18 W for 8% PAA-gels with glycerol depending on the size of PCR amplicons. To visualise the bands, silver-staining technique was used (II.9).

| | **PAA-gel (8%)** | **PAA-gel (8%) with glycerol** |
|---|---|---|
| $ddH_2O$ | 80.0 ml | 67.5 ml |
| Acrylamide/bisacrylamide (30%) | 33.0 ml | 33.0 ml |
| 10 × TBE | 12.5 ml | 12.5 ml |
| Glycerol (100%) | - | 12.5 ml |
| 10% APS | 1.0 ml | 1.0 ml |
| TEMED | 24.0 µl | 24.0 µl |

**Tab. 2: Composition of the PAA-gels used for SSCP technique**

Under denaturating conditions, proteins can be electrophoretically separated by SDS-PAGE due to their molecular weight (Laemmli, 1970). Sodium dodecyl sulfate (SDS) is an anionic detergent that binds quantitatively to proteins and gives them linearity and negative charge, so that they can be separated solely on the basis of their size. Gel electrophoresis was performed in a mini-gel apparatus (BioRad, München) in 1 x SDS-running buffer. For the separation of proteins in the size of 50-55 kDa, a 12.5% PAA-gel was used. 3.9% PAA concentration was used for the stacking gel (Tab. 3). The protein lysates (II.11.1) were mixed in ratio 3:1 with protein loading buffer and pressed through a 20 G syringe needle. Finally, the protein lysates were denaturated at 95°C for 5 min and 20-30 µl were loaded on the SDS-PAA-gel. The electrophoresis of the stacking gel was performed at 90 V and of separating gel at 120-130 V. As a marker, Precision Plus Protein™ Standards- All Blue (BioRad, München) was used.

| | **Separating gel (12.5%)** | **Stacking gel (3.9%)** |
|---|---|---|
| $ddH_2O$ | 1.65 ml | 2.10 ml |
| Separating gel buffer (4 ×) | 1.25 ml | - |
| Stacking gel buffer (4 ×) | - | 0.84 ml |
| Acrylamide/Bis (30%) | 2.10 ml | 0.45 ml |
| APS (10%) | 70.0 µl | 70.0 µl |
| TEMED | 4.0 µl | 4.0 µl |

**Tab. 3: Composition of the separating and stacking SDS-PAA-gels**

## 4.4 Purification of DNA fragments

For purification of DNA fragments, the JETquick PCR Purification Spin Kit (Genomed, Löhne) was used according to the manufacturer's protocol. The DNA was eluted from the column in 30 µl HPLC water.

## 4.5 Precipitation of DNA

To eliminate oligonucleotides, PCR products were precipitated before sequencing reaction. Therefore, 1 volume of 4 M ammonium acetate and 6 volumes of absolute ethanol were added to the sample and the samples were centrifuged at 13.000 rpm for 25 min. The pellet was washed with 70% (v/v) ethanol, centrifuged again for 10 min, dried, and resuspended in 20 µl HPLC water.

After sequencing reaction (II.4.6), DNA was precipitated by addition of 1/10 volume of 3 M natrium acetate (pH 5.2) and 2.5 volumes of absolute ethanol. After 25 min centrifugation at 13.000 rpm, the pellet was washed with 70% (v/v) ethanol, centrifuged, and dried.

## 4.6 Cycle sequencing

DNA sequencing was performed at the Institute of Human Genetics by the dideoxy method (Sanger et al., 1977). Automatic sequencing analysis was done using ABI Prism Dye Terminator Kit and an ABI Prism 377 DNA Sequencer (PE Applied Biosystems, Weiterstadt) according to the supplier's instructions.

| Sequencing reaction: | Program: |
|---|---|
| 5 µl PCR product or 1-3 µl plasmid DNA | 1. 96°C 5 min |
| 2 µl Big Dye Terminator (BDT) | 2. 96°C 30 s |
| 1 µl primer (10 pmol/µl) | 3. 55°C 15 s |
| ad 10 µl HPLC $H_2O$ | 4. 60°C 4 min |
| | 5. step 2-4 repeat 24-29 times |

## 4.7 Determination of DNA concentration

DNA concentration was determined by UV spectrophotometry using photometer Ultrospec® 2000 (Pharmacia Biotech, Freiburg). The absolute volume necessary for measurement was 500 µl and DNA was diluted 1:100 with water. Concentration was determined by measuring the absorbance at 260 nm ($A_{260}$). A ratio $A_{260}/A_{280}$ between 1.8 and 2 showed a sufficient purity of the DNA preparation.

# 5. Cloning of DNA fragments in plasmid vectors

## 5.1 Generation of competent *Escherichia coli* cells for chemical transformation

Competent cells (DH10B) were prepared by the rubidium method (Sambrook and Russell, 2001). One single colony was inoculated in 2 ml ψB-medium and incubated ON at 37°C with constant agitation at 220 rpm. 1 ml from this culture was inoculated in 100 ml ψB-medium and incubated until the optical density at 550 nm ($OD_{550}$) was 0.3-0.4. To generate 500 ml final volume, five times 5 ml from the 100 ml culture were inoculated in 100 ml fresh ψB-medium and incubated at 37°C until $OD_{550}$ 0.3-0.4. The bacterial suspension was transferred in 50 ml tubes and incubated in ice water for 5 min, then centrifuged at 4°C and 2.500 rpm for 8 min. The supernatant was decanted and the pellet was resuspended in 15 ml cold TfBI. The cells were incubated in ice water for 30 min. After another centrifugation step at 4°C and 2.500 rpm for 8 min, the cells were resuspended in 2 ml cold TfBII. 200 µl aliquots were made and the bacterial cells were immediately frozen in liquid nitrogen. Competent cells were kept at -80°C and thaw on ice directly before use.

One Shot® TOP10 Chemically Competent cells were supplied with TOPO TA Cloning® Kit (Invitrogen, Karlsruhe).

## 5.2 Cloning of PCR products

PCR amplicons were cloned in pCR®2.1-TOPO® vector from TOPO TA Cloning® Kit according to the manufacturer's instructions.

## 5.3 Ligation of DNA fragments

T4 DNA ligase combines covalent double stranded DNA fragments with blunt- or cohesive-compatible ends. The linearized vector DNA was mixed with 3 to 5-fold molar excess of restricted DNA insert. The ligation was catalyzed by 1 U T4 DNA Ligase (Invitrogen, Karlsruhe) in ligation buffer at RT for 4-6 h or at 16°C ON, or with 1 U Quick T4 DNA Ligase (New England Biolabs, USA) in ligase buffer at RT for 5 min. Half of the ligation mix (10 µl) was used directly for transformation.

## 5.4 Transformation of competent cells with plasmid DNA

For transformation of competent *E.coli* cells (Hanahan, 1983), one vial of TOP10 or 100 µl DH10B cells was gently mixed with 2 µl of the TOPO TA cloning reaction (II.5.2) or 10 µl of ligation mix (II.5.3), respectively, and incubated on ice for 20-30 min. After a heat-shock at 42°C for 0.5-1.5 min and incubation on ice for 5 min, 250-700 µl SOC-medium was added and the suspension was incubated at 37°C for 1 h. Then, different volumes of the suspension were plated on prewarmed agar plates containing the appropriate antibiotic (eventually also X-gal) and incubated ON at 37°C. Due to the insertion of foreign DNA into the multiple cloning site of the TOPO vector, the *lacZα* gene encoding N-terminal part of β-galactosidase is disrupted. Due to the inactivation of the *lacZα* gene in recombinant clones, X-gal is not degraded. Bacteria carrying recombinant plasmids therefore form white colonies.

# 6. Polymerase chain reaction

## 6.1 DNA amplification by PCR

Polymerase chain reaction (PCR; Mullis and Faloona, 1987) was performed in 25 µl reaction volume containing 50-100 ng genomic DNA, 0.5 U *Taq* DNA Polymerase (Qiagen, Hilden), 5 pmol of each primer, 0.2 mM of each dNTP (Invitrogen, Karlsruhe) and 1 × PCR Buffer containing 1.5 mM $MgCl_2$ (Qiagen, Hilden). PCR conditions were optimized and addition of 6% (v/v) DMSO or $MgCl_2$ was done if necessary. FailSafe™ PCR System (Biozym, Hess. Oldendorf) was used for amplification of certain PCR products. PCR amplification was done in thermocycler PTC-200 (MJ Research, USA) using the following programs. After initial denaturation (95°C, 4 min) amplification was performed at 95°C for 15 s, 48-68°C for 10 s and 72°C for 20 s - 3 min (35 cycles). Final elongation was performed at 72°C for 4-10 min. Annealing temperature depends on the average melting temperature (Tm) of both primers. To enhance specificity in certain PCRs, the so-called "touch-down PCR" was used. Here, the starting annealing temperature was relatively high (e.g. 68°C) for the first 3 cycles. For the next 3 cycles the temperature was 2°C lower (e.g. 66°C) and for the final 30 cycles again 2°C lower (e.g. 64°C). The quality of the PCR product was examined by agarose gel electrophoresis.
Junction fragments of the derivative chromosome 1 were amplified with primers PDGFB5-1 and AL355520-5. Nested PCR was performed with primers PDGFB5-2 and AL355520-6. For amplification of the junction fragment of the derivative chromosome 22, primer AL355520-8 was combined with primer PDGFBin6-1. PCR products were cloned into TA cloning vector and sequenced.

## 6.2 Colony PCR of *E.coli* cells

To screen a large amount of bacterial colonies for a desired insert, single colonies were picked from a transformation plate with a sterile tooth picker and spotted on a selective agar plate. The rest of the colony on the tooth picker was used as template for a PCR reaction. Primers m13uni and m13rev were used for the amplification of fragments cloned into TA cloning vector.

| Single colony PCR: | Program: |
|---|---|
| 0.5 µl dNTPs (10 mM) | 1. 95°C 5 min |
| 0.5 µl primer 1 (10 pmol/µl) | 2. 95°C 45 s |
| 0.5 µl primer 2 (10 pmol/µl) | 3. 55°C 30 s |
| 3.25 µl 10 x PCR Buffer | 4. 72°C 30-90 s |
| 0.1 µl *Taq* DNA Polymerase | 5. steps 2-4 repeat 34 times |
| 20.15 µl HPLC $H_2O$ | 6. 72°C 10 min |

## 6.3 Rapid amplification of 5' cDNA ends (5'RACE-PCR)

To obtain the complete 5'-end sequence of a novel gene, the GeneRacer™ Kit (Invitrogen, Karlsruhe) was used according to the supplier's protocol. The kit ensures amplification of only full-length transcripts via elimination of truncated messages from the amplification process.

## 6.4 Generation of expression vector pMT2SM⁻

Plasmid pMT2SM-HA was restricted with *Pst*I and *Sal*I and purified (II.4.4). Subsequent degradation of 3' and 5' extensions was done by Mung Bean Nuclease (New England Biolabs, USA) generating blunt ends. After a second purification step, the plasmid was ligated and transformed into competent *E.coli* cells DH10B. The clones obtained represent vector pMT2SM⁻ that was sequenced for integrity.

## 6.5 Megaprime PCR

Megaprime PCR was used for the generation of EGFP/DsRed2 fusion constructs. Various PCR products were generated comprising the 5'- and the 3'-end coding region of *PDGFB* wild-type and of the two fusion transcripts, respectively, as well as the coding region of the *EGFP* or *DsRed2* gene. For generation of EGFP fusion constructs, the coding region of EGFP without ATG start and TAG stop codon was amplified using plasmids pEGFP-N3 or pEGFP-C3 as template, and primers EGFP-F and EGFP-R. For amplification of the 5'- ends of the *PDGFB* wild-type coding region, pMSU42 was used as template with primers PDGFB-NotI and PDGFBex1-4EGFP. In case of *EGFP* inserted in exon 5, primer PDGFBex1-5EGFP was used instead of PDGFBex1-4EGFP. For amplification of the 3'-end of the wild-type *PDGFB* coding region, pMSU42 was used as template with primers PDGFBex4-6EGFP (insertion in exon 4) or PDGFBex5-6EGFP (insertion in exon 5) with primer PDGFB-EcoRI. To amplify the 3'-end of the coding region of the first fusion transcript, template pMSU11 and primer PDGFBex4-6EGFP or PDGFBex5-6EGFP in combination with primer AL355520-1-EcoRI were used. To amplify the 3'-end of the coding region of the second fusion transcript, pMSU77 was used as template with primer PDGFBex4-6EGFP or PDGFBex5-6EGFP and primer AL355520-2-EcoRI. For generation of DsRed2 fusion constructs, the coding region of DsRed2 without ATG start and TAG stop codon was amplified using plasmid pDsRed2-N1 or pDsRed2-C1 as template and primers DsRed2-up and DsRed2-dn. For amplification of the 5'- ends of the *PDGFB* wild-type coding region, pMSU42 was used as template with primers PDGFB-NotI and PDGFBex1-4 (insertion in exon 4) or PDGFBex1-5 (insertion in exon 5). For amplification of the 3'-end of the wild-type *PDGFB* coding region, pMSU42 was used as template with primers PDGFBex4-6 or PDGFBex5-6 with primer PDGFB-EcoRI. To amplify the 3'-end of the coding region of the first fusion transcript, template

pMSU11 and primer PDGFBex4-6 or PDGFBex5-6 in combination with primer AL355520-1-EcoRI were used. To amplify the 3'-end of the coding region of the second fusion transcript, pMSU77 was used as template with primer PDGFBex4-6 or PDGFBex5-6 and primer AL355520-2-EcoRI.
Each of the PCR amplicons was amplified twice, PCR products were pooled and purified (II.4.4). Then, 6.6 µl of the purified PCR was taken to set up the megaprime PCR. During first three PCR cycles (program 1), the overlapping DNA fragments annealed and overhanging single strands were filled-up. Then two oligonucleotides (PDGFB-NotI and PDGFB-EcoRI for wild-type *PDGFB*, PDGFB-NotI and AL355520-1-EcoRI for the first fusion transcript, PDGFB-NotI and AL355520-2-EcoRI for the second fusion transcript) were added and the PCR proceeded for 20 cycles (program 2). All amplifications were done by the *Pfu Turbo* DNA Polymerase (Stratagene, Netherlands). The megaprime PCR products were purified (II.4.4), restricted with *Not*I and *Eco*RI (II.4.1), and ligated into vector pMT2SM$^-$ (II.5.3). All constructs were sequenced for integrity.

Megaprime-PCR:
6.6 µl PCR product 1
6.6 µl PCR product 2
6.6 µl PCR product 3
0.5 µl dNTPs (10 mM)
2.5 µl *Pfu* 10 x Buffer
0.2 µl *Pfu Turbo* DNA Polymerase

Program 1:
1. 95°C 3 min
2. 95°C 15 s
3. 40°C 20 s
4. 72°C 5 min
5. steps 2-4 repeat 2 times

Addition of the primers:
1 µl primer 1 (10 pmol/µl)
1 µl primer 2 (10 pmol/µl)

Program 2:
1. 95°C 3 min
2. 95°C 15 s
3. 55°C 10 s
4. 72°C 3 min
5. steps 2-4 repeat 19 times
6. 72°C 10 min

## 7. Reverse transcription and RT-PCR

First-strand cDNA was synthesized using 1 µg total RNA and SuperScript™ II RNase H$^-$ Reverse Transcriptase (Invitrogen, Karlsruhe) and oligo dT or random hexanucleotides (both Invitrogen, Karlsruhe) according to the manufacturer's protocol. Of each first-strand reaction, 2 µl was taken as template in PCR reactions using cDNA Advantage Polymerase (BD Biosciences Clontech, Heidelberg). For amplification of 3'RACE-PCR products (III.1.2), cDNA from the translocation patient and an unaffected person was used with forward primers located in PDGFB exons 1-6 (PDGFB1A-1, PDGFB2-1, PDGFB3-1, PDGFB4-1, PDGFB5-1, or PDGFB6-1) and the reverse primer S-ag3'E1. Nested PCR reactions were performed with forward primers PDGFB1A-2, PDGFB2-2, PDGFB3-2, PDGFB4-2, PDGFB5-2, or PDGFB6-2 and the reverse primer S-ag3'E.

For amplification of the coding region of wild-type *PDGFB* (II.6.5 and III.2.1), cDNA derived from human testis poly $A^+$ RNA (BD Biosciences Clontech, Heidelberg) was used with primers PDGFB-10 and PDGFB-7R. PCR products were cloned into TA cloning vector and sequenced.
Human testis poly $A^+$ RNA and human brain total RNA (both BD Biosciences Clontech, Heidelberg) were used for RT-PCR.

## 8. Fluorescence *in situ* hybridization (FISH)

PAC and cosmid DNA, and *Sac*I/*Hin*dIII restriction fragments of cosmid LL22NC03-10C3 were labeled with biotin-16-dUTP (Roche, Mannheim) by nick translation (Nick Translation Mix; Roche, Mannheim) for 1 h at 16°C.

Biotin labeling:
4 µl cosmid or PAC DNA, or 1 µg of each *Sac*I/*Hin*dIII restr. fragment
10 µl BIO-MIX
4 µl Nick Translation Mix
ad 20 µl $H_2O$

BIO-MIX:
10 µl 0.4 mM dATP
10 µl 0.4 mM dCTP
10 µl 0.4 mM dGTP
2 µl 0.4 mM dTTP
15 µl biotin-16-dUTP

To precipitate DNA, 2 µl 0.5 M EDTA (pH 8.0), 2 µl 3 M NaAc (pH 5.2), 4 µl Cot 1-DNA, 0.5 µl salmon sperm (both Invitrogen, Karlsruhe) and 60 µl absolute ethanol were added and mixed, the sample was kept at -20°C for 1 h. The following centrifugation was carried out at 4°C and 13.000 rpm for 20 min. The pellet was washed twice with 70% (v/v) ethanol and dried. Then, the pellet was resuspended in 10 µl deionized formamide (pH 7.0) at 37°C for 5 min and 10 µl master mix [20% (w/v) dextran sulfate in 2 × SSC] was added. The probe was denatured at 95°C for 5 min, placed on ice, and incubated at 37°C for 1 h. During the incubation Cot 1-DNA binds to repetitive sequences in genomic DNA to prevent unspecific hybridization signals on the chromosomes. The TEL 1q DNA probe labeled by Texas Red (Appligene Oncor, France) was used to identify the long arm of chromosome 1. The TEL 1q DNA probe was incubated at 73°C for 5 min and put on ice. In the next step, 10 µl probe labeled by biotin was combined with 1 µl TEL 1q DNA probe. Metaphase spreads from peripheral blood lymphocytes of the translocation patient were made by standard procedure. The chromosomal DNA on the slides was denatured in 70% (v/v) deionized formamide (in 2 × SSC) at 70°C for 4 min. The slides were immediately transferred to ice-cold 2 × SSC for 5 min and dehydrated in an ethanol row [ice-cold 70%, 80%, and 95% (v/v) ethanol; 2 min for each step] to fixate the material. Then the slides were air dried. The biotin labeled probe was pipetted on the slide and covered by a coverslip that was fixated with Fixogum (Marabu, Germany). Hybridization was performed in humid chamber ON at 37°C. After that, the slide was washed first in 2 × SSC for 5 min, then, to eliminate unspecific bounded probes, in 50% (v/v) deionized formamid (in 2 × SSC) at 43°C for 5 min, and finally to eliminate the rest of the formamid, in 2 × SSC / 0.1% (v/v) Tween 20 for 5 min.

Fluorescein isothiocyanate (FITC) labeled avidin diluted in blocking solution (II.13.5) was used for detection of biotin labeled probe. Signal was amplified with anti-avidin (II.13.6) by the sandwich principle. The chromosomes were counterstained with DAPI. Slides were analysed with the Zeiss Axioplan fluorescence microscope equipped with Smart Capture Software (Vysis).

# 9. Single strand conformation polymorphism

SSCP analysis was originally described by Orita et al. (1989). The principle is to take a PCR amplicon, denature it, and electrophorese it through a non-denaturing polyacrylamide gel. Thus, as the PCR product moves into and through the gel, it will regain a secondary structure that is sequence dependent. The mobility of single-stranded PCR products will depend upon their secondary structure.
PAGE was performed as described in II.4.3. To detect the single and double strands alleles a silver-staining technique was used. First, the gel was fixed with 10% (v/v) ethanol for 5-10 min followed by 1% (v/v) nitric acid for 3 min. Then, the gel was rinsed two times with water and was left in silver nitrate solution for 20 min. After washing the gel two times with water, reducer solution was added. Developing needed few minutes, when the bands started to appear, the solution was discarded, and fresh reducer solution was added. Finally, the reaction was stopped with 10% (v/v) acetic acid and the gel was rinsed with water. All staining steps were performed in glass dishes with constant agitation.

# 10. Cell biology methods

## 10.1 Culture of adherent cells

COS-7 and CHO-K1 cells were cultured in Dulbecco's Modified Eagle Medium (D-MEM) or F-12 Nutrient Mixture (Ham), respectively, supplemented with 10% (v/v) fetal calf serum (FCS) and 1% (v/v) penicillin-streptomycin (P/S) (all Gibco, Karlsruhe) at 37°C, with relative humidity of 95% and with 5% $CO_2$ concentration (NUaire™ $CO_2$ Water Jacketed Incubator; Zapf, Sarstedt). Cells were passaged until they were 90-95% confluent. Medium was removed, cells were washed in PBS (without $MgCl_2$ and $CaCl_2$), and detached by incubation with Trypsin-EDTA-Solution (2 ml/10-cm plate; Gibco, Karlsruhe). Redundant trypsin was inactivated by addition of 8 ml fresh pre-warmed complete medium. Then, the resuspended COS-7 and CHO-K1 cells were split either 1/10 or 1/20 for maintenance, or the cells were seeded in 24-, 6-well or 10-cm plates for transfection experiments.

## 10.2 Freezing and thawing of adherent cells

Freezing medium was composed of 9 volumes of medium and 1 volume of dimethyl sulfoxide (DMSO). Cells were grown in 10-cm plates or flasks until they were 90-95% confluent. After trypsination, 10 ml fresh pre-warmed medium was added and the cell suspension was centrifuged at 950 rpm for 5 min. Pellet was carefully resuspended in 3 ml chilled freezing medium and 1 ml aliquots of the cell suspension were pipetted in cryovials. Cells were frozen in steps (4°C, -80°C) and for long-term storage kept in liquid nitrogen.
Thawing of the cells was done by incubation in water bath at 37°C, then the cell suspension was immediately transferred to pre-warmed medium.

## 10.3 Transient transfection by liposome mediated DNA-transfer

Negatively loaded nucleic acids and synthetic, positively loaded liposomes build up a complex that is brought near to the cells and fuses with the cell membrane.
24 h before transfection, $3 \times 10^4$ or $1.2 \times 10^5$ cells were seeded on coverslips in a 24- or 6-well plate. COS-7 or CHO-K1 cells grown on coverslips in D-MEM or Ham medium, respectively, were transfected with the PDGFB-EGFP fusion constructs using Lipofectamine™ 2000 (Invitrogen, Karlsruhe) according to the manufacturer's instructions. The plasmids and Lipofectamine™ 2000 were separately diluted with serum- and antibiotic-free medium Opti-MEM® I (Gibco, Karlsruhe) (Tab. 4), incubated 5 min at RT, combined, and left at RT for 20-30 min. Meanwhile, the cells were washed with PBS (without $MgCl_2$ and $CaCl_2$) and left in Opti-MEM® I medium until transfection. DNA-Lipofectamine™ 2000 complexes were carefully added to each well and incubated for 5-6 h at 37°C, then the COS-7 or CHO-K1 cells were washed once with pre-warmed complete medium (D-MEM or Ham) and cultivated in the medium ON.

| Culture vessel | DNA | Lipofectamine™ 2000 | Dilution volume of Opti-MEM® I | Volume of plating medium |
|---|---|---|---|---|
| 24-well | 50 ng / well | 1 µl / well | 50 µl | 500 µl |
| 6-well | 0.25-1 µg / well | 5-6 µl / well | 250 µl | 2 ml |
| 10-cm | 4 µg | 10 µl | 400 µl | 10 ml |

**Tab. 4: Reagent quantities for transient transfection with Lipofectamine™ 2000**

CHO-K1 cells that were cultured on coverslips in 6-well plates in Ham were transfected with the PDGFB-DsRed2 fusion constructs using Lipofectamine™ 2000 according to the manufacturer's protocol and as described above.

### 10.4 Immunofluorescence and EGFP/DsRed2-fluorescence

20-21 h after transfection, the coverslips with COS-7 cells transfected with the PDGFB-EGFP fusion constructs were rinsed with PBS +/+ (4°C) and fixed in filtrated 4% (w/v) paraformaldehyde (in PBS +/+, 4°C) for 10 min. After washing with PBS +/+ three times for 10 min, cells were incubated with 2% (w/v) BSA, 3% (v/v) goat serum, and 0,5% (v/v) Nonidet P40 in PBS +/+ for 60 min. For detection of laminin, cells were incubated with rabbit anti-laminin antibody followed by incubation with anti-rabbit secondary antibody (II.13.5 and II.13.6). After washing twice with high salt PBS +/+ and three times with PBS +/+, cells on coverslips were mounted in glycerol gelatin containing 1% (w/v) phenol (Sigma, Taufkirchen). Cells were examined with the fluorescence microscope Leica DM RA (Leica Mikrosysteme, Bensheim) and the CytoVision™-Software (Applied Imaging, GB).
24 h after transfection, the coverslips with CHO-K1 cells transfected with the PDGFB-DsRed2 fusion constructs were rinsed with PBS, put on slides without fixation and mounted with nail enamel. Living cells were examined by fluorescence microscopy.

## 11. Standard protein methods

### 11.1 Extraction of proteins

20-21 h after transfection, COS-7 cells were washed with PBS and lysed with ice-cold cell lysis buffer (1 ml/dish) and then scraped off. Cell lysates were incubated on ice for 5 min and then half of the cell lysates was stored at -20°C (whole cell lysate). The other half of the cell lysates was centrifuged at 4°C and 14.000 rpm for 10 min to remove cell debris, supernatant was kept again at -20°C (cytosolic fraction).

### 11.2 Western blotting

Protein lysates were mixed with loading buffer and separated by SDS-PAGE (II.4.3). After electrophoresis, the SDS-gel as well as filter papers (Gel Blotting Paper; Schleicher & Schuell, Dassel) were equilibrated in semi dry transfer buffer. A western blotting PVDF membrane (Roche, Mannheim) was shortly equilibrated in dd$H_2O$, methanol, and finally in semi dry transfer buffer. Then, a sandwich containing filter papers, PVDF membrane, SDS-gel, and filter papers was assembled from the bottom. The proteins were transferred from the SDS-gel to the PVDF membrane using a semi dry blotting apparatus (Biometra, Göttingen) at 300 mA for 20-25 min.

## 11.3 Immunological detection of proteins on nitrocellulose membrane

After electrophoretic transfer, the membrane was removed from the sandwich and placed (protein-binding side up) in glass vessels. The membrane was blocked with 4% non-fat dry milk powder in 1 × TBST for 1 h at RT or ON at 4°C. After two times washing with antibody solution, the membrane was incubated in a Falcon tube for 2 h in 5 ml of antibody solution containing the primary antibody (II.13.5). Then, the membrane was washed three times for 10 min with 1 × TBST and incubated for 1 h with the secondary antibody coupled to horseradish peroxidase (II.13.6). The membrane was again washed three times for 15 min with 1 × TBST.

## 11.4 Detection of bounded antibodies using enhanced chemiluminescence (ECL)

Immunoreactive signals were visualized using ECL plus Western Blotting Detection System (Amersham Biosciences, Freiburg) according to the supplier's instructions. The membrane was soaked for 1 min in the mixture of detection solutions, then the mixture was removed and the blot was wrapped in a foil. The membrane was exposed to Hyperfilm ECL X-ray film (Amersham Biosciences, Freiburg) for several time periods, starting from 15 s to 10 min.

# 12. Computer based analysis

Accession numbers and URLs for data presented herein are as follows:

**BLAST:** http://www.ncbi.nlm.nih.gov/BLAST (for homology searches)

**GenBank:** http://www.ncbi.nlm.nih.gov/GenBank/ [for sequence of the breakpoint region on chromosome 22q13.1 (accession numbers Z81010.2 and NT_011520.9), for sequence of the breakpoint region on chromosome 1q24.3 (accession number AL355520.8 and NT_004487.16), for ***PDGFA*** mRNA sequence (accession number NM_002607) and genomic sequences (accession numbers M20488, M20489, M20490, M20491, M20492, and M20493), for ***PDGFB*** mRNA sequences (accession numbers M12783, NM_002608, and NM_033016) and genomic sequence (accession number Z81010), for ***PDGFC*** mRNA sequences (AF091434 and NM_016205) and genomic sequences (accession numbers AC093325 and AC092608), for ***PDGFD*** mRNA sequences (AF113216 and NM_025208) and genomic sequences (accession numbers AP004551 and AP003043), for ***PDGFRA*** mRNA sequences (accession numbers M21574 and NM_006206), and genomic sequences (accession numbers AC138799 and AC098587), for ***PDGFRB*** mRNA sequences (accession numbers J03278 and NM_002609) and genomic sequences (accession numbers AC005895

and AC011382), for ***TGFB1*** mRNA sequence (accession number NM_000660) and genomic sequence (accession number NT_011109), for ***FOXO1A*** mRNA sequences (accession numbers U02310 and NM_002015) and genomic sequences (accession numbers AL355132 and AL133318), and for ***LMNA*** mRNA sequences (accession numbers NM_170707, NM_005572, and NM_170708) and genomic sequence (accession number AL135927)]

**Online Mendelian Inheritance in Man (OMIM):** http://www.ncbi.nlm.nih.gov/Omim [for Costello syndrome (OMIM 218040), Noonan syndrome (OMIM 163950), cardiofaciocutaneous syndrome (OMIM 115150), cutis laxa (e.g. OMIM 219200), neurofibromatosis type 2 (OMIM 101000), Hutchinson-Gilford progeria syndrome (OMIM 176670)]

**GENESCAN:** http://genes.mit.edu/GENSCAN.html and **GrailEXP:** http://compbio.ornl.gov/grailexp/ (for gene prediction)

**ClustalW**, http://searchlauncher.bcm.tmc.edu/multi-align/multi-align.html and **BOXSHADE**, http://www.ch.embnet.org/software/BOX_form.html (for alignment of homologous sequences)

**Peptide Mass (ExPASy)**, http://us.expasy.org/tools/peptide-mass.html (to predict size of the PDGFB-EGFP fusion proteins)

# 13. Reagents and Materials

## 13.1 Buffers and Solutions

| | |
|---|---|
| Agar plates | 15 g select agar<br>in 1000 ml LB-medium; autoclave<br>add antibiotic and/or X-gal |
| Antibody solution [western blotting (WB)] | 0.2% (w/v) non-fat dry milk in 1 × TBST |
| Antibody solution [immunofluorescence (IF)] | 3% (v/v) goat serum<br>0.1% (v/v) Nonidet P40<br>in 1 ×PBS +/+ |
| Blocking solution<br>[fluorescence *in situ* hybridization (FISH)] | 2 × SSC<br>1% (w/v) BSA<br>0.1% (v/v) Tween 20 |
| Cell lysis buffer | 50 mM Tris-HCl, pH 7.5<br>1% (v/v) Nonidet P40<br>2 mM $MgCl_2$<br>150 mM NaCl<br>10% (v/v) glycerol<br>add 1 tablet complete mini and 1 mM PMSF per 10 ml |

| | |
|---|---|
| DNA-loading buffer I | 25 ml glycerol 100 %<br>25 ml 1 × TBE<br>~ 20 mg orange G |
| DNA-loading buffer II (6 ×) | 30% (v/v) glycerol in $ddH_2O$<br>0.25% (w/v) bromphenol blue<br>0.25% (w/v) xylene cyanol FF |
| LB-medium | 10 g trypton<br>5 g yeast extract<br>10 g NaCl<br>in 1000 ml $ddH_2O$; pH 7.0 |
| PBS (20 ×) | 160 g NaCl<br>4 g KCl<br>21.49 g $Na_2HPO_4$<br>1.725 g $KH_2PO_4$<br>in 1000 ml $ddH_2O$; pH 7.3<br>for PBS +/+ add 0.5 mM $MgCl_2$ and 1 mM $CaCl_2$ |
| PBS +/+ high salt | add 500 mM NaCl |
| Protein loading buffer | 4 volumes of NU Page LDS Sample Buffer 4 ×<br>(Invitrogen, Karlsruhe)<br>1 volume of mercaptoethanol |
| ψB-medium | 5 g yeast extract<br>20 g bactotryptone<br>0.75 g KCl<br>pH 7.6 with KOH; autoclave<br>add 34 ml sterile 1M $MgSO_4$ / l |
| Reducer solution | 29.6 g sodium carbonate anhydrous<br>540 µl formaldehyde solution 36.5%<br>in 1000 ml $ddH_2O$ |
| SDS-running buffer (10 ×) | 40 g SDS<br>50.6 g Tris<br>288.4 g glycin<br>in 2000 ml $ddH_2O$; pH 8.3 |
| Semi dry transfer buffer | 25 mM Tris-HCl; pH 8.3<br>150 mM glycin<br>10% (v/v) methanol |
| Separating gel buffer (4 ×) | 2 g SDS<br>91 g Tris<br>in 500 ml $ddH_2O$<br>pH 8.8 adjust with $H_3PO_4$ |
| Silver nitrate solution | 2.02 g silver nitrate<br>in 1000 ml $ddH_2O$ |

| | |
|---|---|
| SOC-medium | 20 g trypton<br>5 g yeast extract<br>0.5 g NaCl<br>in 980 ml $ddH_2O$; pH 7.0; autoclave<br>10 ml sterile 1 M $MgSO_4$<br>10 ml sterile 1 M $MgCl_2$<br>10 ml sterile 40% glucose |
| Solution I | 50 mM glucose<br>25 mM Tris-HCl, pH 8.0<br>10 mM EDTA |
| Solution II | 0.2 M NaOH<br>1% (w/v) SDS |
| Solution III | 29.4 g potassium acetate resusp. in 50 ml $ddH_2O$<br>11.5 ml acetic acid (glacial)<br>fill up to 100 ml with $ddH_2O$ |
| SSC (20 ×) | 3 M NaCl<br>0.3 M sodium citrate<br>pH 7.0 |
| SSCP-loading buffer | 98% (v/v) formamid<br>10 mM EDTA<br>0.025% (w/v) bromphenol blue<br>0.025% (w/v) xylene cyanol FF |
| Stacking gel buffer (4 ×) | 2 g SDS<br>30.3 g Tris<br>in 500 ml $ddH_2O$<br>pH 6.8 adjust with $H_3PO_4$ |
| TBE-buffer (10 ×) | 216 g Tris<br>110 g boric acid<br>14.9 g EDTA<br>in 2000 ml $ddH_2O$ |
| TBST (10 ×) | 200 mM Tris-HCl, pH 7.4<br>1500 mM NaCl<br>1% (v/v) Tween 20<br>in 1000 ml $ddH_2O$; pH 7.8 |
| TE-buffer (1 ×) | 10 mM Tris<br>1 mM EDTA<br>pH 8.0 |
| TfBI | 1.47 g potassium acetate<br>4.95 g $MnCl_2$<br>6.05 g RbCl<br>0.74 g $CaCl_2$<br>75 ml glycerol<br>pH 5.8 with 0.2 M acetic acid<br>filter sterilize and store at +5°C |

| | |
|---|---|
| TfBII | 10 ml 100 mM MOPS (pH 7.0)<br>1.10 g $CaCl_2$<br>0.12 g RbCl<br>15 ml glycerol<br>filter sterilize and store at +5°C in the dark |
| X-gal | 2% (w/v) X-Gal in dimethylformamid<br>storage at -20°C |

## 13.2 Chemicals

All basic chemicals were purchased from Sigma (Taufkirchen) or Merck (Darmstadt). The source of some chemicals was already described in the text.

| | |
|---|---|
| Acrylamide/Bis | BioRad (München) |
| Acrylamide/bisacrylamide | Severn Biotech Ltd. (USA) |
| Ammonium persulfate | Sigma (Taufkirchen) |
| Ampicillin | Sigma (Taufkirchen) |
| Bacto™ Tryptone | BD (France) |
| Blotting Grade Blocker Non-Fat Dry Milk | BioRad (München) |
| Bovine serum albumin | Sigma (Taufkirchen) |
| Bromphenol blue | Sigma (Taufkirchen) |
| Chloramphenicol | Sigma (Taufkirchen) |
| Complete Mini Protease Inhibitor Cocktail Tablets | Roche (Mannheim) |
| DAPI | Sigma (Taufkirchen) |
| Dimethyl Sulphoxide (DMSO) Hybri-Max® | Sigma (Taufkirchen) |
| Formaldehyde solution 36.5% | Fluka (Steinheim) |
| Formamide | Merck (Darmstadt) |
| Glucose | Sigma (Taufkirchen) |
| Glycerol | Fluka (Steinheim) |
| Glycin | Merck (Darmstadt) |
| Goat serum | Sigma (Taufkirchen) |
| HPLC water | LiChrosolv® (Merck, Darmstadt) |
| Kanamycin sulfate | Fluka (Steinheim) |
| Mercaptoethanol | Merck (Darmstadt) |
| MOPS | Sigma (Taufkirchen) |
| Nonidet P40 / Igepal | ICN (Eschwege) |
| Orange G | Sigma (Taufkirchen) |
| Paraformaldehyde | Sigma (Taufkirchen) |
| Phenol | Roth (Karlsruhe) |
| Phenylmethyl sulphonyl fluoride | Roche (Mannheim) |
| Restore™ Western Blot Stripping Buffer | Pierce/Perbio (Bonn) |
| Select agar | Invitrogen (Karlsruhe) |
| Sodium dodecyl sulfate | Sigma (Taufkirchen) |
| TEMED | Sigma (Taufkirchen) |
| Tetracycline | Sigma (Taufkirchen) |
| Titriplex® III (ethylenedinitrilo tetraacetic acid) | Merck (Darmstadt) |
| TRIZMA® BASE (Tris) | Sigma (Taufkirchen) |
| Tween 20 (polyoxyethylenesorbitan monolaurate) | Sigma (Taufkirchen) |
| Yeast extract | Oxoid (England) |
| X-Gal | Invitrogen (Karlsruhe) |
| Xylene cyanol FF | Sigma (Taufkirchen) |

## 13.3 Plasmids

### 13.3.1 Vector plasmids

| | Name | Characteristics | Source/Reference |
|---|---|---|---|
| **Cloning vectors** | pACYC184 | $Cm^r$ $Tc^r$ | Chang and Cohen, 1978 |
| | pBluescript-Cm | $Cm^r$ | R. Waldschütz |
| | pCR®2.1-TOPO® | $Km^r$ $Amp^r$, *lacZα* | Invitrogen (Karlsruhe) |
| **Eukaryotic expression vectors** | pMT2SM-HA | $Amp^r$, HA-tag | Kaufman et al., 1987 |
| | pEGFP-N3 | $Km^r$/$Neo^r$, *EGFP* | Prasher et al., 1992 |
| | pEGFP-C3 | $Km^r$/$Neo^r$, *EGFP* | Prasher et al., 1992 |
| | pDsRed2-N1 | $Km^r$/$Neo^r$, *DsRed2* | Matz et al., 1999 |
| | pDsRed2-C1 | $Km^r$/$Neo^r$, *DsRed2* | Matz et al., 1999 |

### 13.3.2 Hybrid plasmids

| Name | Characteristics | Source/Reference |
|---|---|---|
| pMSU1 | 1177 bp *Sac*I fragment from cosmid LL22NC03-10C3 in pBluescript-Cm | this work |
| pMSU2 | 935 bp *Sac*I fragment from cosmid LL22NC03-10C3 in pBluescript-Cm | this work |
| pMSU3 | 3895 bp *Sac*I fragment from cosmid LL22NC03-10C3 in pBluescript-Cm | this work |
| pMSU4 | 4134 bp *Sac*I fragment from cosmid LL22NC03-10C3 in pBluescript-Cm | this work |
| pMSU5 | 3447 bp *Sac*I fragment from cosmid LL22NC03-10C3 in pBluescript-Cm | this work |
| pMSU6 | 1875 bp *Hin*dIII fragment from cosmid LL22NC03-10C3 in pACYC184 | this work |
| pMSU7 | 5201 bp *Hin*dIII fragment from cosmid LL22NC03-10C3 in pACYC184 | this work |

| Name | Characteristics | Source/Reference |
|---|---|---|
| pMSU8 | 4889 bp *Hin*dIII fragment from cosmid LL22NC03-10C3 in pACYC184 | this work |
| pMSU9 | 2070 bp *Hin*dIII fragment from cosmid LL22NC03-10C3 in pACYC184 | this work |
| pMSU10 | 6139 bp *Hin*dIII fragment from cosmid LL22NC03-10C3 in pACYC184 | this work |
| pMSU11 | first fusion transcript in pCR®2.1-TOPO® | this work |
| pMSU42 | wild type *PDGFB* in pCR®2.1-TOPO® | this work |
| pMSU49 | second fusion transcript in pCR®2.1-TOPO® | this work |
| pMSU62 | second fusion transcript in pCR®2.1-TOPO® | this work |
| pMSU77 | second fusion transcript in pCR®2.1-TOPO® | this work |

## 13.4 Bacterial strains and eukaryotic cell lines

| | Name | | Source | Reference |
|---|---|---|---|---|
| **Bacterial strains** | DH10B | F- *mcr*A Δ(*mrr-hsd*RMS-*mcr*BC) Φ80d*lacZ*ΔM15 Δ*lac*X74 *deo*R *rec*A1 *end*A1 *ara*D139 Δ(*ara*, *leu*)7697 *gal*U *gal*K λ- *rps*L (Str$^R$) *nup*G | Invitrogen (Karlsruhe) | |
| | TOP10 | F- Δ(*mrr-hsd*RMS-*mcr*BC) Φ80d*lacZ*ΔM15 Δ*lac*X74 *deo*R *rec*A1 *ara*D139 Δ(*ara*, *leu*)7697 *gal*U *gal*K *rps*L (Str$^R$) *end*A1 *nup*G | Invitrogen (Karlsruhe) | |
| **Cell lines** | COS-7 | African green monkey kidney; fibroblast-like cells growing as monolayers | DSMZ (Braunschweig) ACC 60 | Gluzman, 1981 |
| | CHO-K1 | Chinese hamster ovary cells; adherent, fibroblastoid cells | DSMZ (Braunschweig) ACC 110 | Puck, 1965 |

## 13.5 Primary antibodies

| Name | Species | Antigen | Concentration | Source |
|---|---|---|---|---|
| Fluorescein avidin DN | – | biotin | FISH 1:200 | Vector Laboratories, Inc. (USA) |
| Anti-laminin | rabbit | laminin from basement membrane of Englebreth Holm-Swarm (EHS) mouse sarcoma | IF 1:100 | Sigma (Darmstadt) |
| Living Colors® A.v. Peptide Antibody | rabbit | GFP | WB 1:100 | BD Biosciences Clontech (Heidelberg) |

## 13.6 Secondary antibodies

| Name | Species | Konjugat | Concentration | Source |
|---|---|---|---|---|
| Biotinylated anti-avidin D | goat | – | FISH 1:200 | Vector Laboratories, Inc. (USA) |
| Alexa Fluor® 546 goat anti-rabbit IgG | goat | Alexa Fluor 546 | IF 1:1500 | Molecular Probes / MoBiTec (Göttingen) |
| Anti rabbit Ig, Horseradish Peroxidase linked $F(ab')_2$ fragment | donkey | Horseradish peroxidase | WB 1:5000 | Amersham Biosciences (Freiburg) |

## 13.7 Synthetic oligonucleotides

Oligonucleotides were supplied from Sigma (Taufkirchen) or Metabion (Planegg-Martinsried), lyophilizated and desalted. Only primers used for amplification of the coding region of *PDGFB* wild-type and of the two fusion transcripts, were purified by HPLC. All oligonucleotides were resuspended in 1 x TE to 100 pmol/µl concentration before use. When needed, aliquots from this stock solution were diluted with HPLC water to 10 pmol/µl.

**General primers**

| | |
|---|---|
| m13uni: | 5'-GTAAAACGACGGCCAG-3' |
| m13rev: | 5'-CAGGAAACAGCTATGAC-3' |
| GeneRacer™ 5'Primer: | 5'-CGACTGGAGCACGAGGACACTGA-3' |
| GeneRacer™ 5'Nested Primer: | 5'-GGACACTGACATGGACTGAAGGAGTA-3' |

**Primers used for 3'RACE-PCR**

| | |
|---|---|
| PDGFB1A-1: | 5'-GAATCGCTGCTGGGCGCTCTTC-3' |
| PDGFB1A-2: | 5'-GTCTCTCTGCTGCTACCTGCTTCTG-3' |
| PDGFB2-1: | 5'-GACCCCATTCCCGAGGAGCTTTATG-3' |
| PDGFB2-2: | 5'-GAGATGCTGAGTGACCACTCGATC-3' |
| PDGFB3-1: | 5'-GGAAGATGGGGCCGAGTTGGACCTG-3' |
| PDGFB3-2: | 5'-CATGACCCGCTCCCACTCTGGAG-3' |
| PDGFB4-1: | 5'-GTTCCCTGACCATTGCTGAGC-3' |
| PDGFB4-2: | 5'-CCATGATCGCCGAGTGCAAGACG-3' |
| PDGFB5-1: | 5'-GTGAGAAAGATCGAGATTGTGC-3' |
| PDGFB5-2: | 5'-GGAAGAAGCCAATCTTTAAGAAG-3' |
| PDGFB6-1: | 5'-CAAAACGCCCCAAACTCGGGTGAC-3' |
| PDGFB6-2: | 5'-GACCATTCGGACGGTGCGAGTCC-3' |
| S-ag3'E1: | 5'-GCATGCGCGCGGCCGCGGAGGCCTTTTTTTTTTTTTTT-3' |
| S-ag3'E: | 5'-GCATGCGCGCGGCCGCGGAGGCC-3' |

**Primers located on the insert of clone LL22NC03-10C3 (accession number Z81020.2)**

| | |
|---|---|
| PDG-Ex5L2: | 5'-CTCCTGGCTGTGTGGTCTCTAC-3' |
| PDGFBin-5-2: | 5'-CAGCGCCATTTCCAGTCTTGCTACC-3' |
| PDGFBin-5-3: | 5'-TAGCCCCCTGCTTTGTTGGATGTGG-3' |
| PDGFBin5-9: | 5'-GAATCATACTCCCACCATGAAGCTG-3' |
| PDGFBin5-10: | 5'-TCCTTAGCTTGACCTACTATTGAGG-3' |
| PDGFBin6-1: | 5'-CATCCCATGTTCATATGTCCCCGATG-3' |
| PDGFB-7R: | 5'-CAATATTATCACTCCAAGGACCCCATG-3' |
| PDGFB-10: | 5'-GGAGTCGGCATGAATCGCTGCTG-3' |

**Primers located on the insert of clone RP4-595C2 (accession number AL355520.8)**

| | |
|---|---|
| AL355520-5: | 5'-CTGTTTACACCTGGCTCAATGC-3' |
| AL355520-6: | 5'-GTACATCAAACACGTATTTCAAAC-3' |
| AL355520-8: | 5'-GTAGTTAAGAGGAGCTGCTCTTTATG-3' |
| AL355520-12: | 5'-AGCGTGGAAGATTGATGCTGCGGTC-3' |
| AL355520-13: | 5'-CAGGAGGGGACTTTGGGGAACAGAG-3' |
| AL355520-14: | 5'-CTGGAGGCTAGAAAATCCAACATCAAG-3' |
| AL355520-17: | 5'-CAAAGAAGACAGACCATTATCAAC-3' |
| AL355520-20: | 5'-CTGGGACTACAGGCATGCACCACCACG-3' |
| AL355520-21: | 5'-AGGAAACAATCAGAATGGGTCTGGAAC-3' |
| AL355520-27: | 5'-GATGACCCTGCAAACAGCTACTGG-3' |
| AL355520-28: | 5'-GAGCATGGAGACAGGGGGTTGAG-3' |

**Primers for megaprime PCR**

Recognition sequences for restriction endonucleases are shadowed. Start and stop codons are underlined.

| | |
|---|---|
| EGFP-F: | 5'-GTGAGCAAGGGCGAGGAGCTGTTC-3' |
| EGFP-R: | 5'-CTGGGCCCGGATCCTCTTGTACAG-3' |
| PDGFB-NotI: | 5'-AAGGAAAAAAGCGGCCGCGCAGCCATGAATCGCTGCTGGGCGC TCTTC-3' |
| PDGFBex1-4EGFP: | 5'-AGCTCCTCGCCCTTGCTCACCGGCTCAGCAATGGTCAGGG AACC-3' |
| PDGFBex1-5EGFP: | 5'-AGCTCCTCGCCCTTGCTCACACACTTGCATGCCAGGTGGT CTTC-3' |
| PDGFBex4-6EGFP: | 5'-ACAAGAGGATCCGGGCCCAGGCCATGATCGCCGAGTGCAA GACG-3' |
| PDGFBex5-6EGFP: | 5'-ACAAGAGGATCCGGGCCCAGGAGACAGTGGCAGCTGCACG GCCTG-3' |
| PDGFB-EcoRI: | 5'-CCGGAATTCTTACTAGGCTCCAAGGGTCTCCTTCAG-3' |
| AL355520-1-EcoRI: | 5'-CCGGAATTCTTACTACAAAATACAGTATATTAAAAAAAC-3' |
| AL355520-2-EcoRI: | 5'-CCGGAATTCTTATCAGGAGGGGACTTTGGGGAACAG-3' |
| | |
| DsRed2-up: | 5'-GCCTCCTCCGAGAACGTCATCACC-3' |
| DsRed2-dn: | 5'-CAGGAACAGGTGGTGGCGGCCCTC-3' |
| PDGFBex1-4: | 5'-ATGACGTTCTCGGAGGAGGCCGGCTCAGCAATGGTCAGGG AACC-3' |
| PDGFBex1-5: | 5'-ATGACGTTCTCGGAGGAGGCACACTTGCATGCCAGGTGGT CTTC-3' |
| PDGFBex4-6: | 5'-GCCGCCACCACCTGTTCCTGGCCATGATCGCCGAGTGCAA GACG-3' |
| PDGFBex5-6: | 5'-GCCGCCACCACCTGTTCCTGGAGACAGTGGCAGCTGCACG GCCTG-3' |

**Primers for mutation screening**

*PDGFA*

| | |
|---|---|
| PDGA-1F: | 5'-GCCACAGGAGACCGGCTGGAG-3' |
| PDGA-1R2: | 5'-AGGAACCAAAACGCTCTCTGCAGAG-3' |
| PDGA-2F3: | 5'-GGCCGCGGGCGCTGACCGTG-3' |
| PDGA-2R2: | 5'-GATTGGATTCTGACCTTTCGGTG-3' |
| PDGA-3F: | 5'-ACAGCGCACGGGGCATTCAC-3' |
| PDGA-3R: | 5'-ATCGCGGCCTCCTGGACTCAC-3' |
| PDGA-4F2: | 5'-CTGGCCTGTGGGTTACCCTGGTTGC-3' |
| PDGA-4R: | 5'-CACCTTGACGCTGCGGTGGTG-3' |
| PDGA-5F: | 5'-CGAAGCTCCATGCAGGCATTC-3' |
| PDGA-5R: | 5'-CACCCCAAAAGCAAGGCTCTG-3' |
| PDGA-6F: | 5'-TGCCGTAGGTATTTGTTGCTTC-3' |
| PDGA-6R: | 5'-CTTGCATGCCTAGCAGGACTC-3' |

*PDGFB*

| | |
|---|---|
| PD-Ex1L2: | 5'-CCCCCGGCCGTGGATGCT-3' |
| PD-Ex1R2: | 5'-GGAGAGGAGGGGGCGGTCAGAAG-3' |
| PDG-Ex1BL: | 5'-AGAGCCCTGGAGGTGTGCAAG-3' |
| PDG-Ex1BR: | 5'-TCACAGAAGAGGCTCCTCAATGTG-3' |

| | |
|---|---|
| PDG-Ex2L: | 5’-GGAGACAGCCATGCTGGAAAG-3’ |
| PDG-Ex2R: | 5’-GCTGCCATGGGCCTCTAGTTC-3’ |
| PDG-Ex3L: | 5’-CCTCCCGCCTGCCCAGACAC-3’ |
| PDG-Ex3R: | 5’-GCCCGCCCCCGTTCTCTTTC-3’ |
| PD-Ex4L2: | 5’-TGAAGGGCGTGAGAAAGAGCAGTC-3’ |
| PD-Ex4R2: | 5’-GAGCCCAGGAACAAATCAGGAATG-3’ |
| PDGFB-5F: | 5’-TTGCTGCAGGGGACACCGGGGTG-3’ |
| PDG-Ex5R: | 5’-CTGCAGGGGAAGGGGGCTGAG-3’ |
| PDG-Ex6L: | 5’-GGTCCACATGCTGACGAGGTC-3’ |
| PDG-Ex6R: | 5’-GCCCTCACCTGCCCACACACTC-3’ |

*PDGFC*

| | |
|---|---|
| PDGFC-ex1-F: | 5’-GGATGGGATTATGTGGAAACTACC-3’ |
| PDGFC-ex1-R2: | 5’-CATACCAACGCACAATGCCAACG-3’ |
| PDGFC-ex2-F2: | 5’-CACTCAGCACTTGTCTGAGGTAAAG-3’ |
| PDGFC-ex2-R2: | 5’-CTTCAAATAAAACATAGCTTCAATAAG-3’ |
| PDGFC-ex3-F: | 5’-CACAGACATGAAACTTGTAATTGC-3’ |
| PDGFC-ex3-R: | 5’-TTCTGATTCTCATGTGTAAGAGG-3’ |
| PDGFC-ex4-F2: | 5’-CTTCACACATATTTCCAGCCTCAG-3’ |
| PDGFC-ex4-R2: | 5’-AGCTGTGGCAGAAGAATCTGAAAC-3’ |
| PDGFC-ex5-F2: | 5’-GAGCTTAATGAAATACATTCAGGCTC-3’ |
| PDGFC-ex5-R: | 5’-ACGCATTTCAGATTCACTGTTTTG-3’ |
| PDGFC-ex6-F: | 5’-TTGTTTATAAAAGCCAGTCATAGAC-3’ |
| PDGFC-ex6-R: | 5’-GGATGGAGATAACGCATACGTTCTC-3’ |

*PDGFD*

| | |
|---|---|
| PDGFD-ex1-F: | 5’-AGCCCGAGTTCACATTCAAGATTC-3’ |
| PDGFD-ex1-R: | 5’-TCGGAAAGTTCAGCATGCAGGAAG-3’ |
| PDGFD-ex2-F2: | 5’-CTTTCCTGTAATTGGAGCAACATAC-3’ |
| PDGFD-ex2-R2: | 5’-CTATCTTGTCTGTTAGGGTCTTTAG-3’ |
| PDGFD-ex3-F: | 5’-CAGTGAAAGTATGAATTTCAAAATC-3’ |
| PDGFD-ex3-R: | 5’-AATTGATCTCTACACTTCATGAAAC-3’ |
| PDGFD-ex4-F2: | 5’-CAGAAGGCTGAGATGTTGAAACTGTG-3’ |
| PDGFD-ex4-R: | 5’-GGTTGACCTTAGCTGTTCCATCC-3’ |
| PDGFD-ex5-F2: | 5’-GTTCCTTCCGTATAGTTGAATGACTG-3’ |
| PDGFD-ex5-R: | 5’-GGATAAGGGATACTCAGCTTGTAC-3’ |
| PDGFD-ex6-F: | 5’-CAAAACACATGCTGAGCAATTGTGC-3’ |
| PDGFD-ex6-R: | 5’-CAATGGCCCTGTCTTCCTGAATCC-3’ |
| PDGFD-ex7-F: | 5’-GGTAATAAGTAGGTGGCATCTGAC-3’ |
| PDGFD-ex7-R: | 5’-GCTGAGACTCAGCAACCACTTGTG-3’ |

*PDGFRA*

| | |
|---|---|
| PDGFRA-2F: | 5’-CAAAGAGAACTAGGCTCCAGGGTTG-3’ |
| PDGFRA-2R: | 5’-GTAAAAAACCCATGCAGCACAAAGC-3’ |
| PDGFRA-3F: | 5’-CTCTCAGTTGTCGGGATGAGACTGTC-3’ |
| PDGFRA-3R: | 5’-GTTTAAAACCTTAGTACATTTAACAG-3’ |
| PDGFRA-4F2: | 5’-CATACCTAATATCAATAATGCCAG-3’ |
| PDGFRA-4R: | 5’-CCTACACGCACCTTATGATTTTGC-3’ |
| PDGFRA-5F: | 5’-CCTTTATAAGATCCTGGCTATCCTG-3’ |
| PDGFRA-5R: | 5’-GAGCTCAAATGCAGGTCTTCTGAGC-3’ |
| PDGFRA-6F: | 5’-GTTTATCTTAGAGTTCACTCCTAG-3’ |
| PDGFRA-6R: | 5’-ATGATTACCACATATGGATCCCGAG-3’ |
| PDGFRA-7F: | 5’-GTCAGTTGTCCATGCTGCTCGGGATC-3’ |

PDGFRA-7R: 5’-CACACACAAACCTCAGTCCGCCTCTG-3’
PDGFRA-8F: 5’-GAGTACAATTGTTTAAACAATTGGAAC-3’
PDGFRA-8R: 5’-GTGCCAGGCTTTCCTTGGAAGACAC-3’
PDGFRA-9F: 5’-CCACTTTGTAGTCTCATATGTTCTG-3’
PDGFRA-9R: 5’-GTATTTGACATCATTTGTGTCAAGGGAG-3’
PDGFRA-10F: 5’-GTGTTCCCGTGGCTCCACTCATTGC-3’
PDGFRA-10R: 5’-GGATTCAAAGTTCCGCCTGGGGCAG-3’
PDGFRA-11F2: 5’-CCACACTACCTTGCTGCCCCTGTGC-3’
PDGFRA-11R2: 5’-GTTCACTCCACATGTAATTGCTGAG-3’
PDGFRA-12F: 5’-CTGCTTCAGTGAAGCTCTGGTGCAC-3’
PDGFRA-12R: 5’-CTGCCAAGGCCTATAAATTGTAAAG-3’
PDGFRA-13F2: 5’-TGGCTACGGTGCAGAAAGCTGAGGAG-3’
PDGFRA-13R: 5’-GAAATTCCCTTAATATCCCCATGCTC-3’
PDGFRA-14F: 5’-CAATCACAGGATTAGTCATATTCTTG-3’
PDGFRA-14R: 5’-CTGATTGAACAGTTTTCACAACCAC-3’
PDGFRA-15F: 5’-GCAGGACAATTCATGGCTTTTCTGTTC-3’
PDGFRA-15R: 5’-GACATGGGTCTTTCCATTTGTGATGC-3’
PDGFRA-16F: 5’-CATCTACTGAAAGTGGAATGACCAC-3’
PDGFRA-16R: 5’-CTTACCATCCCTATACACTTCCCTC-3’
PDGFRA-17F: 5’-CTTTGGGCATGCCTCTGCAACCTGATG-3’
PDGFRA-17R: 5’-CTAGCATCTCCTTCCACACTCCACTC-3’
PDGFRA-18F: 5’-GTCTTGCAGGGGTGATGCTATATCAG-3’
PDGFRA-18R: 5’-TCTGCTGCCAAGGCAGTGTACTGAC-3’
PDGFRA-19F2: 5’-CACTCAAATGGGACAAGATAATTAG-3’
PDGFRA-19R: 5’-GAAAGAACACATTTTCCTTCCAGTG-3’
PDGFRA-20F: 5’-CATGCCAAGTGTTTCACCGATGCAC-3’
PDGFRA-20R: 5’-CTCAGGGCCCCTCCCTCCCCCTAGAC-3’
PDGFRA-21F: 5’-CTGTGTTCACAGTCTGTGGGTCTAG-3’
PDGFRA-21R: 5’-GAACAGCACAGCTCACTGGTATAAC-3’
PDGFRA-22F: 5’-CTGAGTGTCTCTATTCATTTTTGAG-3’
PDGFRA-22R: 5’-CGGGAAAATGGGTCCTCTCCTTCAG-3’
PDGFRA-23F: 5’-GAATGCCAAAGGCTTTCGTTTGTCTC-3’
PDGFRA-23R: 5’-CTGGGAACTTCTCTTTAAACATCAAC-3’

*PDGFRB*

PDGFRB-2F: 5’-CAAGCTGGGGCTCATTCTGCAGGAGC-3’
PDGFRB-2R: 5’-CTAAAGCTGAAGGGCAGGGCAGTGTG-3’
PDGFRB-2R2: 5’-CTGAAGGGCAGGGCAGTGTGCCTG-3’
PDGFRB-3F: 5’-CAAGGACCTGAGGGCTGTGCATACG-3’
PDGFRB-3R: 5’-CTTTTCTAGGATGGCTGCATTTCAC-3’
PDGFRB-4F: 5’-GATGGCAAATGACTTGCCACACAGC-3’
PDGFRB-4R: 5’-CTGTAAAGGGCTATTCCTCTGTGGAG-3’
PDGFRB-5F: 5’-CATCAGTCATCCTTTCCCTCTCTAG-3’
PDGFRB-5R: 5’-GAAATCAGCCTGCAAGCCAGATATC-3’
PDGFRB-6F: 5’-GATATCTGGCTTGCAGGCTGATTTC-3’
PDGFRB-6R: 5’-GCAACTCTCACCATCACTCTGCACC-3’
PDGFRB-7F: 5’-CAGGCTGGCCTCCTTTGGGATTCAG-3’
PDGFRB-7R: 5’-CTGGGCCTAGGTTTGTGGCTGAAAG-3’
PDGFRB-8F: 5’-GTTCCTCTTTATACCAGGAGGGTG-3’
PDGFRB-8R: 5’-CTAGAATCCATCTCCTGAGTTCCAG-3’
PDGFRB-9F: 5’-GTTCACCTGCAGTCTACAGCCCTC-3’
PDGFRB-9R: 5’-GAACGGGCGGGACTAGATAACCTTC-3’
PDGFRB-10F: 5’-CTTCCACCAGTTTCTCCTCAGTTTC-3’
PDGFRB-10R: 5’-CATGGGCACATTACCAATTAGGCAG-3’
PDGFRB-11F: 5’-GAGGGATCTATGATGCCAAAGATG-3’

PDGFRB-11R: 5’-GATCACGCAGCATTCAAGGAGGGCAG-3’
PDGFRB-12F: 5’-GTGTCCTAGACGGACGAACCTAATG-3’
PDGFRB-12R: 5’-CAAGACACCAGCCCTAGGTCTCATAG-3’
PDGFRB-13F2: 5’-GCAGCTGGGGGAGCGGTGCAGCTTC-3’
PDGFRB-13R: 5’-CTCTAGTGCCTGCAAATCAGCATCAG-3’
PDGFRB-14F: 5’-GCAGAAGAGTCAGAATAGGCTCCTG-3’
PDGFRB-14R: 5’-CAGCAGGAGTGTGCTGTTGTGCAAG-3’
PDGFRB-15F: 5’-CTAGCCGTCATGCCAAAGTGTCTC-3’
PDGFRB-15R: 5’-CTGCCCTGTCACAGCCTCAGCTTC-3’
PDGFRB-16F: 5’-GATGAGTGAGTGTGTGAGTGAGAG-3’
PDGFRB-16R: 5’-CAAGGCTGGGCATGTGAAGAGCATC-3’
PDGFRB-17F: 5’-CACCTGTCTTGGACATTCAGTCTC-3’
PDGFRB-17R: 5’-CTGGTGTGCTCTTGGAGGATGCTG-3’
PDGFRB-18F: 5’-GCACATGGGCAGTGTTGTATTTTC-3’
PDGFRB-18R: 5’-CACAGATTTCCTATGAGCTGCAGC-3’
PDGFRB-19F: 5’-CACAGGGAATGGGACGGAGAAGTG-3’
PDGFRB-19R: 5’-CCTGAACCAGGATCCCTGTATCAG-3’
PDGFRB-20F: 5’-CTTACCCATACCAGGGCCAGCATG-3’
PDGFRB-20R: 5’-CCAAGGCTTTCTAGATCTCTGAGC-3’
PDGFRB-21F: 5’-CCATGGCTCACCTTGTTCTGAGAG-3’
PDGFRB-21R: 5’-CTAAATGCCAGCCCATCACGCAGAG-3’
PDGFRB-22F: 5’-CTCAACCATGTGGCTTGGGCAAATC-3’
PDGFRB-22R: 5’-GTAACTTACCTCTGAGGCAAACCTG-3’
PDGFRB-23F: 5’-ACACCGAAGGCTCTTCATGACTGC-3’
PDGFRB-23R: 5’-CAGCTGATAAGGGCAGCCTGGCTG-3’

*TGFB1*

TGFB1-1F: 5’-CCCACCACACCAGCCCTGTTC-3’
TGFB1-1R: 5’-CTACCCGTGGCCCCGGCACTC-3’
TGFB1-2F: 5’-TCACCTCTGCCAAACCCCTGATC-3’
TGFB1-2R: 5’-CTTGGTCACAGCTCACCCTCTC-3’
TGFB1-3F: 5’-TGAAGGATTCAGTTAGTGTATGTG-3’
TGFB1-3R: 5’-AGAGGGGTCCTAGGCAAAGTGAC-3’
TGFB1-4F: 5’-GTGAGCTGCACTCTCAGACTG-3’
TGFB1-4R: 5’-CACACGTCACAACTGGGCATGG-3’
TGFB1-5F: 5’-GTGTGTGTGTATGTCCCCTATC-3’
TGFB1-5R: 5’-CTGGTCAGCAGATGGCAGTCATG-3’
TGFB1-6F: 5’-GCATGTGGCTTCTATGGTGGTAG-3’
TGFB1-6R: 5’-TCCTGGCTCCCCCCAAGCGCATC-3’

*FOXO1A*

FKHR-1AF: 5’- GTCCGCCCCCAGTGCTGCGTTCTC-3’
FKHR-1AR: 5’-CAAGCTCAGGTTGCTCATGAAGTC-3’
FKHR-1BF: 5’-GTCAGCGCCGACTTCATGAGCAAC-3’
FKHR-1BR: 5’-CAAACCTGCACAGCTGCGCCCTCG-3’
FKHR-2AF2: 5’-CTGTTCAGATGGAAATCTGTAGCAC-3’
FKHR-2AR: 5’-GAATGCACATCCCCTTCTCCAAG-3’
FKHR-2BF: 5’-GACTCTCACCCATTATGACCGAAC-3’
FKHR-2BR: 5’-GATTCATCATTTTGTTATGAGATG-3’
FKHR-2CF: 5’-GTCATGTCAACCTATGGCAGCCAG-3’
FKHR-2CR: 5’-CCATGGCAAGTTACTGTGTTCCTC-3’

*LMNA*

| | |
|---|---|
| LMNA-1F: | 5’-GACTCCGAGCAGTCTCTGTCCTTC-3’ |
| LMNA-1R: | 5’-CAGGCCCTCTCACTCCCTTCCTG-3’ |
| LMNA-2F: | 5’-GAGCCTGGCACTGTCTAGGCAC-3’ |
| LMNA-2R: | 5’-CCTAGGTAGAAGAGTGAGTGTAC-3’ |
| LMNA-3F: | 5’-CCTCTCAGCTTCCTTCCAGTTC-3’ |
| LMNA-3R: | 5’-CTAGGGCAAGGGACTCAGGAAG-3’ |
| LMNA-4F: | 5’-CTTGGCCTCCCAGGAACTAATTC-3’ |
| LMNA-4R: | 5’-CAGAAGGCATAGCCCAGCGTGG-3’ |
| LMNA-5F: | 5’-CAGTGATGCCCAACTCAGGCCTG-3’ |
| LMNA-5R: | 5’-TGGTTGTGGGGACACTTTTCATCC-3’ |
| LMNA-6F: | 5’-CGTCCCTCCTTCCCCATACTTAG-3’ |
| LMNA-6R: | 5’-GGTCTAGTCAAGGCCAGTTGC-3’ |
| LMNA-7F: | 5’-AGACGTCGGGGAGGTGCTGGCAG-3’ |
| LMNA-7R: | 5’-CCACATGCCATCCTTCTGTCTTG-3’ |
| LMNA-8+9F: | 5’-CTTTGAGCAAGATACACCCAAGAG-3’ |
| LMNA-8+9R: | 5’-CTGGCTCCGATGTTGGCCATCAG-3’ |
| LMNA-10F: | 5’-GTAGACATGCTGTACAACCCTTC-3’ |
| LMNA-10R: | 5’-CAGGCCAGCGAGTAAAGTTCC-3’ |
| LMNA-11F: | 5’-GGTTGGGCCTGAGTGGTCAGTC-3’ |
| LMNA-11R: | 5’-CCTCGTCCTACCCCTCGATGACC-3’ |
| LMNA-12F: | 5’-GGAGATGCTACCTCCCTTCTAGG-3’ |
| LMNA-12R: | 5’-TAAGGCAGATGTGGAGTTTCCTG-3’ |

# III. Results

In this project, a female patient initially diagnosed with Costello syndrome and carrying an apparently balanced chromosome translocation, t(1;22)(q25;q11) (Czeizel and Tímár, 1995), was studied. In order to delineate and define the breakpoints of the 1;22 translocation, Maróti and colleagues (2002) performed fluorescence *in situ* hybridization (FISH) analyses with YAC, PAC, and cosmid clones. The breakpoint on chromosome 1q25 was confirmed and mapped to a 109-kb region, whereas the breakpoint on chromosome 22 was refined to the region q13.1.

## 1. Characterization of the translocation breakpoint regions in 22q13.1 and 1q25

### 1.1 Delineation of the breakpoint in 22q13.1 by FISH

By FISH experiments, cosmid clone LL22NC03-10C3 was found to overlap the breakpoint on chromosome 22. Signals were obtained on wild-type chromosome 22 and on both derivative chromosomes 1 and 22 (Fig. 6). Analysis of the DNA sequence of chromosome 22 deposited at the NCBI database (Z81010.2, NT_011520.9) revealed that the gene encoding the platelet-derived growth factor beta *(PDGFB)* is located on the insert of the cosmid (Fig. 8).

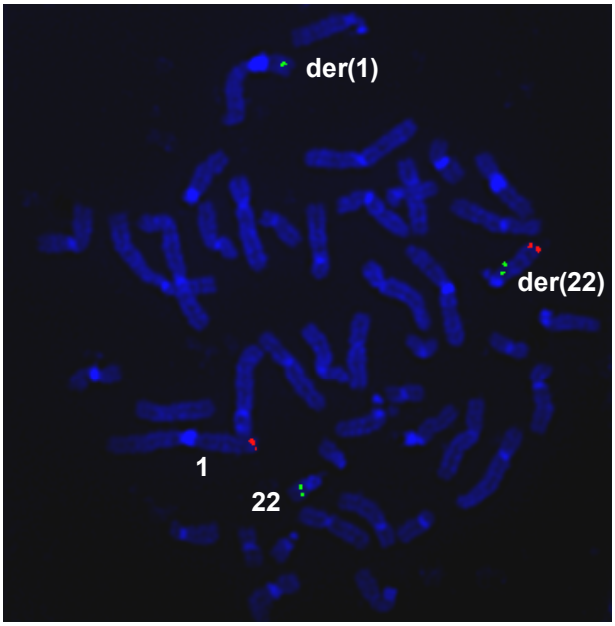


**Fig. 6: FISH with cosmid clone LL22NC03-10C3 on lymphocyte metaphase spreads of the translocation patient**

The probe is labeled by FITC (green). Cosmid LL22NC03-10C3 produced a signal on the wild-type chromosome 22 as well as on der(1) and der(22) indicating that this clone is spanning the breakpoint. A telomeric 1q DNA probe labeled by Texas red (red) was used to identify the end of the long arm of chromosome 1. Chromosomes are counter-stained with DAPI.

In order to define the translocation breakpoint more precisely, five *Sac*I and five *Hin*dIII restriction fragments of cosmid LL22NC03-10C3 were cloned in pBluescript-Cm (pMSU1-pMSU5) and pACYC184 (pMSU6-pMSU10), respectively. These ten restriction fragments covering the genomic sequence of the *PDGFB* gene were pooled and used as a probe in FISH experiments. Again, breakpoint overlapping signals were observed (Fig. 7) suggesting that the breakpoint is located in the *PDGFB* gene.

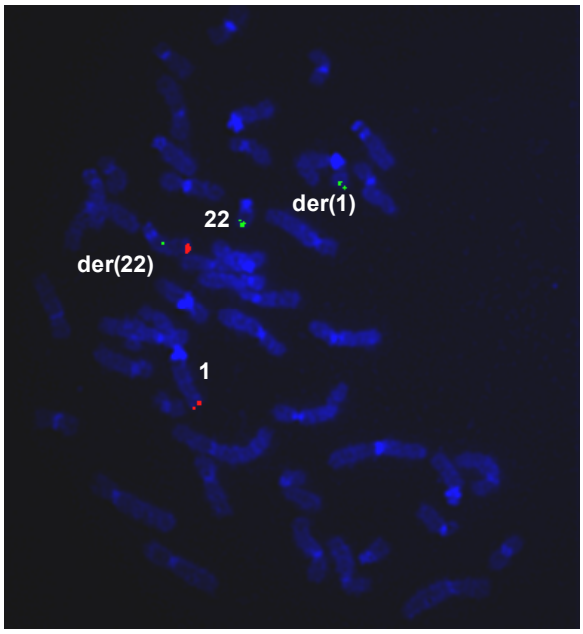


**Fig. 7: FISH with pooled *Hin*dIII and *Sac*I fragments on lymphocyte metaphase spreads of the translocation patient**

The probe is labeled by FITC (green). A signal was obtained on the wild-type chromosome 22 as well as on der(1) and der(22) indicating that the pooled fragments overlap the breakpoint. A telomeric 1q DNA probe labeled by Texas red (red) was used to identify the end of the long arm of chromosome 1. Chromosomes are counterstained with DAPI.

The signal on derivative chromosome 1 was stronger than the signal on derivative chromosome 22. Thus, it could be speculated that the translocation breakpoint lies closer to the 3' end of the *PDGFB* gene (Fig. 8).

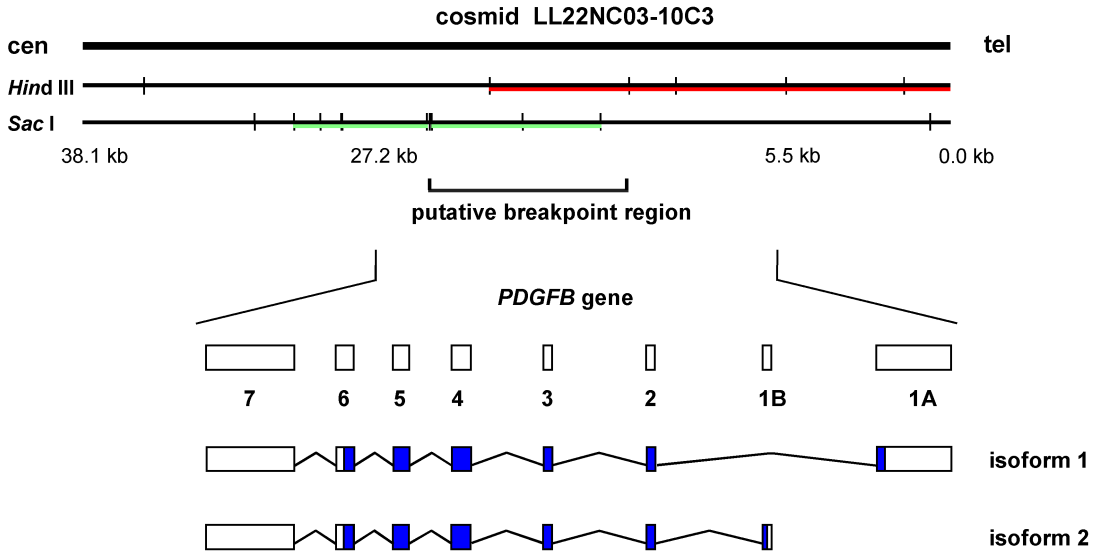


**Fig. 8: Schematic representation of the insert of cosmid LL22NC03-10C3 and localization of the *PDGFB* gene**

The upper line represents the insert of cosmid LL22NC03-10C3. On the middle line, vertical bars indicate *Hin*dIII sites. *Hin*dIII fragments shown in red were used in FISH experiments. On the lower line, vertical lines indicate *Sac*I sites. *Sac*I fragments shown in green were used in FISH experiments. In the insert, the exon-intron structure of *PDGFB* is shown schematically. Boxes represent exons; blue boxes indicate the coding region of *PDGFB* whereas white boxes represent untranslated regions. Alternative splicing of exon 1 (1A or 1B) gives rise to two isoforms of the protein.

## 1.2 Identification of the breakpoint in the *PDGFB* gene

To characterize the breakpoint in 22q13.1 at the molecular level, RT-PCR was performed using RNA isolated from peripheral blood of the patient and a control individual. Nested 3'RACE-PCR experiments on cDNA with forward primers located in *PDGFB* exon 3, 4, 5, or 6 in combination with a polyT primer yielded specific PCR products only in the translocation patient but not in the control (Fig. 9 and data not shown).

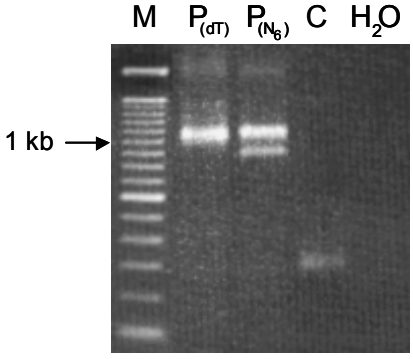


**Fig. 9: Amplification of putative aberrant *PDGFB* mRNAs by 3'RACE-PCR**

cDNA was reverse transcribed with oligo dT primer (dT) or random hexamers ($N_6$). By 3'RACE-PCR, various PCR products of ~1 kb were obtained with primers PDGFB3-2 and S-ag3'E in the translocation patient (P) but not in control (C). $H_2O$ was used as negative control. A 100-bp ladder (M) was used as DNA size marker. The arrow points to one band of the DNA marker, respective size is given.

The amplicons were cloned and inserts of 37 clones were sequenced. By database searches, four *PDGFB* fusion RNAs that contained different sequences from chromosome 1q24.3 (GenBank accession no. AL355520.8, PAC clone RP4-595C2) at their 3'-end were identified (Fig. 10). In the first fusion transcript (3 clones), the first 124 bp of the total 145 bp of *PDGFB* exon 5 were fused to a 589-bp region of clone RP4-595C2 (139.204-138.616 bp of sequence AL355520.8). At the junction site, an overlap of 6 bp (gcccgg) was present both in the *PDGFB* cDNA sequence and the sequence of clone RP4-595C2. The putative PDGFB protein encoded by this transcript lacks the last 7 amino acids encoded by exon 5 and all residues encoded by exon 6 of *PDGFB*. In addition, 11 unrelated amino acids are present at the carboxyl terminus of this PDGFB ligand. In the second fusion transcript (19 clones), exon 5 of *PDGFB* was spliced to two different regions of PAC clone RP4-595C2 (127.917-127.800 bp and 126.819-126.580 bp). These two different regions of RP4-595C2 seem to represent exons of a putative novel gene on chromosome 1q24.3 and were named exon B and exon C. The derived open reading frame predicts a protein that lacks the 41 amino acids encoded by exon 6 of *PDGFB* and, instead, contains 28 unrelated amino acids present at the C-terminal end of the protein that are encoded by the mRNA portion transcribed from chromosome 1. The third and fourth fusion transcripts (10 and 5 clones, respectively) consisted of the coding exons of the *PDGFB* gene including the natural TAG stop codon located in exon 6. However, adjacent sequences from the breakpoint region of chromosome 1q24.3 were different in the two transcripts. The sequence from 139.354-138.616 bp of PAC RP4-595C2 was present in the third transcript. In contrast, three different parts of RP4-595C2 (139.354-139.333 bp, 127.917-127.800 bp, and 126.819-126.580 bp) were present in the fourth mRNA and fused to *PDGFB* exon 6. These latter parts of RP4-595C2 seem to represent exons of a putative novel gene on chromosome 1q24.3 that were named exon A, exon B, and exon C. In both transcripts, an overlap of 4 bp (cagg) was identified at the junction sites. Although untranslated exon 7 of *PDGFB* is missing in the two latter mRNAs, which may affect mRNA stability, both transcripts might give rise to wild-type PDGFB protein.

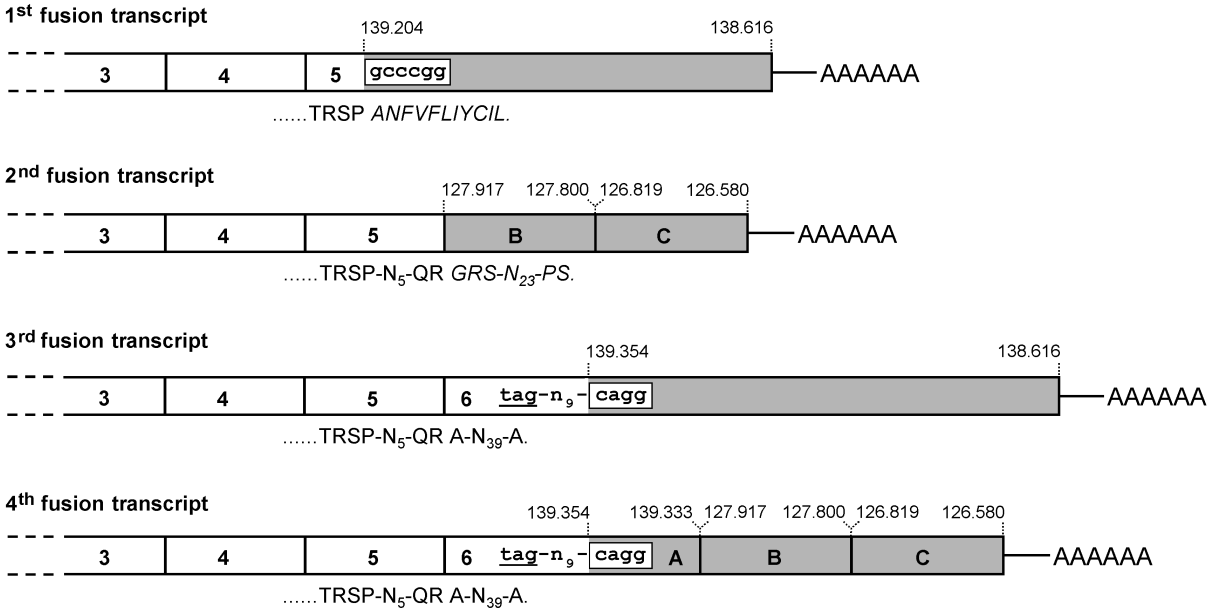


**Fig. 10: Schematic representation of the four fusion transcripts identified in the translocation patient**

White boxes that are numbered schematically indicate various exons of *PDGFB* whereas grey boxes indicate sequence parts from the breakpoint region on chromosome 1q24.3. Short sequences that overlap at the junction sites are boxed. The stop codon of *PDGFB* is underlined. Numbers above the grey boxes indicate the positions in the sequence of clone RP4-595C2 (GenBank accession no. AL355520.8). Amino acid residues (single letter code) of the partial open reading frame derived from the coding region of each fusion transcript are given below each transcript. PDGFB-unrelated residues are in italics.

To confirm the identity of the fusion RNAs, specific RT-PCRs using RNA isolated from peripheral blood of the patient and controls were performed. cDNA was reverse transcribed with oligo dT primer or random hexamers. Forward primers located in *PDGFB* exon 3, 4 or 5 were used in combination with a primer located at position 127.809-127.833 bp in sequence AL355520.8 (in exon B of the putative novel gene on chromosome 1q24.3). Various PCR products (Fig. 11) that were obtained only for the patient, were cloned and sequenced. Sequence analysis revealed that the amplicons of 549 bp, 460 bp, and 254 bp, obtained for three different primer combinations, corresponded to the second fusion transcript. A second band was only obtained in the patient when cDNA was used that had been reverse transcribed with hexanucleotides (Fig. 11). By sequence analysis of this fragment it was shown that it represents the fourth fusion transcript.

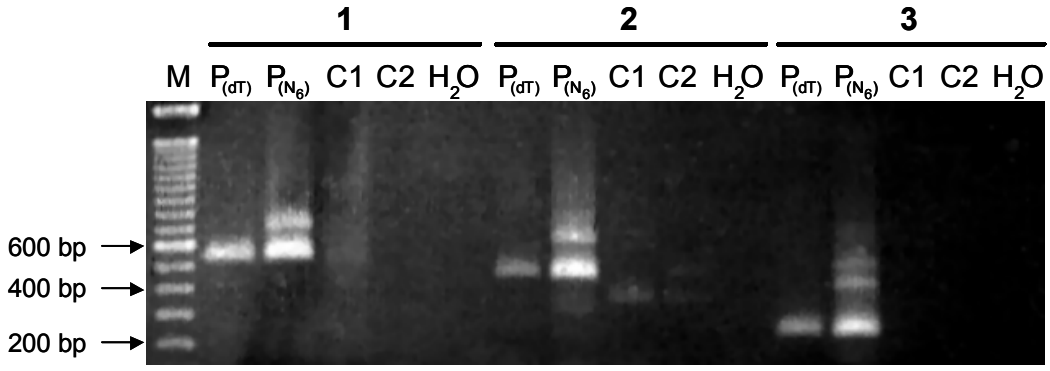


**Fig. 11: Amplification of the second and fourth fusion transcripts by specific RT-PCRs**

cDNA was reverse transcribed with oligo dT primer (dT) or random hexamers ($N_6$). Various PCR products were obtained with primer combinations PDGFB3-1 and AL355520-12 **(1)**, PDGFB4-1 and AL355520-12 **(2)**, and PDGFB5-1 and AL355520-12 **(3)** in the translocation patient (P) but not in controls (C1, C2). $H_2O$ was used as negative control. As DNA size marker a 100-bp ladder (M) was used. The arrows point to three bands of the DNA marker, respective sizes are given.

The identity of the third fusion transcript was confirmed by another RT-PCR. A forward primer located in *PDGFB* exon 5 was used in combination with a primer located at position 138.341-138.364 bp in sequence AL355520.8. Two PCR products of ~800 bp and ~1.3 kb were obtained from the patient's cDNA (Fig. 12) which were cloned and sequenced. Sequence analysis revealed that the ~1.3-kb amplicon corresponds to the third fusion transcript, whereas the 800-bp product was unspecific.

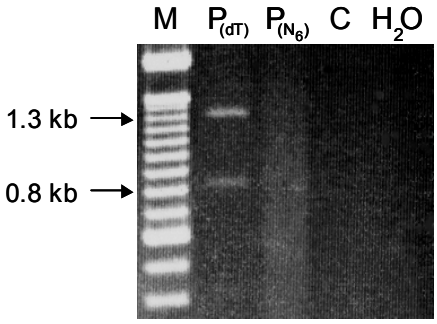


**Fig. 12: Amplification of the third fusion transcript by a specific RT-PCR**

cDNA was reverse transcribed with oligo dT primer (dT) or random hexamers ($N_6$). Primer combination PDGFB5-2 and AL355520-6 was used that amplified ~800-bp and ~1.3-kb fragments in the translocation patient (P) but not in control (C). $H_2O$ was used as negative control. A 100-bp ladder (M) was used as DNA size marker. The arrows point to two bands of the DNA marker, respective sizes are given.

## 1.3 Confirmation and refinement of the breakpoint on chromosome 1q24.3

To confirm that the breakpoint on chromosome 1 is located on the insert of PAC RP4-595C2, FISH experiments on metaphase spreads of the patient were performed. Signals were obtained on wild-type chromosome 1 and on both derivative chromosomes 22 and 1 indicating that this clone indeed spans the breakpoint (Fig. 13).

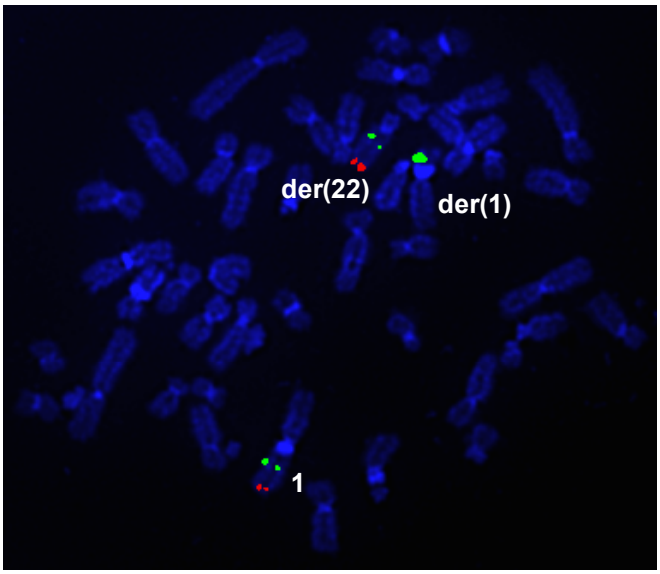


**Fig. 13: FISH with the breakpoint spanning PAC clone RP4-595C2 on lymphocyte metaphase spreads of the translocation patient**

The probe is labeled by FITC (green). PAC RP4-595C2 produced a signal on the wild-type chromosome 1 as well as on der(22) and der(1), indicating that this clone is spanning the breakpoint. A telomeric 1q DNA probe labeled by Texas red (red) was used to identify the end of the long arm of chromosome 1. Chromosomes are counterstained with DAPI.

Previously, the breakpoint was shown to be located in 1q25 (Maróti et al., 2002). However, by database analysis, PAC clone RP4-595C2 was found to map to 1q24.3, thereby refining the breakpoint to this chromosomal subband.

## 1.4 Identification and characterization of both translocation breakpoints on genomic DNA

The breakpoints of the translocation patient were also characterized at the genomic DNA level. For derivative chromosome 1, a primer located in *PDGFB* exon 5 was combined with a primer located at position 138.341-138.364 bp in sequence AL355520.8 to amplify genomic DNA of the patient and controls. Two different PCR products of ~3.3 kb and ~1.8 kb were obtained for the patient but not for the controls (Fig. 14). The amplicons were cloned and the inserts were sequenced.

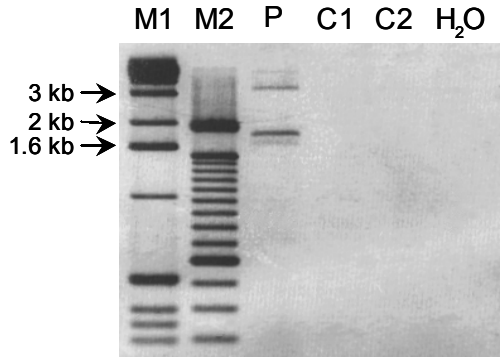


**Fig. 14: Amplification of junction fragments from the derivative chromosome 1 by PCR**

Primer pair PDGFB5-2 and AL355520-6 was used on genomic DNA of the patient (P). Two fragments of ~3.3 kb and ~1.8 kb were amplified that were not obtained in controls (C1, C2). $H_2O$ was used as negative control. 1-kb ladder (M1) and 100-bp ladder (M2) were used as DNA size markers. The arrows point to three bands of the DNA marker, respective sizes are given.

In the 3.3-kb junction fragment [der(1A) in Fig. 15], the breakpoint in *PDGFB* is located within 10-13 bps following the stop codon in exon 6 (at position 24.838 bp in the genomic sequence with GenBank accession no. Z81010.2). The breakpoint on chromosome 1 is in an *Alu*Sg repeat at position 139.354 bp of sequence AL355520.8. The sequence of this genomic junction fragment corresponds to that of the third fusion mRNA described above. At the junction of the translocation, an overlap of 4 bp (cagg) was found. Additionally, an internal deletion of 2.2 kb in intron 5 of *PDGFB* (Fig. 15) was identified. The breakpoints of this deletion could not be determined precisely since the sequence of the three cloned fragments varied at the junction sites. One deletion breakpoint is located in an *Alu* repeat (*Alu*Jb) from 21.182-21.248 bp, whereas the other one is in a 67-bp region of an *Alu*Sx repeat at position 23.410-23.476 bp in sequence Z81010.2. In the 1.8-kb junction fragment [der(1B) in Fig. 15], the breakpoint was in the *Alu*Jb repeat at position 21.231 bp of sequence Z81010.2 (in intron 5 of *PDGFB*) and at position 139.247 bp in sequence AL355520.8. Again, a 6-bp (ctcagc) overlap is present at the junction site. It is worth mentioning that the translocation breakpoint in intron 5 of *PDGFB* lies in an *Alu* repeat which also seems to be involved in the internal deletion of intron 5 (position 21.182-21.248 bp). Thus, the latter derivative chromosome 1 carries a deletion of 109 bp of chromosome 1 material and 3607 bp of chromosome 22 (including the previously mentioned 2.2-kb deletion in *PDGFB* intron 5) (Fig. 15).

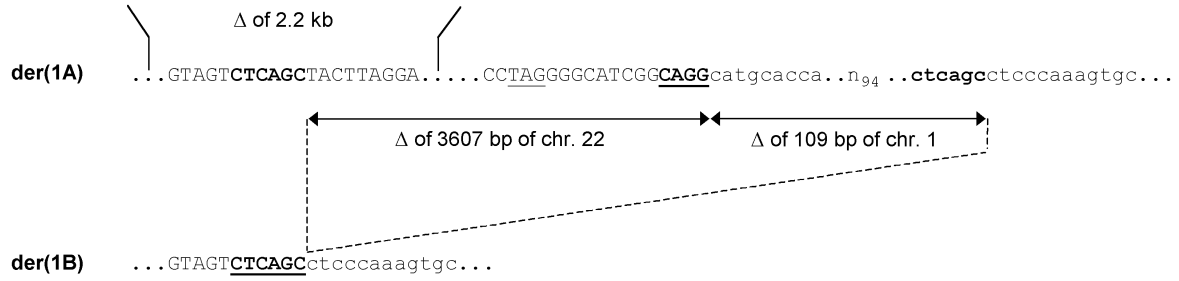


**Fig. 15: DNA sequences of the junction fragments from the two derivative chromosomes 1 [der(1A) and der(1B)]**

Chromosome 22-derived sequences are shown in uppercase letters, and chromosome 1-derived sequences in lowercase letters. Overlapping breakpoint sequences at both derivative chromosomes 1A and 1B are shown in bold and underlined. Regular stop codon of *PDGFB* is underlined. The internal deletion of 2.2 kb identified in intron 5 of der(1A) is shown schematically by two brackets. Der(1B) differs from der(1A) by the presence of material deleted both from chromosome 1 and 22 that is indicated by two arrows.

Taken together, the data suggest that the translocation patient is a mosaic of two different derivative chromosomes 1 [der(1A) and der(1B)] that can only be distinguished at the molecular level. Since only DNA isolated from peripheral blood of the patient is available, it is not known whether the patient is also mosaic in other tissues, e.g. fibroblasts.

For amplification of the breakpoint region on the derivative chromosome 22, a primer located at position 140.243-140.218 bp in sequence AL355520.8 was combined with a primer located in intron 6 of *PDGFB*. A ~1.2-kb PCR product was amplified only on the DNA of the translocation patient (Fig. 16) that was cloned and sequenced.

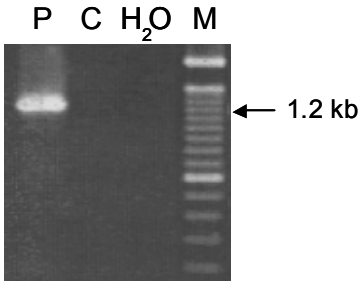


**Fig. 16: Amplification of a junction fragment of the derivative chromosome 22**

Primer combination AL355520-8 and PDGFBin6-1 amplified a ~1.2-kb junction fragment in the patient (P). This amplicon was not obtained in the control (C). $H_2O$ was used as negative control. As DNA size marker a 100-bp ladder (M) was used. The arrow marks one band of the DNA marker and respective size is given.

The breakpoint in the *PDGFB* gene was located in the untranslated region of exon 6 (at position 24.835 bp of Z81010.2), whereas the breakpoint on chromosome 1 was at position 139.351 bp in sequence AL355520.8. A 4-bp overlap (cagg) was identified at the site of junction. An alignment between the breakpoint sequences of der(1A) and der(22) showed that no additional rearrangement occurred (Fig. 17). However, a subsequent rearrangement of derivative chromosome 1 led to a deletion of both chromosome 1 and chromosome 22 material.

| | |
|---|---|
| **WT chr. 22** | CCTAGGGGCATCGG**CAGG**AGAGTGTGTGGGCAG |
| **der(1A)** | CCTAGGGGCATCGG**CAGG**catgcaccaccacgc |
| **der(22)** | tgtagctgggacta**CAGG**AGAGTGTGTGGGCAG |
| **WT chr. 1** | tgtagctgggacta**cagg**catgcaccaccacgc |

**Fig. 17: Alignment of chromosome 22, der(1A), der(22), and chromosome 1 sequences at the translocation breakpoints**

Chromosome 22-derived sequences are shown in uppercase letters, and chromosome 1-derived sequences in lowercase letters. Overlapping sequence at the breakpoints is shown in bold and underlined. The stop codon of *PDGFB* is underlined on the chromosome 22-derived sequences.

## 1.5 Database searches for the identification of putative novel genes in 1q24.3

As described in III.1.2, the breakpoint region on chromosome 1 was localized within the sequence 127.917-139.354 on the insert of clone RP4-595C2 (total insert sequence 157.575 bp). BLAST analysis with the genomic sequence of clone RP4-595C2 did not reveal any homologies to EST (expressed sequence tag) sequences in the breakpoint region of chromosome 1 suggesting that no gene is present in this region. By additional database searches, no known gene or EST sequence could be identified in the 1q24.3 breakpoint region (Fig. 18) confirming the results of the BLAST analysis. Nevertheless, two genes are located on the insert of clone RP4-595C2 (AL355520.8), the angiopoietin-like 1 (*ANGPTL1*) gene and the 3' end of the gene encoding the Ral-A exchange factor RalGPS2 (*FLJ10244*) (Fig. 18).

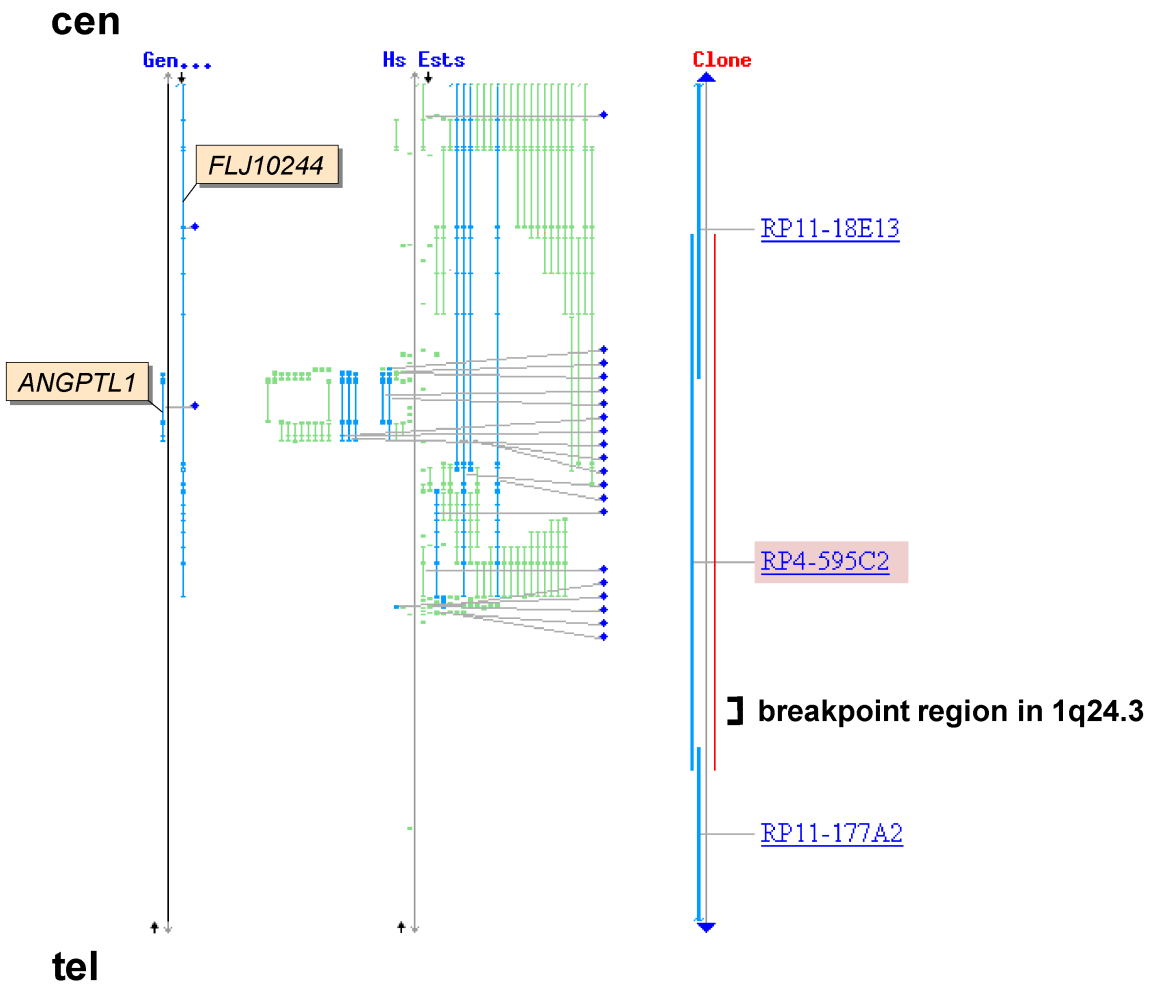


**Fig. 18: Localization of two known genes and numerous EST sequences on the insert of clone RP4-595C2**

This is a segment cut from Map View at NCBI. On the right, the insert of clone RP4-595C2 (GenBank accession no. AL355520.8) is shown as a vertical blue line as well as a red line. The breakpoint region identified in 1q24.3 is indicated and marked by a vertical black line. On the left, blue lines indicate the genes *ANGPTL1* and *FLJ10244*. The *ANGPTL1* gene is orientated from telomere to centromere and the *FLJ10244* gene from centromere to telomere. In the middle, blue and green lines indicate EST sequences.

The genomic sequence of clone RP4-595C2 was also analysed by the gene prediction programs GENESCAN and GrailEXP. Only one of the eight genes identified by GENESCAN was located close to the breakpoint region in 1q24.3, in telomere to centromere orientation (Fig. 19B). Four other exons were also predicted by the GrailEXP program (Fig. 19C). However, none of the computer predicted exons was corresponding to one of the three exons of the putative novel gene identified by 3'RACE-PCR experiments (Fig. 19A).

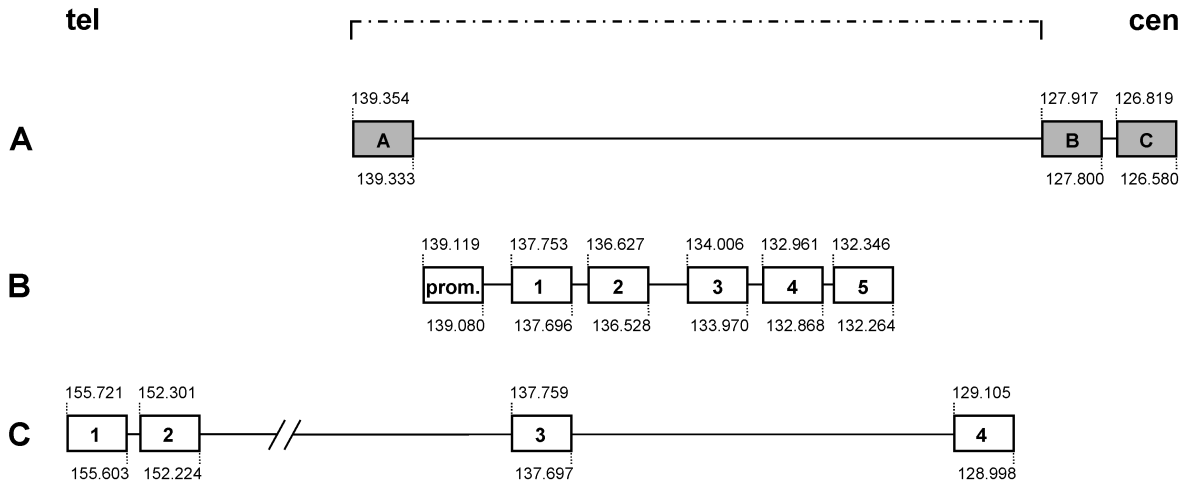


**Fig. 19: Schematic representation of the exon-intron structure of three putative genes in the 1q24.3 breakpoint region**

**(A)** Putative gene identified by 3'RACE-PCR. Grey boxes indicate exons A, B, and C. Putative gene predicted by GENESCAN **(B)** or GrailEXP **(C)**. White boxes that are numbered indicate various exons of the respective gene. Numbers above and below the boxes indicate the positions in the sequence of clone RP4-595C2 (GenBank accession no. AL355520.8). The breakpoint region is marked by a dashed line and the orientation of genes from telomere to centromere is given.

## 1.6 Characterization of a novel gene in 1q24.3 by 5'RACE- and RT-PCR

By 3'RACE-PCR experiments previously described (III.1.2), a putative gene consisting of exons A-C was identified in the breakpoint region on chromosome 1q24.3. First, expression of this putative gene was examined by RT-PCR and revealed that the gene is expressed strongly in human testis and brain (Fig. 20 and data not shown).

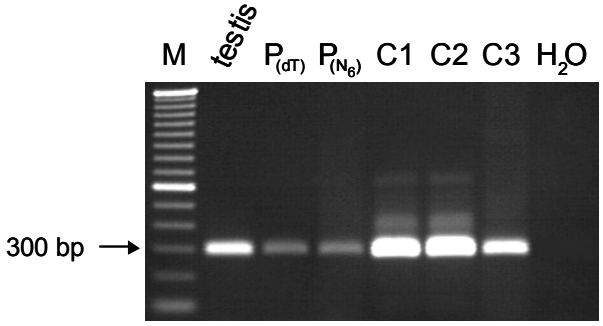


**Fig. 20: RT-PCR analysis of the putative novel gene in 1q24.3**

cDNA of the translocation patient was reverse transcribed with oligo dT primer (dT) or random hexamers ($N_6$). Primer combination AL355520-14 and AL355520-17 was used to amplify a 297-bp product from human testis cDNA (testis), cDNA of the translocation patient (P) and of a control person (C3). As positive controls plasmid pMSU62 (C1) and pMSU49 (C2) containing the second fusion transcript were used. $H_2O$ was used as negative control. A 100-bp ladder (M) was used as DNA size marker. The arrow marks one band of the DNA marker and respective size is given.

In order to characterize the gene and to extend the cDNA sequence in 5' direction, 5'RACE-PCRs on GeneRacer™ cDNA obtained from human testis RNA were carried out. Therefore reverse primers located in exon B were combined with GeneRacer 5' primers. Various PCR products were obtained and cloned (Fig. 21 and data not shown).

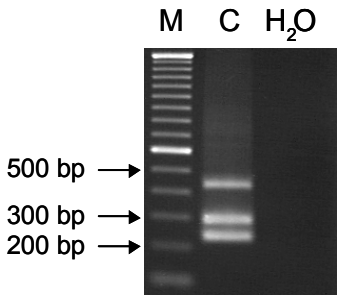


**Fig. 21: 5'RACE-PCR on testis GeneRacer™ cDNA with reverse primers located in exon B**

Various PCR products were obtained with primers AL355520-13 and GeneRacer™ 5'nested primer on human testis cDNA (C). $H_2O$ was used as negative control. As DNA size marker a 100-bp ladder (M) was used. The arrows mark three bands of the DNA marker; respective sizes are given.

DNA sequence analysis of 38 inserts cloned from different 5'RACE experiments revealed the existence of six different splice variants containing various exon combinations. For five of the transcript variants, an open reading frame was identified (Fig. 22). However, no ATG start codon or Kozak consensus sequence (GCC(**A/G**)**CC**ATG**G**; Kozak, 1996) was found.

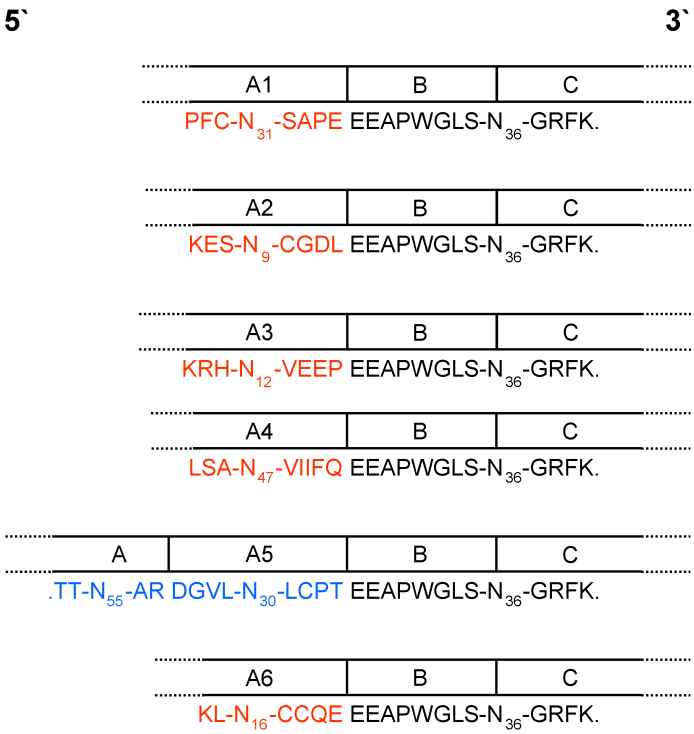


**Fig. 22: Schematic representation of six splice variants of the putative novel transcript**

White boxes containing letters indicate various exons of the putative novel gene. Amino acid residues of the partial open reading frame of each splice variant are given below. Different residues encoded by newly identified exons are shown in red.

The identity of some newly identified exons of the putative gene located in the breakpoint region on chromosome 1 was confirmed by RT-PCR. Therefore, various amplifications were performed with exon-specific primers on human testis and brain cDNAs (data not shown). Specific products were obtained that were cloned and sequenced. The splice variants containing exons A1+B, A4+B, A+A5+B, A6+B were confirmed; a new splice variant, A6+A2+B that does not contain an open reading frame was identified. Finally, it is of interest to mention that the majority of the exons identified are located in repetitive DNA regions on chromosome 1, like *Alu* or L1 elements, suggesting that this gene might represent a pseudogene. Due to this observation and the fact that no EST sequence corresponds to the cDNA sequences obtained, I did not proceed to further characterize this gene/ pseudogene.

## 2. Expression analysis of wild-type and mutant PDGFB proteins

Exon 6 of *PDGFB* encodes a stretch of basic amino acids, the retention motif, that mediates interaction of PDGFB with components of the extracellular matrix (ECM) (LaRochelle et al., 1991; Östman et al., 1991; Raines and Ross, 1992). After maturation and cleavage of the C-terminal retention sequence, the PDGFB molecule becomes diffusible. Thus, PDGFB ligands that lack the COOH-terminal retention motif may not attach properly to the extracellular matrix.

Of the four fusion transcripts identified in the translocation patient (III.1.2), two contain all *PDGFB* coding exons whereas the other two lack exon 6. In one of these latter mRNAs, only the first 124 bp of exon 5 were detected. The existence of fusion transcripts in the patient leaves the possibility open that PDGFB proteins translated from these mRNAs might show differences in conformation and/or function compared to wild-type protein.

### 2.1 Generation of PDGFB-EGFP/DsRed2 fusion constructs

To analyse the subcellular localization of wild-type and mutant PDGFB proteins, the open reading frame of the gene encoding enhanced green fluorescent protein (EGFP; 729 bp) was inserted in frame in exon 4 (after position c.273) or exon 5 (after position c.540) of the *PDGFB* wild-type coding sequence and also at the corresponding position in the first and second fusion transcript. There was no option to add EGFP at the N- or C-terminus of PDGFB since exon 1 encodes a signal peptide, exons 2 and 3 encode the precursor sequence that is removed during processing, and exon 6 encodes a COOH-terminal sequence that is also

cleaved off (Heldin and Westermark, 1999). Only *PDGFB* exons 4 and 5 encode the mature protein and therefore EGFP was inserted either in exon 4 or in exon 5. Various PCR amplicons were generated comprising the 5'- or the 3'-end coding region of *PDGFB* wild-type or that of the two fusion transcripts as well as the coding region of the *EGFP* gene. PCR products comprising the 5'-end of *PDGFB* contain a stretch of 20 bp at their 3'-end that is complementary to the beginning of the *EGFP* coding region. The amplicons comprising the 3'-end of *PDGFB* begin with 20 bp that are complementary to the end of the *EGFP* coding region. The coding region of *EGFP* without ATG start and TAG stop codon was amplified. To set up a megaprime PCR reaction, a PCR product comprising the 5'-end of *PDGFB*, an amplicon containing the *EGFP* coding region, and a product comprising the 3'-end of wild-type *PDGFB* or the fusion transcripts were combined. Primers PDGFB-NotI and PDGFB-EcoRI were added to amplify wild-type *PDGFB* containing the coding region of *EGFP* inserted in exon 4 or exon 5 (Fig. 23). Similar megaprime PCRs were performed for amplification of the fusion transcripts. The megaprime PCR products were purified, restricted with *Not*I and *Eco*RI, and cloned into the eukaryotic expression vector pMT2SM⁻.

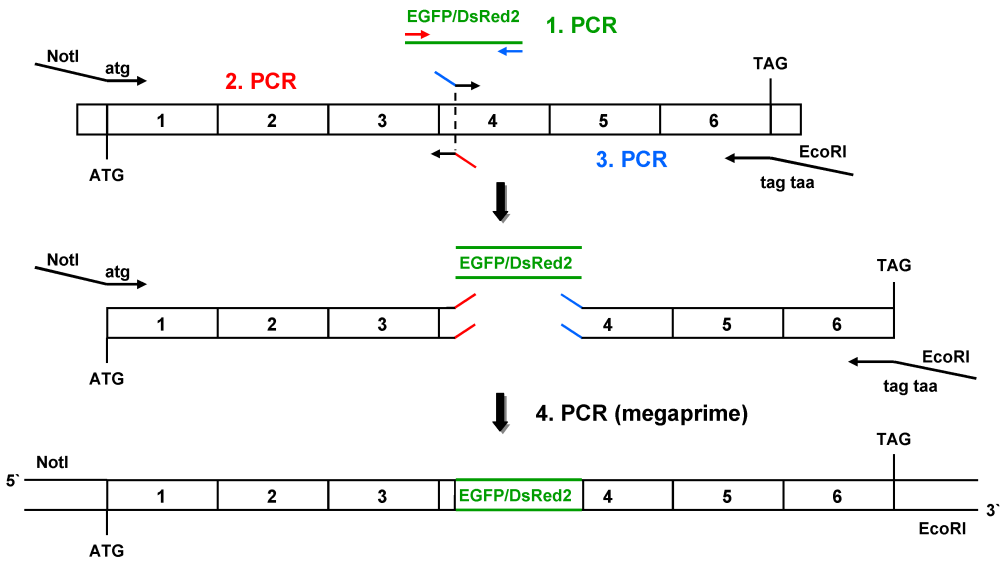


**Fig. 23: Scheme of the PCR reactions required for in frame insertion of *EGFP* or *DsRed2* in exon 4 of wild-type *PDGFB***

White boxes that are numbered indicate various exons of wild-type *PDGFB*. The start and stop codons of *PDGFB* are shown by vertical lines. The position in *PDGFB* exon 4 at which *EGFP* or *DsRed2* should be inserted is marked by a dashed line. Coding sequence of *EGFP* or *DsRed2* is shown schematically by a green line (single strand) or two green lines (double strand). Arrows indicate primers used for various PCRs.

The same approach was used to insert the open reading frame of the red fluorescent protein DsRed2 (672 bp) in frame in exon 4 (after position c.273) and exon 5 (after position c.540) of the *PDGFB* wild-type coding sequence and also at the corresponding position in the two fusion transcripts (Fig. 23). All constructs obtained were sequenced for integrity. Two different fluorescent proteins, EGFP and DsRed2, were used simultaneously to exclude possible unspecific localization of the generated fusion proteins in the cell. Similar subcellular localization pattern for EGFP and DsRed2 fusion proteins was expected.

## 2.2 Subcellular localization of PDGFB-EGFP fusion proteins

To study the subcellular localization of wild-type and mutant PDGFB proteins, the EGFP and DsRed2 fusion constructs for wild-type as well as for mutant *PBGFB* cDNAs were used. Expression of wild-type PDGFB fused to EGFP in transiently transfected COS-7 cells showed that PDGFB was present at the cell-plate interface suggesting extracellular matrix localization. To confirm matrix localization of PDGFB, endogenous laminin, a known extracellular matrix protein, was simultaneously detected (data not shown). Both wild-type PDGFB-EGFP fusion protein variants (*EGFP* inserted in exon 4 and exon 5 of *PDGFB*) seem to be present in a well organized network-like structure in the ECM (Fig. 24A-B and G-H). Mutant PDGFB proteins fused to EGFP also localized at the cell-plate interface in transiently transfected COS-7 cells. However, PDGFB mutant proteins lacking the C-terminal retention motif formed large aggregates in the ECM and were not dispersed in the network-like structure seen for the wild-type fusion proteins (Fig. 24C-F and I-J).

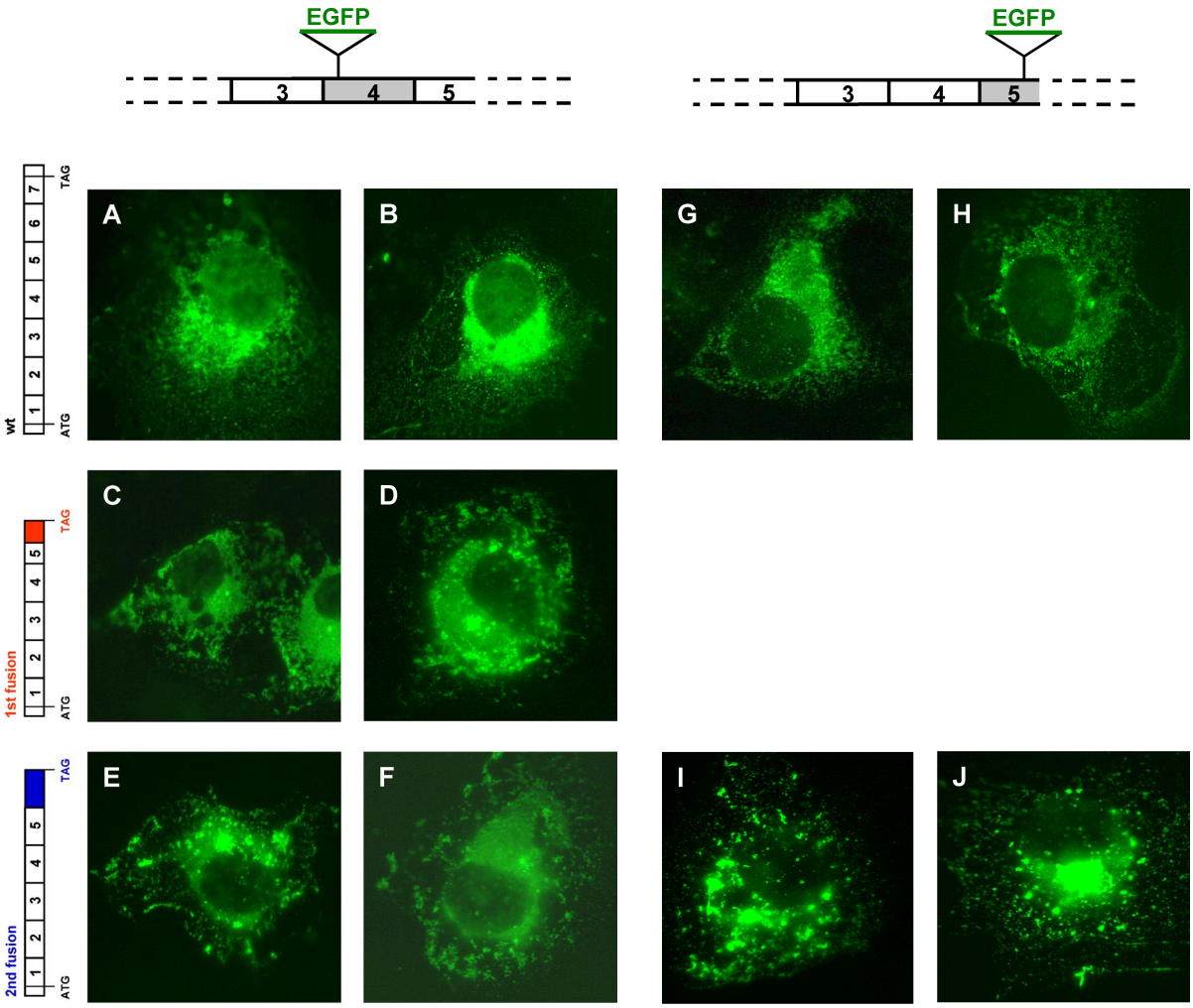


**Fig. 24: Subcellular localization of PDGFB proteins encoded by wild-type and various fusion transcripts**

COS-7 cells were transiently transfected with *PDGFB-EGFP* expression plasmids, fixed, and analysed by fluorescence microscopy. Two representative COS-7 cells were photographed from each transient transfection. **(A, B)** Wild-type PDGFB protein with insertion of *EGFP* in exon 4 of *PDGFB*. **(C, D)** PDGFB protein encoded by the first fusion transcript with insertion of *EGFP* in exon 4 of *PDGFB*. **(E, F)** PDGFB protein encoded by the second fusion transcript with insertion of *EGFP* in exon 4 of *PDGFB*. **(G, H)** Wild-type PDGFB protein with insertion of *EGFP* in exon 5 of *PDGFB*. **(I, J)** PDGFB protein encoded by the second fusion transcript with insertion of *EGFP* in exon 5 of *PDGFB*.

The construct containing the first fusion transcript with insertion of *EGFP* in exon 5 of *PDGFB* showed a very low transfection efficiency in COS-7 cells. The mutant PDGFB protein encoded by this construct seem to accumulate in the cell and formed some kind of aggregates (Fig. 25).

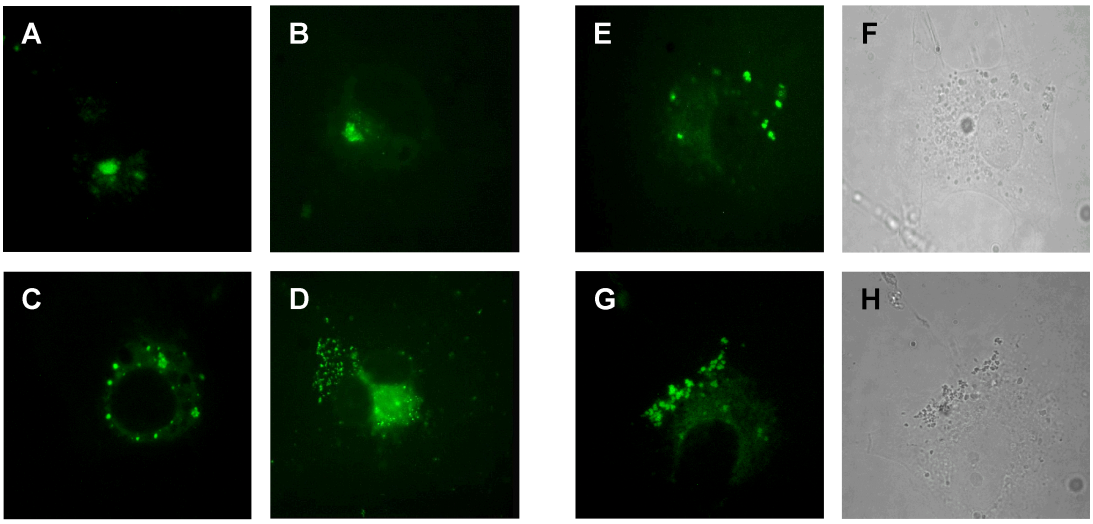


**Fig. 25: Subcellular localization of the PDGFB protein encoded by the first fusion transcript with insertion of *EGFP* in exon 5 of *PDGFB***

COS-7 cells were transiently transfected with the *PDGFB-EGFP* expression plasmid, fixed, and analysed by fluorescence microscopy. Various COS-7 cells from transient transfections were photographed. **(A, B)** The PDGFB protein is present in a large aggregate in the cell. **(C, D)** Localization of the PDGFB protein in small aggregates in the cell. **(E, G)** The PDGFB protein is located in small aggregates that correspond to dots visible in the bright field **(F, H)**.

The pattern detected most likely represents unspecific subcellular localization of the mutant PDGFB protein encoded by the first fusion transcript. To exclude a mutation in the promoter region of the expression vector, the SV40 promoter was sequenced. No differences were found by comparison of the sequences of the original vector and the recombinant plasmid (data not shown).

## 2.3 Expression of PDGFB-EGFP fusion proteins in cell lysates

As described in III.2.2, expression of the mutant PDGFB-EGFP protein encoded by the first fusion transcript showed no specific localization in the cell (Fig. 25). In order to investigate the expression of this mutant PDGFB protein in COS-7 cells, western blot analysis was performed. COS-7 cells were transiently transfected with wild-type and two mutant constructs with insertion of *EGFP* in exon 5 of *PDGFB*. Whole cell lysates were prepared that contained the total cell lysate, whereas cell debris was removed by centrifugation to yield the cytosolic fraction. Western blot analysis was performed and proteins were detected with an anti-EGFP antibody. A comparable pattern of expression of all three PDGFB-EGFP proteins in both types of cell lysates was detected (Fig. 26).

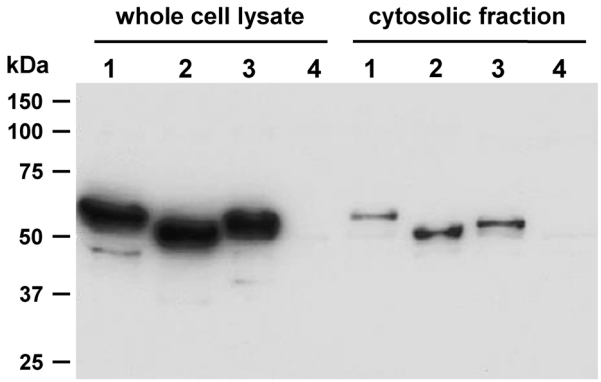


**Fig. 26: Western blot detection of PDGFB-EGFP fusion proteins in lysates from COS-7 cells**

COS-7 cells were transiently transfected with three different *PDGFB-EGFP* expression plasmids (*EGFP* inserted in exon 5 of *PDGFB*). Cells were lysed and aliquots of whole cell lysates and cytosolic fractions were loaded on SDS-PAGE and transferred to a PVDF membrane. PDGFB-EGFP fusion proteins were detected with an anti-EGFP antibody. Sizes of the PDGFB-EGFP fusion proteins were predicted by the Peptide Mass (ExPASy) program. **(1)** Wild-type PDGFB-EGFP protein, calculated molecular weight of the fusion protein is 54.7 kDa. **(2)** PDGFB protein encoded by the first fusion transcript, calculated molecular weight of the fusion protein is 50.5 kDa. **(3)** PDGFB protein encoded by the second fusion transcript, calculated molecular weight of the fusion protein is 53.0 kDa. **(4)** Empty vector pMT2SM$^-$. Six bands of the protein marker used with respective sizes are shown.

Although I was not able to detected a specific subcellular localization of the protein encoded by the first fusion transcript with insertion of *EGFP* in exon 5 of *PDGFB*, western blot analysis showed that this mutant PDGFB protein is expressed at the same level compared to wild-type and the other mutant PDGFB protein.

## 2.4 Subcellular localization of PDGFB-DsRed2 fusion proteins

To study subcellular localization of wild-type PDGFB-DsRed2 fusion proteins, corresponding constructs with insertion in exon 4 or exon 5 were transiently transfected in CHO-K1 cells. Analysis of living cells by fluorescence microscopy revealed that the fusion proteins were present in artificial aggregates in the cell (Fig. 27).

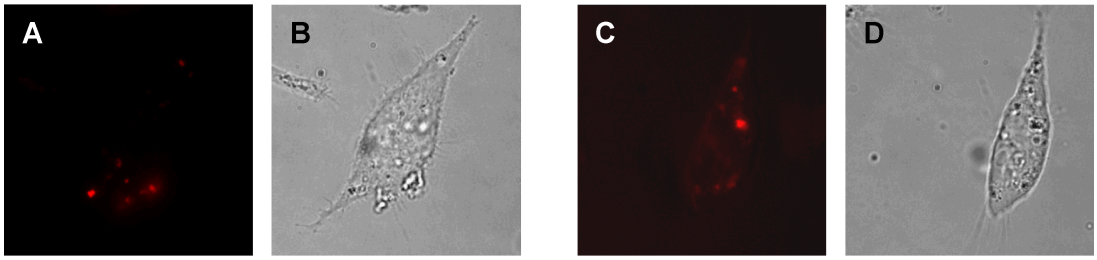


**Fig. 27: Subcellular localization of the PDGFB-DsRed2 wild-type proteins**

CHO-K1 cells were transiently transfected with *PDGFB-DsRed2* expression plasmids, living cells were analysed by fluorescence microscopy. Representative CHO-K1 cells were photographed. **(A)** Wild-type PDGFB protein with insertion of *EGFP* in exon 4 of *PDGFB*. **(C)** Wild-type PDGFB protein with insertion of *EGFP* in exon 5 of *PDGFB*. The same cells were shown in bright field **(B, D)**.

It seems that the DsRed2 fusion proteins are not suitable for subcellular localization analysis. Thus, the six constructs containing insertion of *DsRed2* in the open reading frame of wild-type and mutant *PDGFB* were not used for further studies.

## 3. Mutation screening of genes of the *PDGF/R* family in patients with Costello syndrome

The platelet-derived growth factor beta *(PDGFB)* gene was found to be disrupted in the patient with the 1;22 translocation and presumed Costello syndrome. The considered pattern of inheritance for CS is autosomal dominant and thus, disruption of one *PDGFB* allele by the translocation could result in Costello phenotype in this patient. Therefore, the *PDGFB* gene was good candidate gene for Costello syndrome. We decided to perform mutation screening of the gene in 18 patients with Costello syndrome and normal karyotype. The mutation analysis was done for 7 exons of *PDGFB* that were amplified using genomic DNA from each patient as template. Primers were designed to cover the coding region and adjacent intronic sequences at both sides of the coding region (minimum 40 bp at each side). PCR products for the exons of *PDGFB* were directly sequenced. No pathogenic mutation was identified. Only seven sequence variants were detected, both in introns and the coding regions of *PDGFB* (Tab. 5 and 6).

PDGFB belongs to a family of paracrine growth factors, including PDGFA, PDGFC, and PDGFD, that exert their effects on target cells by activating two structurally related protein tyrosine kinase receptors, α and β encoded by *PDGFRA* and *PDGFRB*. Since no pathogenic mutation was found in *PDGFB* in sporadic Costello patients, the other ligands of the PDGF family as well as the two receptors have been considered candidate proteins/genes for

Costello syndrome. Mutation screening was done for 6 exons of *PDGFA*, 6 exons of *PDGFC*, 7 exons of *PDGFD*, 22 exons of *PDGFRA* and 22 exons of *PDGFRB* that were amplified using genomic DNA from 18 Costello patients as template. PCR products for the exons of *PDGFA*, *PDGFC*, and *PDGFD* were directly sequenced whereas amplicons for *PDGFRA* and *PDGFRB* were initially analysed by single strand conformation polymorphism. Fragments that showed mobility shifts of single strands and/or heteroduplex formation were subsequently sequenced. Again, no pathogenic mutation was identified.

In summary, mutation screening of the coding exons of all six *PDGF/R* genes revealed no pathogenic mutation in the 18 Costello patients. Numerous sequence variants were identified both in the introns and coding regions of the six genes studied. Most of the variants were also found in unaffected controls (Tab. 5) and thus, they most likely represent polymorphisms.

| Gene | Nucleotide change | Amino acid change | Frequency of second allele in patients | controls |
|---|---|---|---|---|
| ***PDGFA*** | c.207C>T[a] | p.H69 | 30/36 (12)[b] | 18/22 (8) |
| | IVS5+12C>T[a] | | 18/36 (5) | 3/4 (1) |
| ***PDGFB*** | IVS2+15C>A | | 3/36 | 1/4 |
| ***PDGFC*** | c.113A>G | p.Q38R | 1/36 | 2/220 |
| | c.855C>G | p.A285 | 1/36 | 1/224 |
| | c.1032A>G | p.G344 | 4/36 | 11/50 (3) |
| ***PDGFD*** | c.568A>G | p.I190V | 2/36 | 2/52 |
| | c.1080T>C | p.C360 | 16/36 (3) | 3/4 (1) |
| ***PDGFRA*** | c.939T>G | p.G313 | 2/36 | 1/8 |
| | c.1432T>C | p.S478P | 1/36 | 13/116 (2) |
| | c.1701G>A | p.P567 | 1/36 | 0/58[c] |
| | IVS13-44A>T | | 6/36 (3) | 2/6 (1) |
| | IVS20-52G>A[a] | | 2/36 | 1/114 |
| ***PDGFRB*** | IVS2+90G>A[a] | | 8/36 (3) | 13/100 (4) |
| | c.1453G>A | p.E485K | 1/36 | 1/4 |
| | IVS10+50T>C | | 14/36 (4) | 3/4 (1) |
| | c.1854G>A | p.T618 | 3/36 (1) | 6/116 |
| | IVS18-41T>A | | 2/36 | 1/4 |
| | c.2601A>G | p.L867 | 11/36 (3) | 2/4 |
| | c.3246A>G | p.P1084 | 12/36 (6) | 2/4 (1) |

**Tab. 5: Polymorphisms identified in six *PDGF/R* genes of 18 patients with Costello syndrome**

[a] Respective sequence variant was also identified in unaffected family member/s of the patients.

[b] Total number of homozygotes.

[c] Respective sequence variant was not identified on 58 control chromosomes, but was found in the unaffected father of the patient and is already listed in the dbSNP (rs1873778) at NCBI.

Nevertheless, ten nucleotide changes were found in five patients with Costello syndrome that were not detected in at least 220 control alleles (Tab. 6). Seven of these sequence variants were identified in unaffected members of the patients' families suggesting that they are rare polymorphisms. Three of these sequence variants that were detected in a single patient of Afro-American origin were not found in over 220 alleles of control persons from European population. The parents of this patient were not available for the analysis.

| Patient id# | Gene | Nucleotide change[a] | Amino acid change | Presence in patients' unaffected family members[b] | |
|---|---|---|---|---|---|
| 8 | *PDGFA* | IVS3+42G>A | | F | |
| | *PDGFRA* | c.1320G>A | p.T440 | F | |
| | *PDGFRB* | c.2164G>T | p.V722F | F, S | |
| 9 | *PDGFB* | c.453C>G | p.V151 | F | |
| | | c.635C>T | p.T212M | F | |
| 11 | *PDGFB* | IVS2+36G>C | | n.a. | (0/222)[c] |
| | | IVS2+70A>G | | n.a. | (0/222)[c] |
| | | IVS3+22A>G | | n.a. | (0/224)[c] |
| 15 | *PDGFB* | g.24832C>T | | M | |
| 6 | *PDGFRA* | c.3083T>C | p.V1028A | M | |

**Tab. 6: Rare nucleotide changes identified in the *PDGF/R* genes in 5 patients with Costello syndrome**

[a] All changes were heterozygous.
[b] Father (F), mother (M), sister (S), not available (n.a.).
[c] Frequency of second allele in controls.

Of the 18 nucleotide substitutions detected in the coding regions in total, seven should result in an amino acid change (Tab. 5 and 6). None of the isocoding sequence variants are predicted to affect splicing.

Although autosomal dominant inheritance was suggested for Costello syndrome, it can not yet be excluded that it could be also a very rare autosomal recessive disorder. Therefore, a mutation screening in the second allele of the *PDGFB* gene in the translocation patient was performed. A single nucleotide change, IVS2+15C>A, was identified that was also present in three other Costello patients and in the unaffected mother of the translocation patient. Therefore this change represents a polymorphism.

## 4. Re-evaluation of the phenotype of the patient with the 1;22 translocation

Molecular characterization of the 1;22 translocation was performed with the assumption that a gene or a control element is disrupted by one of the breakpoints that caused the phenotype (presumed Costello syndrome) of the patient. I showed that the *PDGFB* gene in 22q13.1 was indeed disrupted by the chromosome rearrangement and this led to a hypothesis that *PDGFB* is candidate gene for Costello syndrome. However, no pathogenic mutation was detected in *PDGFB* in 18 sporadic patients with CS. In addition, five other genes belonging to *PDGF/R* family were considered to be candidate genes for the syndrome. Nevertheless, no pathogenic mutation was detected in five *PDGF/R* genes in 18 sporadic patients with CS. These results suggest that six genes of the *PDGF/R* family are not the major genes for Costello syndrome. These findings together prompted us to re-evaluate the clinical diagnosis of the translocation patient.

Two papers describe the phenotype of the patient at the age of 17 months (Selypes et al., 1992) and six years (Czeizel and Tímár, 1995). In the latter report, several features are mentioned that are present in patients with Costello syndrome, such as coarse face with full cheeks, depressed nasal bridge, low set ears, as well as loose and wrinkled skin. However, the pictures published (Fig. 1a-d in Czeizel and Tímár, 1995) revealed that, in total, she did not have the characteristic facial “gestalt” of a Costello patient. In particular, she has no thick lips, a short neck, and epicanthal folds, all symptoms typical for patients with Costello syndrome. It was reported that she showed a progeroid, senile-like appearance (Czeizel and Tímár, 1995). More recent clinical photographs of the patient (Fig. 28A and B) show that she has sagging of cheeks and wrinkling of facial skin. Moreover, the patient has no sparse and curly hair. In contrast to the majority of Costello patients that have macrocephaly, high birth weight, and poor feeding during infancy, the translocation patient is microcephalic, showed normal weight at birth with neither failure to thrive nor postnatal growth failure. Although generalized excessive and very loose skin was described, the skin of Costello patients is thickened, soft and velvety in feel that causes deep creases in palms of hands and soles. Yet, the patient’s hands did not show these characteristics (Fig. 1d in Czeizel and Tímár, 1995 and Fig. 28B).

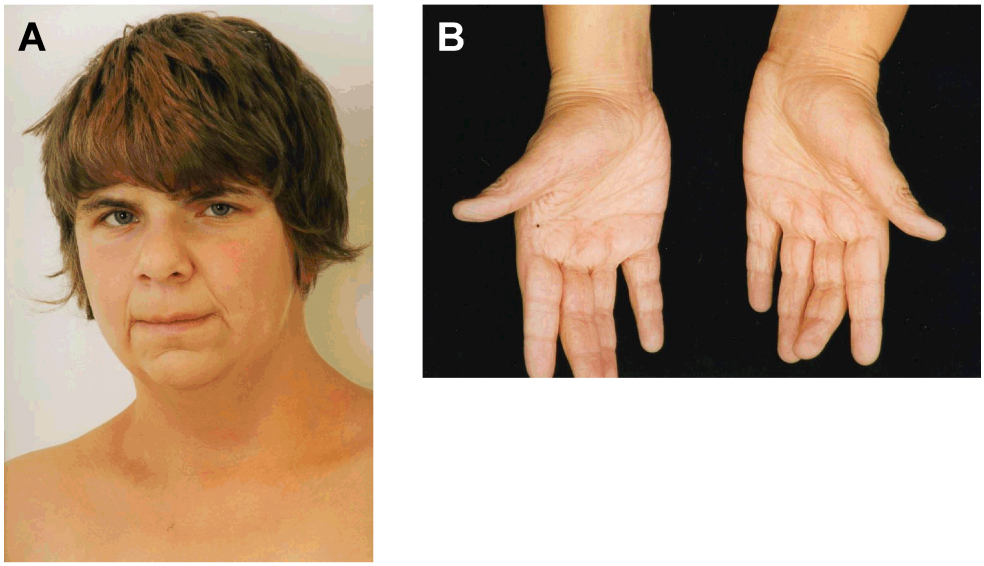


**Fig. 28: Photographs of the translocation patient taken at age of 12 years**

Note the coarse face **(A)** and wrinkled skin on palms **(B)**.

Severe mental retardation (IQ 25-50) is present in the majority of patients with Costello syndrome (Hennekam, 2003). The IQ of the translocation patient was determined twice and was in the range of 71-85 indicating only borderline mental retardation. Finally, congenital heart defects are found in about 60% of the patients (Lin et al., 2002) whereas no cardiovascular abnormality was described in the translocation patient. In Table 7, the typical clinical signs and symptoms seen in patients with Costello syndrome were compiled and compared with those seen in the translocation patient.

| Typical clinical findings in patients with Costello syndrome | %[a] | Translocation patient[b] |
|---|---|---|
| Coarse face with full cheeks, depressed nasal bridge, and low set ears | ~97 | + |
| Loose and wrinkled skin | 99 | + |
| Skin is thickened, soft, and velvety in feel | ~99 | – |
| Short neck | 88 | – |
| Thick lips | 97 | – |
| Sparse and curly hair | 82 | – |
| Macrocephaly | 84 | – |
| High birth weight | 89 | – |
| Failure to thrive | 96 | – |
| Moderate to severe mental retardation | 100 | – |
| Congenital heart defect | 63[c] | – |

**Tab. 7: Clinical signs and symptoms seen in patients with Costello syndrome and in the patient with 1;22 translocation**

[a] Values were taken from Hennekam (2003).

[b] Present (+) and absent (–) in the translocation patient.

[c] Taken from Lin et al. (2002).

Although some of the typical clinical features were also found in the translocation patient (already mentioned above) the majority of them was absent. Therefore, the failure to identify any mutation in the *PDGF/R* genes in 18 patients with Costello syndrome together with the absence of clinical signs and symptoms typical for patients with Costello syndrome in the translocation patient question the clinical diagnosis of Costello syndrome. Instead, it seems more likely that the translocation patient shows a 'unique' phenotype not resembling any known and well-defined syndrome.

## 5. Mutation screening of functional candidate genes for Costello syndrome

In attempt to identify the disease gene for Costello syndrome we characterized a 1;22 translocation in a patient with presumed Costello syndrome and in parallel, we searched for functional candidate genes for this disorder. A candidate gene for Costello syndrome was selected based on

1/ its potential involvement in pathways that might be implicated in the pathogenesis of Costello syndrome

2/ its possible role in the development of rhabdomyosarcoma, a tumor which has been described in numerous patients with CS
3/ its implication in an inherited disorder that showed overlapping features with CS.

## 5.1 Mutation analysis of the *TGFB1* gene

Benign ectodermal tumors such as facial papillomas are often present in patients with Costello syndrome (Kerr et al., 1998). In addition, rare malignancies, e.g. rhabdomyosarcoma and bladder carcinoma, are more common in these patients than expected (Gripp et al., 2002). Proud and colleagues (2001) proposed that alterations in growth signaling proteins such as transforming growth factor-alpha (TGF-α) or -beta (TGF-β) may explain many of the clinical features of Costello syndrome. TGF-α facilitates epithelial growth and is overexpressed in breast and bladder cancers (Ciardiello et al, 1991; Inui et al., 1996; Thogersen et al., 1999). TGF-β is a multifunctional peptide growth factor that stimulates or inhibits proliferation depending on the cell type and dynamic state of the organism (Waite and Eng, 2003). Aberrant TGF-β function in Costello syndrome could facilitate the development of rhabdomyosarcoma and cardiac hypertrophy and may lead to tissue laxity, soft palmar creases, and lax joints since it is an elastin processing protein (Proud et al., 2001). In mammals, three different TGF-βs, β1, β2 and β3, exist that are encoded by three genes (*TGFB1*, *TGFB2*, *TGFB3*) and function through the same receptor signaling system (Massagué, 1998). Of these, TGF-β1 is most frequently upregulated in tumor cells and most studies focus on the role of TGF-β in tumorigenesis (Derynck et al., 2001). These data led to the assumption that *TGFB1* is a candidate gene for CS and therefore, six exons covering 87% of the coding region of *TGFB1* were screened for mutations in 18 Costello patients. PCR products were directly sequenced and no pathogenic mutation was detected. Four sequence variants were identified, one in intron 5 and three in the analysed coding region of *TGFB1* (Tab. 8).

| Gene | Nucleotide change | Amino acid change | Frequency of second allele in patients | controls | dbSNP[b] |
|---|---|---|---|---|---|
| ***TGFB1*** | c.29C>T | p.P10L | 23/36 (8)[a] | 1/4 | rs1982073 |
| | c.74C>T | p.R25P | 4/36 | 1/4 | rs1800471 |
| | c.788C>T | p.T263I | 2/36 | 1/4 | rs1800472 |
| | IVS5-20C>T | | 7/36 (1) | 0/4 | rs8179181 |

**Tab. 8: Sequence variants identified in the *TGFB1* gene in 18 patients with Costello syndrome**

[a] Total number of homozygotes among the individuals screened.
[b] Respective sequence variants have already been deposited to the dbSNP at NCBI.

The variantsin the coding region should result in an amino acid change. However, they were also identified in unaffected controls. All four sequence variants have already been deposited to the dbSNP at NCBI and thus they represent most likely polymorphisms.

## 5.2 Mutation analysis of the *FOXO1A* gene

Ten cases of rhabdomyosarcoma were reported in patients with Costello syndrome. Of these, the embryonal subtype was present in seven cases, one had alveolar and one pleomorphic histology, and in one case the histology is not known (Gripp et al., 2002). The relatively high prevalence of rhabdomyosarcoma in a rare syndrome such as Costello syndrome is suggestive to represent a causal link (Kerr et al., 1998). In several cases with alveolar rhabdomyosarcoma a recurrent translocation, t(2;13)(q35;q14), was found that result in a fusion gene involving the *PAX3* (paired box gene 3) and the *FKHR* gene. In addition, another chromosome translocation, t(1;13)(p36;q14), results in a fusion of *PAX7* (paired box gene 7) and the *FKHR* gene. The gene on chromosome 13 was called fork head in rhabdomyosarcoma (*FKHR*) (Galili et al., 1993). Nevertheless, a new name was given by the Hugo Gene Nomenclature Committee: forkhead box O1A (rhabdomyosarcoma) (*FOXO1A*).

Due to its obvious involvement in rhabdomyosarcoma, *FOXO1A* was screened for mutations in 8 Costello patients. The two coding exons of *FOXO1A* were amplified using genomic DNA of each patient as template and the PCR products were directly sequenced. No pathogenic mutation was identified. Only one sequence variant, g.60919C>T, was found in the 5' untranslated region of the *FOXO1A* gene. This sequence variant has not yet been deposited to the dbSNP at NCBI and was not investigated further.

## 5.3 Mutation analysis of the *LMNA* gene

Patients with the Hutchinson-Gilford progeria syndrome [HGPS (OMIM 176670)], an extremely rare form of accelerated aging in childhood, are characterized among others by severe growth retardation, short statue, failure to thrive, and hyperkeratosis (DeBusk, 1972; Baker et al., 1981). Recently, mutations in the lamin A/C gene (*LMNA*) were identified to be causative for this disorder (Eriksson et al., 2003; De Sandre-Giovannoli et al., 2003). Some of the symptoms of patients with HGPS listed above are also shared by patients with Costello syndrome. In particular, patients with Costello syndrome also show senescence. For this reason, mutation screening of the *LMNA* gene was performed. The twelve exons of *LMNA* gene were screened for mutations in 9 patients with CS using genomic DNA of each patient as template. The PCR products were directly sequenced. Five sequence variants were identified, two in the introns and three in the coding regions (Tab. 9).

| Gene | Nucleotide change | Amino acid change | Frequency of second allele in patients | controls | dbSNP[a] |
|---|---|---|---|---|---|
| ***LMNA*** | c.861T>C | p.A287 | 1/18 | | rs538089 |
| | IVS6+16G>A | | 1/18 | | rs534807 |
| | IVS8+44C>T | | 1/18 | 6/48 (1)[b] | |
| | c.1698C>T | p.H566 | 7/18 (2) | 12/52 (1) | rs4641 |
| | c.1786G>A[c] | p.D596N | 1/18 | 0/154 | |

**Tab. 9: Sequence variants identified in the *LMNA* gene in 9 patients with Costello syndrome**

[a] Respective sequence variants have already been deposited to the dbSNP at NCBI under given identification numbers.

[b] Total number of homozygotes.

[c] Sequence variant was also identified in unaffected family member of the patient.

Of the variants detected, only one should result in an amino acid change. Four of the sequence variants found were also identified in unaffected controls and/or have been deposited to the dbSNP at NCBI. One nucleotide change, c.1786G>A, was found in an unaffected member of the patient's family. None of the isocoding sequence variants are predicted to affect splicing. Together, all five nucleotide substitutions represent most likely polymorphisms.

In summary, none of the ten nucleotide substitutions detected in the three candidate genes for Costello syndrome seemed to be the causative mutation for this syndrome. Therefore *TGFB1*, *FOXO1A*, and *LMNA* can be excluded as the major causative genes for Costello syndrome.

# IV. Discussion

## 1. Non-homologous recombination as a molecular mechanism for the 1;22 translocation and the intrachromosomal rearrangement

By molecular analysis of the 1;22 translocation, the breakpoints were characterized at the nucleotide level. In the genomic DNA isolated from peripheral blood of the translocation patient, two different breakpoints were found on the derivative chromosome 1. One breakpoint occurred after the stop codon in exon 6 [der(1A) in Fig. 15] whereas the second one was in intron 5 of the *PDGFB* gene [der(1B) in Fig. 15]. Thus, the patient is mosaic for two cell lines in her peripheral blood with two different derivative chromosomes 1. In the junction fragments containing exon 6 breakpoint, an internal deletion of 2.2 kb was also identified that most likely occurred by homologous *Alu*-*Alu*-mediated recombination. It is likely that the generation of two derivative chromosomes 1 occurred in two steps: First, an interchromosomal rearrangement between chromosomes 1 and 22 produced a derivative chromosome 1 with breakpoint in exon 6 and an internal deletion in intron 5 of *PDGFB* [der(1A)]. The potential intrinsic instability of this chromosome resulted in a second, intrachromosomal rearrangement leading to derivative chromosome 1B with a break in an *Alu*Jb element in *PDGFB* intron 5.

*Alu* sequences represent more than 10% of the human genomic DNA and are spread through the entire human genome at varying densities (International Human Genome Sequencing Consortium, 2001). Consensus *Alu* sequences are approximately 280 bp in length and consist of two similar monomers linked by an oligo-d(A) stretch. RNA polymerase III promoter boxes A and B are present in the left monomer. The right *Alu* monomer contains a 31-bp insert that is not present in the left monomer (Fuhrman et al., 1981; Willis, 1993). At the 3' end of the right *Alu* monomer, another oligo-d(A) chain of variable length is present (Hutchinson et al., 1993; Jurka and Klonowski, 1996). Insertions of an *Alu* sequence into coding exons or adjacent introns of a gene as well as recombinations between *Alu* elements have been repeatedly described to be associated with various human diseases (reviewed in Deininger and Batzer, 1999). In general, homologous recombination may be mediated by direct repeats such as *Alu* sequences, and low copy repeats (Stankiewicz and Lupski, 2002) while various types of recombinogenic motifs (DNA polymerase pause site, immunoglobulin heavy chain class switch repeat, heptamer recombination signal, etc.) were shown to promote non-homologous recombination (Abeysinghe et al., 2003).

Analysis of DNA sequences at the breakpoint regions of the 1;22 translocation revealed the presence of an *Alu*Sg repeat in 1q24.3, whereas no repetitive element was found at the 22q13.1 breakpoint of derivative chromosome 1A. An overlap of 4 bp (cagg) is present at the breakpoint, suggesting that the translocation occurred by non-homologous (illegitimate) recombination. Similarly, in the majority of translocations that have been analysed at the nucleotide level, short common sequences were found (Budarf et al., 1995; Bonaglia et al., 2001; McMullan et al., 2002 and references therein; Kalscheuer et al., 2003). A single 1;19 translocation has been described with both breakpoints in *Alu* repetitive elements. The recombination occurred between the left monomer of an *Alu* repeat on chromosome 1 and the right monomer on chromosome 19, suggesting illegitimate recombination as molecular mechanism by which this translocation occurred (Nothwang et al., 2001). It is of interest to note that the breakpoint on chromosome 22 of the derivative chromosome 1B is located in the right monomer of an *Alu*Jb repeat (between nucleotides –5 and +1 in Fig. 29), whereas that on chromosome 1 is in the left monomer of an *Alu*Sg repeat, precisely between the A and B sequences of the *Alu* consensus sequence (between nucleotides -118 and -123 in Fig. 29). No sequence homologies exist between the two *Alu* repeat regions as the *Alu* repeats are in antiparallel orientation. The short motif 'ctcagc' was found at both breakpoint regions (Fig. 29), also suggesting illegitimate recombination as a molecular mechanism for the second intrachromosomal rearrangement. Moreover, a 26-bp *Alu* core sequence overlaps with the 'ctcagc' motif at the breakpoint on chromosome 1 (dashed box in Fig. 29). This core sequence was frequently found at or near recombination breakpoints, suggesting that it stimulates non-homologous recombination events (Rüdiger et al., 1995; Hiltunen et al., 2000).

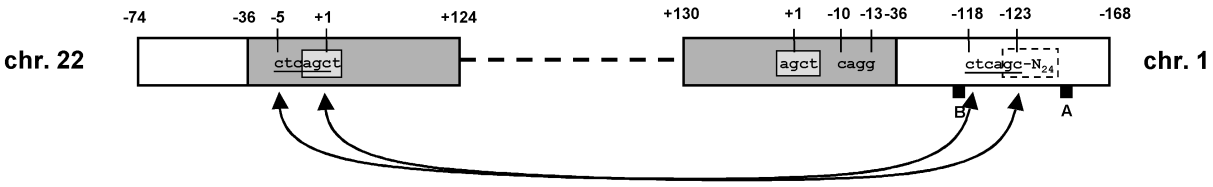


**Fig. 29: Schematic representation of the two *Alu* repetitive elements and their orientation in the breakpoint region of the der(1) chromosome**

Left monomers are indicated by white boxes, right monomers by grey boxes. Nucleotide numbering is as proposed in Deininger et al. (1981). Position +1 refers to the C of the *Alu*I endonuclease recognition site within the motif 'agct' that is boxed. Bipartite promoter sequences A and B of the left monomer are indicated by black boxes below the *Alu* repeat. Arrows point to the breakpoints of the rearrangement. The 'cagg' motif at position –10 to –13 indicate the breakpoint on der(1A), whereas the 'ctcagc' motif, which is underlined in both *Alu* repeats, represents the position of the breakpoints on der(1B). The 26-bp *Alu* core sequence is indicated by a dashed box.

In summary, the initial rearrangement between chromosome 1 and chromosome 22 was mediated by non-homologous recombination between an *Alu* element on chromosome 1 and a single-copy sequence on chromosome 22. The second, intrachromosomal rearrangement occurred between the same *Alu* element on chromosome 1 and an *Alu* element on chromosome 22. Nonetheless, since neither of the *Alu* sequences shared significant sequence homologies, this latter rearrangement also occurred most likely by non-homologous recombination. It has been proposed that repetitive sequence elements such as direct repeats, inverted repeats, symmetric elements, and inversions of inverted repeats may be involved in the formation of secondary structure intermediates between single-stranded DNA ends that recombine during rearrangements (Chuzhanova et al., 2003). These findings extended the model of illegitimate recombination previously proposed by Zucman-Rossi and colleagues (1998). In addition, Gotter and colleagues (2004) described translocations that occurred between genomic regions of similar melting temperature and of propensity to form secondary structure. These authors reported that analysis of the putative secondary structure sequences surrounding translocation breakpoints within low copy repeat B region in 22q11.2 revealed the presence of palindromes forming stem-loop structures that do not share large sequence homology. In general, it was suggested that illegitimate recombination might occur between regions having similar characteristics (but not necessary sequence homology) (Gotter et al., 2004). By searching the DNA sequences surrounding the breakpoints of the 1;22 translocation for the presence of repetitive sequence motifs and palindromes, various short repetitive sequence elements were identified that could possibly participate in the formation of secondary structure and thus, might have facilitated the recombination process.

## 2. Aberrant subcellular localization of the PDGFB fusion proteins in extracellular matrix might have contributed to the disease phenotype of the translocation patient

Various fusion transcripts were identified in the patient with the translocation consisting of *PDGFB* exons and parts of chromosome 1q24.3. Two fusion transcripts that contained the complete coding region of *PDGFB* but not the untranslated exon 7 were identified (third and fourth fusion transcript in Fig. 10). Instead of *PDGFB* exon 7, material from chromosome 1q24.3 was present in these transcripts. Untranslated regions are known to play a crucial role in post-transcriptional regulation of gene expression. It is well established that the 3' untranslated region (UTR) of mRNAs can specifically control nuclear export,

polyadenylation status, subcellular targeting, rates of translation, and degradation of mRNA (reviewed in Mignone et al., 2002). Thus, one of the a.m. processes might be impaired by alteration in the 3' UTR sequence that may cause deregulated expression of the *PDGFB* gene/protein.

The carboxyl terminus of PDGFB (aa 201-241) encoded by exon 6 was shown to be required for membrane retention. PDGFB retention properties were mapped to different residues at the C-terminus (LaRochelle et al., 1991; Östman et al., 1991; Raines and Ross, 1992). These findings provided evidence for a novel mechanism of stably presenting growth factors at the cell surface (LaRochelle et al., 1991). By immunofluorescence and laser confocal microscopy, Kelly and colleagues (1993) investigated the subcellular distribution of PDGFB in CHO cells moderately expressing this protein. Substantial amounts of PDGFB homodimers were deposited in the matrix laid down below the cells. Matrix attachment was shown to be most likely mediated by proteoglycans, at least partly through glycosaminoglycan moieties. However, additional components could also be implicated (Kelly et al., 1993). It has been hypothesized that matrix association of PDGFB may focus and prolong the activity and the response of the growth factor compared to the soluble diffusible form (Raines and Ross, 1992; Kelly et al., 1993). Indeed, PDGFB associated with the extracellular matrix can be made available for binding high affinity PDGF receptors on cells in contact with the matrix (Field et al., 1996). Moreover, PDGFB has a strong local growth enhancing effect that is most likely due to its association with components of the extracellular matrix (Pekny et al., 1994). Taken together, proper matrix association of the platelet-derived growth factor beta is required for its regulated action on receptors.

Two of the fusion transcripts detected in the translocation patient do not contain the complete coding sequence of the *PDGFB* gene since both lack exon 6 (first and second fusion transcript in Fig. 10). In COS-7 cells, overexpressed PDGFB proteins encoded by these transcripts showed an extracellular matrix localization. However, platelet-derived growth factor beta proteins containing novel amino acid residues at their carboxy-terminal end form larger aggregates in the ECM compared to wild-type PDGFB. PDGFB binding to heparan sulfate is likely to involve an electrostatic interaction between positively charged basic residues in the retention motif of PDGFB and negatively charged groups in heparan sulfate (Raines and Ross, 1992). Thus, impaired PDGFB binding to proteoglycans might be implicated in aberrant subcellular localization of both fusion proteins. Moreover, PDGFB was shown to bind to the extracellular matrix proteins fibronectin, laminin, collagen type III, thrombospondin 1, and SPARC (secreted protein, rich in cysteine; also named osteonectin)

(Raines et al., 1992; Field et al., 1996; Hogg et al., 1997). It is possible that binding of PDGFB fusion proteins to one or more of these proteins might be disturbed that might have resulted in aberrant matrix distribution of the fusion proteins.

Deposition of PDGFB into the subcellular matrix provides the potential for a substantial amount of growth factor to be held in preformed storage pools. Thus, this deposited growth factor is available for subsequent mobilization, possibly by the release through appropriate enzymes (Kelly et al., 1993). Indeed, mitogenic activity of matrix-localized PDGFB has been demonstrated (Field et al., 1996). Although the PDGFB fusion proteins without a basic C-terminal end show matrix localization, we assume that cleavage of the PDGF molecule that is necessary for removal of the C-terminal sequences, might be disturbed. Thus, PDGFB proteins lacking the basic C-terminus remain in the extracellular matrix but possibly can not be made available for binding to high affinity PDGF receptors. Conversely, secretion of these PDGFB proteins might be enhanced leading to differences in their paracrine activities as growth factors. Eming and colleagues (1999) initiated a study to investigate the *in vivo* role of cell-associated versus released form of PDGFB produced by the epidermis. They demonstrated that both forms of PDGFB act as paracrine mediators that control cellular events in adjacent dermis. The released isoforms diffuse away and control more distal events whereas cell-associated isoforms control more proximal events. These data suggest that changes in the concentration or availability of PDGFB can influence the type of biological response *in vivo* as well as its spatial organization (Eming et al., 1999). Thus, we hypothesize that the novel PDGFB proteins encoded by the first and second fusion transcripts of the translocation patient have different properties as growth factor compared to wild-type PDGFB that, in turn, might have contributed to the disease phenotype of the patient.

To analyse the subcellular localization of wild-type and mutant PDGFB proteins, the proteins were tagged with enhanced green fluorescent protein (EGFP) or red fluorescent protein (DsRed2). Two different fluorescent proteins were used to exclude abnormal localization of the fusion proteins due to artefacts as already described. For example, Söling and colleagues (2002) expressed Herpes simplex virus type 1 thymidine kinase fused to different fluorescent proteins (EGFP, DsRed1, DsRed2, dsdrFP616) and showed that intracellular localization of these fusion products depends on the type of fluorescent tag. In addition, it was also shown that a fusion of the red fluorescent protein DsRed to another protein may impair the function and localization of this protein due to formation of tetramers or even higher order aggregates of DsRed moiety (Jakobs et al., 2000; Lauf et al., 2001). Furthermore, a direct toxic effect of DsRed on cells has also been discussed (Jakobs et al., 2000; Lauf et al., 2001). Yanushevich

and colleagues (2002) substituted several basic residues located at the N-terminus of DsRed and demonstrated that the mutant protein (DsRed2) had a lower tendency to aggregate. Nonetheless, Söling and colleagues (2002) showed that these N-terminally modified DsRed2 proteins still aggregate. This result is in line with the findings presented in this work showing that wild-type PDGFB-DsRed2 fusion proteins were present in artificial aggregates in the cell. In contrast, green fluorescent protein (GFP) is monomeric and shows only a weak tendency to dimerize (Söling et al., 2002). A mutant form of GFP, EGFP, shows 35-fold higher fluorescence than the wild-type protein (Cormack et al., 1996) and was successfully used in the experiments described in this work. Yet, mutant PDGFB protein encoded by the first fusion transcript and having an insertion of *EGFP* in exon 5 of *PDGFB* showed unspecific localization in the cell. Various forms of aggregates were detected and the biological activity of such a protein is questionable. Nevertheless, this mutant PDGFB protein was found to be expressed in two types of cell lysates by western blotting and the protein amount was comparable to that observed for wild-type PDGFB and mutant PDGFB protein encoded by the second fusion transcript (both with insertion of *EGFP* in exon 5 of *PDGFB*).

In summary, additional experiments are needed to further characterize the biological activity of the mutant PDGFB proteins encoded by the first and second fusion transcripts. To examine the effect of these mutant PDGFB proteins on the activity of their appropriate protein tyrosine kinase receptors, assays to measure the kinase activity of the receptors can be performed.

## 3. Pitfalls in identifying mutations in candidate genes

A number of chromosomal translocations has been shown to be associated with a disease phenotype as a result of interrupting or modifying the expression of gene(s) localized in or close to the breakpoints (Bugge et al., 2000). In an attempt to identify the gene responsible for the trait in question, breakpoint regions should be characterized. If the gene is indeed disrupted by the rearrangement, it is considered a promising candidate gene for the disease. The next important step is then to screen the gene for mutations in patients without a chromosomal rearrangement. In our case, no pathogenic mutation in *PDGFB* was identified in 18 sporadic patients with Costello syndrome. Four sequence variants were detected that most likely represent polymorphisms. Three other sequence variants were identified in introns 2 and 3 of *PDGFB* in a patient of Afro-American origin that were not found in control persons from European population. The different origin of the patient and control persons might explain why the three variants were not detected in the control population used in our study.

Some of the variants may represent (very rare) polymorphisms. Indeed, it has been reported that about 38% of randomly selected SNPs occur at a very low frequency in the general population (Stephens et al., 2001).

In general, mutations present in the promoter region, 5'- and 3'-untranslated regions, as well as in intronic sequences can not be ruled out by the mutation screening approaches used routinely. Varon and colleagues (2003) reported that congenital cataracts, facial dysmorphism neuropathy (CCFDN) is caused by a single nucleotide substitution in intron 6 (IVS6+389C>T) of *CTDP1*. The substitution located 389 bp from the splice donor site of exon 6 results in aberrant splicing and insertion of 95 nucleotides of an *Alu* sequence in the *CTDP1* mRNA. Thereby, the insertion generates a premature termination signal (Varon et al., 2003). Such an intronic mutation would not have been detected by mutation analysis performed in this work. Therefore, sequence analysis of cDNA is recommended not to miss such mutations. Similarly, submicroscopic chromosomal rearrangements not detectable by routine cytogenetic analysis such as larger deletions, insertions, inversions or duplications can also not be identified.

For a number of monogenic disorders the pattern of inheritance has not yet been finally established. In such a case, conclusions drawn from the mutation analysis assuming a monogenic disorder with autosomal dominant inheritance differ from those for an autosomal recessive condition. In the latter case, it can not be excluded that heterozygous nucleotide changes identified in a gene are pathogenic and a second mutation in the same gene has not been identified. For example in dystrophic epidermolysis bullosa (DEB), a group of blistering disorders, mutations in the collagen type VII alpha 1 (*COL7A1*) gene were shown to underlie both recessive and dominant DEB forms. Most of the mutations in recessively inherited forms lead to frameshift and premature termination codons (Hovnanian et al., 1997; Pulkkinen and Uitto, 1999). Heterozygous premature termination codon mutations are silent whereas homozygous mutations or mutations combined with another gene defect on the other allele can result in a drastic modulation of the phenotype. In addition, a mild dominant phenotype can be modulated by a second *COL7A1* mutation resulting in a severe phenotype. It has been shown that homozygozity for *COL7A1* mutations is rare and that most of the DEB patients are compound heterozygous for recessive or recessive and dominant *COL7A1* defects (Bruckner-Tuderman, 1999). Moreover, the possibility of a digenic or polygenic trait has also to be considered. Interestingly, junctional epidermolysis bullosa (JEB) can be caused by heterozygous mutations in the genes encoding collagen XVII (*COL17A1*) and β3 subunit of laminin 5 (*LAMB3*), two functionally related proteins (Floeth and Bruckner-Tuderman, 1999).

*PDGFB* was the only gene identified in the breakpoint regions of the translocation patient. Although various exons of a putative novel gene were identified in the breakpoint on chromosome 1q24.3, the majority of them lies in repetitive DNA sequences. To my knowledge, no gene or pseudogene is known that contains exons in repetitive sequence elements. In addition, database searches revealed no EST sequences matching to the identified putative exons in the 1q24.3 breakpoint region. Usually, a gene is represented by multiple ESTs that correspond to different portions of a transcript or various alternatively spliced transcripts (Schuler et al., 1996).

It is also possible that genes adjacent to the breakpoints are implicated in the disease phenotype of a translocation patient. In a number of cases, chromosomal breakpoints have been found to map outside disease genes (Fantes et al., 1995; Wirth et al., 1996; Krebs et al., 1997; Flomen et al., 1998). Appropriate expression of a gene requires the presence of an intact transcription unit and also the functioning of regulatory elements. Chromosomal breaks that are located outside the transcription unit of a gene may cause a disease phenotype by a position effect (reviewed in Kleinjan and van Heyningen, 1998). For example, mutations in the *TWIST1* gene have been reported in Saethre-Chotzen syndrome, a form of craniosynostosis. *TWIST1* encodes a basic helix-loop-helix (bHLH) transcription factor (Rose and Malcom, 1997). Four patients with translocations have been reported in which the breakpoints do not interrupt the coding sequence of *TWIST1* and thus act most likely through a positional effect (Rose et al., 1997). Furthermore, mutations in the *POU3F4* (POU domain, class 3, transcription factor 4) gene were shown to cause X-linked deafness type 3 (DFN3) (De Kok et al., 1995). Five DFN3 patients were characterized that show a microdeletion of an 8-kb DNA fragment located 900 kb upstream *POU3F4*. The molecular cause in these cases is not known, disruption of another DFN3 gene or of sequences that are involved in transcriptional regulation of the *POU3F4* gene was discussed (De Kok et al., 1996). It is tempting to speculate that the breakpoint in 1q24.3 of the translocation patient described in my work might cause downregulation of a gene located far from the breakpoint and thus causing the ‘unique’ disease phenotype of the patient.

## 4. Re-evaluation of the clinical symptoms of the translocation patient challenges the diagnosis of Costello syndrome in this patient

Comparison of the clinical symptoms of the 1;22 translocation patient with the main characteristics found in patients with Costello syndrome, together with the failure to identify any mutation in the six genes of the *PDGF/R* family in 18 sporadic Costello patients suggested that the initial clinical diagnosis of Costello syndrome in the translocation patient is questionable. Indeed, re-evaluation of the phenotype of the translocation patient led us to the conclusion that the patient has a 'unique' phenotype. Thus, the patient with the chromosome 1;22 rearrangement described originally as having Costello syndrome did not provide the clue to identify the disease gene.

## 5. Functional candidate genes for Costello syndrome

In an alternative approach, mutation analysis of functional candidate genes for Costello syndrome, namely *FOXO1A*, *TGFB1*, and *LMNA*, was performed. No pathogenic mutation of these genes was identified and therefore, they can be excluded as major causative genes for Costello syndrome. The problems associated with mutation screening were already discussed in IV.3.

Although the genetic defect in Costello syndrome (CS) remains unknown, new insights into the possible molecular pathogenesis of CS have been found. Studies on cultured fibroblasts derived from patients with Costello syndrome revealed impaired formation of elastic fibers (Hinek et al., 2000). Normally, tropoelastin, the major component of the extracellular elastic fibers, has to be delivered to the cell surface. During the intracellular secretory pathway, the highly hydrophobic tropoelastin is chaperoned by the 67-kDa elastin-binding protein (EBP) (Hinek and Rabinovitch, 1994; Hinek et al., 1996). Subsequent coordinated release of tropoelastin from its EBP chaperone to the microfibrillar scaffold of developing elastic fibers occurs by interaction of EBP with galactosugars (Hinek et al., 1991). Skin fibroblasts of patients with Costello syndrome showed increased cell surface accumulation of galactosugars such as chondroitin sulfate (Hinek et al., 2000). Remarkably, the clinical phenotype of CS resembles Hurler disease, and skin fibroblasts of these patients accumulate extensively the galactosugar dermatan sulfate (Hinek and Wilson, 2000). Hurler disease belongs to a group of inherited metabolic storage diseases and is caused by deficiency of the lysosomal enzyme α-L-iduronidase. It has been hypothesized that abnormal accumulation of galactosugars at the

cell surface of fibroblasts of patients with CS or Hurler disease interferes with the normal assembly of elastin on the microfibrillar scaffold (Hinek et al., 2004). This hypothesis is supported by observations that fibroblasts of patients with Costello syndrome or Hurler disease synthesize tropoelastin at normal rate but are unable to secrete tropoelastin or assemble extracellular insoluble elastin. Furthermore, impaired secretion of tropoelastin coincides with low amounts of EBP in both types of fibroblasts, suggesting that deficiency of the tropoelastin chaperone is a crucial factor for the disruption of elastic fiber formation (references in Hinek et al., 2004).

Fibroblasts of patients with Costello syndrome or Hurler disease produce normal amounts of EBP but release them quickly into conditioned media (Hinek et al., 2000; Hinek and Wilson, 2000). All these findings support the assumption on a regulatory role of chondroitin sulfate and dermatan sulfate glycosaminoglycans in elastin fiber assembly. Recently, a variant of chondroitin sulfate proteoglycan versican, V3, which lacks chondroitin sulfate chains, has been shown to stimulate elastic fiber assembly and decrease proliferation when expressed in arterial smooth muscle cells (Merrilees et al., 2002; Lemire et al., 2002). Hinek and colleagues (2004) showed that retroviral transduction of skin fibroblasts of patients with Costello syndrome or Hurler disease with V3 cDNA reverses the impairment of elastic fiber assembly and restores normal proliferation of the cells, probably by rescuing the function of the tropoelastin chaperone (EBP) (Hinek et al., 2004).

Phenotypic similarities have been described between patients with Costello syndrome, Hurler disease, and other mucopolysaccharidoses (Hinek et al., 2000). Mucopolysaccharidoses are caused by a primary deficiency of specific lysosomal enzymes required for degradation of glycosaminoglycans (GAGs). The inability to degrade GAGs leads to their lysosomal accumulation and subsequent development of these disorders (Horwitz, 1979). Similarly, apparent accumulation of the chondroitin sulfate-bearing proteoglycans CD44 and biglycan in multiple cytoplasmatic vesicles in fibroblasts of patients with Costello syndrome might be caused by a deficiency in an enzyme required for degradation of chondroitin sulfate moieties. This hypothesis was further supported by the fact that exposure of fibroblasts of patients with CS to chondroitinase ABC, an enzyme capable of chondroitin sulfate degradation, restored normal elastic fiber assembly (Hinek et al., 2000). Thus, a gene encoding an enzyme required for the degradation of glycosaminoglycans could be considered a candidate gene for Costello syndrome. Nevertheless, Mancini and colleagues (2003) tested glycosaminoglycan turnover by measurement of total sulfate incorporation in mucopolysaccharides using fibroblasts of patients with Costello syndrome. This test usually leads to abnormal results in the majority of

patients with mucopolysaccharidoses but was normal in five Costello patients suggesting that enzymes involved in degradation of mucopolysaccharides show normal activity in patients with Costello syndrome (Mancini et al., 2003).

Urbán and Boyd (2000) suggested that Costello and Hurler syndromes belong to elastic-fiber diseases, and the pathomechanism that leads to aberrant elastic-fiber accumulation may lie in transport mechanisms secondary to fiber assembly. An example of such a secondary elastinopathy is pseudoxanthoma elasticum (PXE), a hereditary disorder that is characterized by dystrophic mineralization of elastic fibers of the skin, retina, and cardiovascular system (Ohtani and Furukawa, 2002). Remarkably, abnormal amounts of proteoglycans were observed in fibroblasts of patients with PXE (Passi et al., 1996) similar to patients with Costello syndrome (Hinek et al., 2000). Moreover, fibroblasts of patients with PXE as well as of patients with Costello syndrome showed a higher growth rate compared to normal fibroblasts (Quaglino et al., 2000; Hinek et al., 2000). Mutations in the *ABCC6* gene are associated with all forms of PXE. *ABCC6* encodes a member of a family of ATP-binding cassette transporters (subfamily C, member 6) that is also known as multi-drug resistance protein 6 (MRP6) (Ringpfeil et al., 2000; Le Saux et al., 2000; Bergen et al., 2000). The function of the ABC transporter still remains unknown but it has been suggested that it plays a regulatory role on mesenchymal cell behavior and metabolism (Maccari et al., 2003). A similar disease mechanism can be proposed for Costello syndrome, i.e. a defect in a gene encoding a transporter or channel protein might be responsible for this disorder.

As already mentioned, skin fibroblasts of patients with Costello syndrome showed increased cell surface accumulation of chondroitin sulfate and a high rate of cellular proliferation (Hinek et al., 2000). Selective binding between glycosaminoglycans and growth factors is essential for the interaction of these latter proteins with target cells to induce signal transmission. It was shown that growth factor receptors are involved in the pathology of craniosynostoses such as Crouzon and Apert syndromes (Robertson et al., 1998). Fibroblasts obtained from patients with Apert and Crouzon syndromes differed from normal cells in their extracellular matrix macromolecule accumulation (Carinci et al., 2000). Fibroblasts of patients with Crouzon syndrome secreted less total glycosaminoglycans into the medium, particularly hyaluronic acid and heparan sulfate, whereas an increase of chondroitin sulfate secretion was observed. Collagen types I and III were raised in fibroblast medium of patients with Crouzon syndrome whereas the concentration of fibronectin was lower (Bodo et al., 1996). Fibroblasts of patients with Apert syndrome produced more GAGs, collagen types I and III, and fibronectin. The amount of hyaluronic acid was much higher and also the amount

of heparan sulfate, chondroitin sulfate, and dermatan sulfate was increased in the media (Bodo et al., 1997). Both Crouzon and Apert syndromes are autosomal dominant diseases that are caused by point mutations in the fibroblast growth factor receptor 2 (*FGFR2*) gene (Reardon et al., 1994; Wilkie et al., 1995). Binding of basic fibroblast growth factor (bFGF) to FGFR1, FGFR2, and FGFR3 in the presence of heparan sulfate proteoglycans leads to dimerization of two receptor molecules followed by tyrosine autophosporylation of the intracellular kinase domains (Mangasarian et al., 1997). Constitutive receptor activation seems to be the underlying defect in Crouzon syndrome (Robertson et al., 1998). It is tempting to speculate that binding of a growth factor to accumulated glycosaminoglycans (chondroitin sulfate) could be altered in patients with Costello syndrome and thereby, leading to an aberrant signal transduction cascade. Thus genes encoding growth factors as well as growth factor receptors can also be considered functional candidates for Costello syndrome.

Phenotypic similarities have been described between patients with Costello and Noonan syndromes (NS). Mutations in the *PTPN11* gene account for approximately 50% of NS cases (Tartaglia et al., 2001). *PTPN11* encodes a protein tyrosine phosphatase, non-receptor type 11 (SHP2) (Freeman et al., 1992; Feng et al., 1993; Vogel et al., 1993). In general, SHP2 is involved in several intracellular signal transduction pathways that control multiple developmental processes (Dechert et al., 1995; Feng, 1999). For example, SHP2 is required for the epidermal growth factor (EGF) signaling pathway that controls semilunar valvulogenesis of the heart (Chen et al., 2000). It has also been shown that SHP2 is necessary for normal growth and development (Tang et al., 1995; Bennett et al., 1996; Saxton et al., 1997; Saxton et al., 2000). Tartaglia and colleagues (2002) proposed that Noonan syndrome-causative mutations induce a gain of function. Moreover, it has been reported that three of the Noonan syndrome-associated SHP2 mutants expressed in eukaryotic cells showed increased basal protein tyrosine phosphatase activity that could be further augmented through EGF stimulation (Fragale et al., 2004). EGF binds to and activates the epidermal growth factor receptor (EGFR) (Prigent and Lemoine, 1992). Upon EGF stimulation, the Grb2-asssociated binder-1 (GAB1) protein is recruited to the cell membrane, becomes tyrosyl phosphorylated, and acts as docking site for several signaling proteins, including SHP2 (Takahashi-Tezuka et al., 1998; Hibi and Hirano, 2000; Maroun et al, 2000). Thereby, SHP2 positively controls activation of the Ras/MAPK cascade (Cunnick et al., 2002). Recently, *PTPN11* was excluded as the major causative gene for Costello syndrome (Tartaglia et al., 2003; Tröger et al., 2003). Tartaglia and colleagues (2003) described that the gain of function mutations in *PTPN11* result in increased signaling through the Ras/mitogen-activated protein kinase

(ERK2/MAPK1) cascade, leading to cell proliferation. The authors discussed that the phenotypic overlap between patients with Costello and Noonan syndromes suggests that the causative gene(s) for CS might encode protein(s) participating in the signal transduction cascade of the Ras/MAPK pathway. Therefore, the *EGFR* as well as the *GAB1* gene encoding proteins involved in EGF signaling can be considered functional candidate genes for Costello syndrome.

Several reports provided further evidence for the assumption that *EGFR* is an attractive candidate gene for CS. The importance of EGFR during development was shown by the analysis of various mutant mice. Phenotypic abnormalities of these *Egfr* mutant mice can be directly compared to the clinical features observed in patients with Costello syndrome. A null mutation in *Egfr* is lethal during embryonic development, the mice show epithelial and neurodegenerative defects. Only certain strains of mutant mice can survive up to three weeks after birth with severe impairment in development of multiple organs including skin and with failure of hair growth (Miettinen et al., 1995; Threadgill et al., 1995; Sibilia and Wagner, 1995). A point mutation in *Egfr* results in a less severe phenotype of curly whiskers and pronounced waviness in the first hair coat. This mutant mouse is called waved-2 (*wa-2*) (Fowler et al., 1995). Similarly, patients with Costello syndrome show curly and often sparely implanted hair (Hennekam, 2003). The *wa-2* mutation is a single nucleotide change in the *Egfr* gene that results in impairment of tyrosine kinase activity of the receptor (Luetteke et al., 1994; Fowler et al., 1995). In addition, $Egfr^{wa2/wa2}$ mice exhibit semilunar valve enlargement resulting from overabundant mesenchymal cells (Chen et al., 2000). The penetrance and severity of the defects in $Egfr^{wa2/wa2}$ mice can be enhanced by introducing a heterozygous *Ptpn11* mutation. Compound $Egfr^{wa2/wa2}$: $Ptpn11^{+/-}$ mutant mice develop aortic stenosis and regurgitation, and show premature lethality. Thus, Egfr and Shp2 were identified as components of a growth factor signaling pathway required specifically for semilunar valvulogenesis (Chen et al., 2000). In patients with Costello syndrome congenital heart defects were described such as pulmonary valve stenosis, ventricular and atrial septal defects, bicuspid aortic valve, and aortic stenosis (Hennekam, 2003).

Recently, mice in which endogenous *Egfr* was replaced by human *EGFR* cDNA were generated by a knock-in strategy (Sibilia et al., 2003). The humanized EGFR mice ($hEGFR^{KI/KI}$) displayed tissue-specific hypomorphic phenotypes in bone and epithelial cells. In contrast, in epithelial tissues such as skin and hair follicles, where the $hEGFR^{KI/KI}$ allele was poorly expressed, severe defects were observed. Homozygous $hEGFR^{KI/KI}$ mice are growth retarded, show skin and hair defects similar to $Egfr^{-/-}$ mutants and develop a severe

heart hypertrophy with semilunar valve abnormalities (Sibilia et al., 2003). Similarly, patients with Costello syndrome show severe early postnatal growth retardation, thickened skin, curly hair, and cardiovascular abnormalities (Hennekam, 2003).

It is known that EGFR is required for skin development and is implicated in epithelial tumor formation. To investigate EGFR responsive pathways in the skin, transgenic mice (K5-SOS-F) expressing a dominant form of hSOS (SOS-F) under control of a full-length K5 promoter were generated. All K5-SOS-F mice developed skin papillomas (Sibilia et al., 2000). One of the major skin symptoms in patients with Costello syndrome is the presence of papillomata around the nose, mouth, joints, abdomen, and perianally (Hennekam, 2003).

The dark (olive) color of the skin present in patients with Costello syndrome was already mentioned. Remarkably, the mutant mice *Dsk5*, dark skin mutant mice carrying an L863Q substitution within the tyrosine kinase domain of Egfr, developed footpad pigmentation that became apparent only in adult animals and progressed with age (Fitch et al., 2003). Histologically, the epidermis of *Dsk5* skin was thickened with a pattern of excess pigment deposition and an increased number of melanocytes in the epidermis. In three weeks old animals, a wavy coat was identified (Fitch et al., 2003). In comparison, the skin of patients with Costello syndrome is thickened, soft, and velvety in feel, and has a darker color. The presence of acanthosis nigricans in Costello patients has also been reported (Hennekam, 2003). Acanthosis nigricans (AN) is a velvety and papillomatous pigmented hyperkeratosis of the flexures and neck (Schwartz, 1994). In AN associated with malignancy, elevated serum levels of growth factors, in particular TGF-α, are believed to act via EGFR (Ellis et al., 1987; Koyama et al., 1997; Haase and Hunzelmann, 2002). In inherited syndromes of which acanthosis nigricans is a feature, inappropriate activation of the insulin-like growth factor 1 receptor (IGF1R) and FGFRs have been implicated (reviewed in Torley et al., 2002).

Taken together, it can be speculated that some of the phenotypic features identified in various *Egfr* mutant mice might correspond to clinical findings observed in patients with Costello syndrome. Therefore, the gene encoding epidermal growth factor receptor (*EGFR*) should be considered a promising functional candidate gene for Costello syndrome.

# V. Summary

In this work, a female patient with a phenotype resembling Costello syndrome and carrying an apparently balanced *de novo* translocation t(1;22)(q24.3;q13.1) was studied. In general, balanced chromosomal rearrangements associated with a Mendelian disorder are powerful tools for mapping novel disease genes. Molecular analysis of the breakpoint regions may help to identify interrupted gene(s) responsible for the phenotype of the patient. By mutation analysis of gene(s) located in the breakpoint regions in patients with the same disease phenotype and a normal karyotype, the disease causing gene can be identified by discovering additional mutations. Initially, a breakpoint spanning PAC clone for the breakpoint on 1q24.3 as well as a cosmid clone overlapping the breakpoint on chromosome 22 were identified by fluorescence *in situ* hybridization. Subsequent database analysis of the DNA sequence revealed that the gene encoding the platelet-derived growth factor beta *(PDGFB)* is located on the insert of the cosmid. Characterization of the breakpoint regions at the molecular level showed that the translocation patient carries a mosaic of two derivative chromosomes 1 in her peripheral blood lymphocytes, in one of which the coding region of the *PDGFB* gene was disrupted. Both the initial translocation and the secondary intrachromosomal rearrangement appear to have occurred by non-homologous (illegitimate) recombination.

In the 1q24.3 breakpoint region of the patient with the 1;22 translocation and a phenotype resembling Costello syndrome, a putative novel gene was identified and partially characterized suggesting that it represents a pseudogene. The *PDGFB* gene was found to be disrupted by the breakpoint in 22q13.1. The considered pattern of inheritance for Costello syndrome is autosomal dominant and thus, disruption of one *PDGFB* allele by the translocation could result in the Costello phenotype in this patient. Therefore, the *PDGFB* gene was a good candidate gene for Costello syndrome. Mutation analysis of *PDGFB* and five genes belonging to the *PDGF/R* family (*PDGFA*, *PDGFC*, *PDGFD*, *PDGFRA*, and *PDGFRB*) revealed no pathogenic mutations in 18 sporadic patients with Costello syndrome. These negative results prompted us to re-evaluate the clinical symptoms of the translocation patient. Although some of the typical clinical features of patients with Costello syndrome were also found in the translocation patient, the majority of them was absent. Therefore, it seems likely that the translocation patient shows a ‘unique’ phenotype not resembling any known and well-defined syndrome.

In total RNA isolated from lymphocytes of the translocation patient, four fusion transcripts consisting of *PDGFB* exons and various DNA fragments located in the breakpoint region on

1q24.3 were identified. In two of the mRNAs, exon 6 of *PDGFB*, encoding the 41 C-terminal amino acid residues, was absent. *PDGFB* exon 6 encodes a stretch of basic amino acids, the retention motif, that mediates interaction of PDGFB with components of the extracellular matrix. After maturation and cleavage of the C-terminal retention sequence, the PDGFB molecule becomes diffusible. Immunofluorescence analysis showed that the fusion protein between PDGFB wild-type and the green fluorescence protein EGFP was dispersed and formed a network-like structure in the extracellular matrix whereas the two aberrant PDGFB-EGFP fusion proteins (without retention motif) were localized in aggregates. We speculate that the biological consequences of the mutant *PDGFB* allele might have contributed to the disease phenotype of the translocation patient.

In an alternative attempt to identify the disease gene for Costello syndrome, we searched for functional candidate genes for this disorder. Mutation analysis of the *FOXO1A*, *TGFB1*, and *LMNA* genes was performed and no pathogenic mutation was identified in sporadic patients with Costello syndrome. Nevertheless, the identification of disease genes for syndromes showing phenotypic overlap with patients with Costello syndrome, like Noonan syndrome, may help to select novel functional candidate genes for Costello syndrome. For example, *PTPN11*, one causative gene for Noonan syndrome, encodes the protein tyrosine phosphatase SHP2 implicated in epidermal growth factor (EGF) dependent signaling pathways. These data together with the phenotypic features observed in various mutant mice suggest that the gene encoding the epidermal growth factor receptor (*EGFR*) is a promising candidate gene for Costello syndrome.

# V. Zusammenfassung

In dieser Arbeit wurde eine balanciert erscheinende *de novo* Translokation, t(1;22)(q24.3;q13.1), bei einer Patientin mit einer Erkrankung, die dem Costello-Syndrom ähnelt, molekular charakterisiert. Im allgemeinen kann bei Personen, die ein *de novo* chromosomales Rearrangement aufweisen und einen Mendel'schen Krankheitsphänotyp zeigen, vermutet werden, dass die chromosomale Anomalie ursächlich für die Erkrankung ist. Je nachdem, ob in einer der Bruchregionen ein Gen gefunden wird, das unterbrochen wurde oder nicht, kommen ein Gen oder mehrere Gene für eine Mutationsanalyse bei einem Patientenkollektiv mit dem gleichen Krankheitsbild und einem normalen Karyotyp in Frage. Mit dem Auffinden weiterer Mutationen wird schließlich das Krankheitsgen identifiziert. Durch Fluoreszenz-*in-situ*-Hybridisierung wurde ein bruchpunktüberspannender PAC-Klon für die Bruchregion 1q24.3 und ein Cosmid für den Bruchpunkt auf dem Chromosom 22 gefunden. Datenbankrecherchen mit der DNA-Sequenz des Cosmides zeigten, dass sich das Gen, das für den Blutplättchenwachstumsfaktor B (PDGFB) kodiert, auf dem Insert des Cosmids befindet. Durch die molekulare Aufklärung der Translokation auf RNA- und DNA-Ebene konnte gezeigt werden, dass die Patientin ein Mosaik, bestehend aus zwei verschiedenen derivativen Chromosomen 1, aufweist. Das *PDGFB*-Gen ist auf beiden dieser derivativen Chromosomen 1 unterbrochen, wobei nur in einem Fall die Kodierregion direkt betroffen ist. Sowohl die ursprüngliche Translokation als auch das zweite intrachromosomale Rearrangement sind vermutlich durch eine nicht-homologe (illegitime) Rekombination entstanden.

In der Bruchpunktregion 1q24.3 der Patientin mit der 1;22-Translokation und dem möglichen Costello-Syndrom wurde ein putatives neues Gen gefunden und partiell charakterisiert, bei dem es sich vermutlich um ein Pseudogen handelt. Das *PDGFB*-Gen in 22q13.1 wurde durch den Bruch unterbrochen. Der für das Costello-Syndrom angenommene autosomal-dominante Erbgang ist mit der Annahme vereinbar, dass die Unterbrechung des *PDGFB*-Allels zum Costello-ähnlichen Phänotyp der Translokationspatientin geführt haben könnte. Daher wurde *PDGFB* als Kandidatengen für das Costello-Syndrom angesehen. Eine Mutationsanalyse des *PDGFB*-Gens sowie von fünf weiteren Genen (*PDGFA*, *PDGFC*, *PDGFD*, *PDGFRA* und *PDGFRB*), die zur *PDGF/R*-Familie gehören, ergab keine pathogene Mutation bei 18 sporadischen Patienten mit Costello-Syndrom. Diese negativen Befunde ließen die Frage aufkommen, ob der als Costello-Syndrom beschriebene klinische Phänotyp der Translokationspatientin tatsächlich zutrifft. Zusammenfassend fanden sich zwar einige phänotypische Überlappungen der Translokationspatientin mit Symptomen von Patienten mit Costello-Syndrom, aller-

dings weist sie nicht die Mehrzahl der häufig beobachteten, typischen Auffälligkeiten von Patienten mit Costello-Syndrom auf. Daher ist davon auszugehen, dass sie einen „privaten" Phänotyp zeigt, der in dieser Form noch nicht beschrieben wurde.

In der Gesamt-RNA aus Lymphozyten der Translokationspatientin wurden vier verschiedene Fusionstranskripte zwischen Anteilen des *PDGFB*-Gens und Anteilen aus der Bruchregion 1q24.3 identifiziert. Bei zwei der *PDGFB*-Fusions-RNAs fehlte das Exon 6 des *PDGFB*-Gens, das für eine Reihe basischer Aminosäuren, das sogenannte *Retention*-Motiv, kodiert. Das *Retention*-Motiv ist dafür verantwortlich, dass der Wachstumsfaktor zunächst noch mit der extrazellulären Matrix in Kontakt bleibt und erst bei Bedarf durch proteolytische Spaltung freigesetzt wird. Mit Hilfe von Immunfluoreszenzanalysen konnte gezeigt werden, dass ein Fusionsprotein zwischen PDGFB-Wildtyp mit dem grünen Fluoreszenzprotein EGFP in einem feinen Netzwerk verteilt in der extrazellulären Matrix vorliegt, wohingegen die beiden aberranten PDGFB-EGFP-Fusionsproteine (ohne *Retention*-Motiv) relativ große Aggregate in der extrazellulären Matrix bilden. Diese Daten führten zu der Hypothese, dass die mutierten PDGFB-Proteine andere biologische Eigenschaften haben als das Wildtyp-Protein und dieser Umstand zur Entstehung des Phänotyps der Translokationspatientin beigetragen haben könnte.

In einem alternativen Ansatz wurde nach funktionellen Kandidatengenen für das Costello-Syndrom gesucht. Mutationsanalysen der *FOXO1A*-, *TGFB1*- und *LMNA*-Gene ergaben keine pathogenen Mutationen bei sporadischen Patienten mit Costello-Syndrom. Zur Zeit gibt es wenig Anhaltspunkte für die physikalische Lokalisation des Gens für das Costello-Syndrom im menschlichen Genom. Phänotypische Überschneidungen zwischen Patienten mit Costello-Syndrom und anderen Erkrankungen, z.B. dem Noonan-Syndrom, können bei dem Auffinden neuer Kandidatengene helfen. Das *PTPN11*-Gen, ein für das Noonan-Syndrom ursächliches Gen, kodiert für die Proteintyrosin-Phosphatase SHP2, die bei der vom epidermalen Wachstumsfaktor (EGF)-abhängigen Signalkaskade eine Rolle spielt. Diese Befunde zusammen mit den phänotypischen Merkmalen verschiedener Mausmutanten weisen auf das den epidermalen Wachstumsfaktorrezeptor kodierende *EGFR*-Gen als ein vielversprechendes Kandidatenprotein/-gen für das Costello-Syndrom hin.

# VI. References


Abeysinghe, S.S., Chuzhanova, N., Krawczak, M., Ball, E.V. and Cooper, D.N. (2003) Translocation and gross deletion breakpoints in human inherited disease and cancer I: Nucleotide composition and recombination-associated motifs. *Hum Mutat*, **22**, 229-244.

Andersson, M., Ostman, A., Westermark, B. and Heldin, C.H. (1994) Characterization of the retention motif in the C-terminal part of the long splice form of platelet-derived growth factor A-chain. *J Biol Chem*, **269**, 926-930.

Baker, P.B., Baba, N. and Boesel, C.P. (1981) Cardiovascular abnormalities in progeria. Case report and review of the literature. *Arch Pathol Lab Med*, **105**, 384-386.

Bennett, A.M., Hausdorff, S.F., O'Reilly, A.M., Freeman, R.M. and Neel, B.G. (1996) Multiple requirements for SHPTP2 in epidermal growth factor-mediated cell cycle progression. *Mol Cell Biol*, **16**, 1189-1202.

Bergen, A.A., Plomp, A.S., Schuurman, E.J., Terry, S., Breuning, M., Dauwerse, H., Swart, J., Kool, M., van Soest, S., Baas, F., ten Brink, J.B. and de Jong, P.T. (2000) Mutations in ABCC6 cause pseudoxanthoma elasticum. *Nat Genet*, **25**, 228-231.

Bergsten, E., Uutela, M., Li, X., Pietras, K., Ostman, A., Heldin, C.H., Alitalo, K. and Eriksson, U. (2001) PDGF-D is a specific, protease-activated ligand for the PDGF beta-receptor. *Nat Cell Biol*, **3**, 512-516.

Betsholtz, C., Karlsson, L. and Lindahl, P. (2001) Developmental roles of platelet-derived growth factors. *Bioessays*, **23**, 494-507.

Billerey, C., Chopin, D., Aubriot-Lorton, M.H., Ricol, D., Gil Diez de Medina, S., Van Rhijn, B., Bralet, M.P., Lefrere-Belda, M.A., Lahaye, J.B., Abbou, C.C., Bonaventure, J., Zafrani, E.S., van der Kwast, T., Thiery, J.P. and Radvanyi, F. (2001) Frequent FGFR3 mutations in papillary non-invasive bladder (pTa) tumors. *Am J Pathol*, **158**, 1955-1959.

Birnboim, H.C. and Doly, J. (1979) A rapid alkaline extraction procedure for screening recombinant plasmid DNA. *Nucleic Acids Res*, **7**, 1513-1523.

Bodkin, N.M., Mortimer, E.S. and Demmer, L.A. (1999) Male to male transmission of Costello syndrome consistent with autosomal dominant inheritance. *49th Annual Meeting of the American Society of Human Genetics*, San Francisco, Vol. October 19 - 23.

Bodo, M., Carinci, F., Baroni, T., Becchetti, E., Giammarioli, M., Bellucci, C., Pezzetti, F., Evangelisti, R. and Carinci, P. (1996) Effects of interleukins on Crouzon fibroblast phenotype *in vitro*. Release of cytokines and IL-6 mRNA expression. *Cytokine*, **8**, 772-783.

Bodo, M., Carinci, F., Baroni, T., Giammarioli, M., Bellucci, C., Bosi, G., Pezzetti, F., Becchetti, E., Evangelisti, R. and Carinci, P. (1997) Apert's syndrome: differential *in vitro* production of matrix macromolecules and its regulation by interleukins. *Eur J Clin Invest*, **27**, 36-42.

Bonaglia, M.C., Giorda, R., Borgatti, R., Felisari, G., Gagliardi, C., Selicorni, A. and Zuffardi, O. (2001) Disruption of the ProSAP2 gene in a t(12;22)(q24.1;q13.3) is associated with the 22q13.3 deletion syndrome. *Am J Hum Genet*, **69**, 261-268.

Boström, H., Willetts, K., Pekny, M., Leveen, P., Lindahl, P., Hedstrand, H., Pekna, M., Hellstrom, M., Gebre-Medhin, S., Schalling, M., Nilsson, M., Kurland, S., Tornell, J., Heath, J.K. and Betsholtz, C. (1996) PDGF-A signaling is a critical event in lung alveolar myofibroblast development and alveogenesis. *Cell*, **85**, 863-873.

Bruckner-Tuderman, L. (1999) Hereditary skin diseases of anchoring fibrils. *J Dermatol Sci*, **20**, 122-133.

Budarf, M.L., Collins, J., Gong, W., Roe, B., Wang, Z., Bailey, L.C., Sellinger, B., Michaud, D., Driscoll, D.A. and Emanuel, B.S. (1995) Cloning a balanced translocation associated with DiGeorge syndrome and identification of a disrupted candidate gene. *Nat Genet*, **10**, 269-278.

Bugge, M., Bruun-Petersen, G., Brondum-Nielsen, K., Friedrich, U., Hansen, J., Jensen, G., Jensen, P.K., Kristoffersson, U., Lundsteen, C., Niebuhr, E., Rasmussen, K.R., Rasmussen, K. and Tommerup, N. (2000) Disease associated balanced chromosome rearrangements: a resource for large scale genotype-phenotype delineation in man. *J Med Genet*, **37**, 858-865.

Cakir, M., Arici, C., Tacoy, S. and Karayalcin, U. (2004) A case of Costello with parathyroid adenoma and hyperprolactinemia. *Am J Med Genet*, **124A**, 196-199.

Cappellen, D., De Oliveira, C., Ricol, D., de Medina, S., Bourdin, J., Sastre-Garau, X., Chopin, D., Thiery, J.P. and Radvanyi, F. (1999) Frequent activating mutations of FGFR3 in human bladder and cervix carcinomas. *Nat Genet*, **23**, 18-20.

Carinci, P., Becchetti, E. and Bodo, M. (2000) Role of the extracellular matrix and growth factors in skull morphogenesis and in the pathogenesis of craniosynostosis. *Int J Dev Biol*, **44**, 715-723.

Chang, A.C. and Cohen, S.N. (1978) Construction and characterization of amplifiable multicopy DNA cloning vehicles derived from the P15A cryptic miniplasmid. *J Bacteriol*, **134**, 1141-1156.

Chen, B., Bronson, R.T., Klaman, L.D., Hampton, T.G., Wang, J.F., Green, P.J., Magnuson, T., Douglas, P.S., Morgan, J.P. and Neel, B.G. (2000) Mice mutant for Egfr and Shp2 have defective cardiac semilunar valvulogenesis. *Nat Genet*, **24**, 296-299.

Chuzhanova, N., Abeysinghe, S.S., Krawczak, M. and Cooper, D.N. (2003) Translocation and gross deletion breakpoints in human inherited disease and cancer II: Potential involvement of repetitive sequence elements in secondary structure formation between DNA ends. *Hum Mutat*, **22**, 245-251.

Ciardiello, F., Kim, N., McGeady, M.L., Liscia, D.S., Saeki, T., Bianco, C. and Salomon, D.S. (1991) Expression of transforming growth factor alpha (TGF alpha) in breast cancer. *Ann Oncol*, **2**, 169-182.

Cormack, B.P., Valdivia, R.H. and Falkow, S. (1996) FACS-optimized mutants of the green fluorescent protein (GFP). *Gene*, **173**, 33-38.

Costello, J.M. (1971) A new syndrome. *NZ Med J*, **74**, 397.

Costello, J.M. (1977) A new syndrome: mental subnormality and nasal papillomata. *Aust Paediatr J*, **13**, 114-118.

Cunnick, J.M., Meng, S., Ren, Y., Desponts, C., Wang, H.G., Djeu, J.Y. and Wu, J. (2002) Regulation of the mitogen-activated protein kinase signaling pathway by SHP2. *J Biol Chem*, **277**, 9498-9504.

Czeizel, A.E. and Tímár, L. (1995) Hungarian case with Costello syndrome and translocation t(1,22). *Am J Med Genet*, **57**, 501-503.

Datson, N.A., Semina, E., van Staalduinen, A.A., Dauwerse, H.G., Meershoek, E.J., Heus, J.J., Frants, R.R., den Dunnen, J.T., Murray, J.C. and van Ommen, G.J. (1996) Closing in on the Rieger syndrome gene on 4q25: mapping translocation breakpoints within a 50-kb region. *Am J Hum Genet*, **59**, 1297-1305.

De Kok, Y.J., van der Maarel, S.M., Bitner-Glindzicz, M., Huber, I., Monaco, A.P., Malcolm, S., Pembrey, M.E., Ropers, H.H. and Cremers, F.P. (1995) Association between X-linked mixed deafness and mutations in the POU domain gene POU3F4. *Science*, **267**, 685-688.

De Kok, Y.J., Vossenaar, E.R., Cremers, C.W., Dahl, N., Laporte, J., Hu, L.J., Lacombe, D., Fischel-Ghodsian, N., Friedman, R.A., Parnes, L.S., Thorpe, P., Bitner-Glindzicz, M., Pander, H.J., Heilbronner, H., Graveline, J., den Dunnen, J.T., Brunner, H.G., Ropers, H.H. and Cremers, F.P. (1996) Identification of a hot spot for microdeletions in patients with X-linked deafness type 3 (DFN3) 900 kb proximal to the DFN3 gene POU3F4. *Hum Mol Genet*, **5**, 1229-1235.

De Sandre-Giovannoli, A., Bernard, R., Cau, P., Navarro, C., Amiel, J., Boccaccio, I., Lyonnet, S., Stewart, C.L., Munnich, A., Le Merrer, M. and Levy, N. (2003) Lamin a truncation in Hutchinson-Gilford progeria. *Science*, **300**, 2055.

DeBusk, F.L. (1972) The Hutchinson-Gilford progeria syndrome. Report of 4 cases and review of the literature. *J Pediatr*, **80**, 697-724.

Dechert, U., Duncan, A.M., Bastien, L., Duff, C., Adam, M. and Jirik, F.R. (1995) Protein-tyrosine phosphatase SH-PTP2 (PTPN11) is localized to 12q24.1-24.3. *Hum Genet*, **96**, 609-615.

Deininger, P.L. and Batzer, M.A. (1999) Alu repeats and human disease. *Mol Genet Metab*, **67**, 183-193.

Deininger, P.L., Jolly, D.J., Rubin, C.M., Friedmann, T. and Schmid, C.W. (1981) Base sequence studies of 300 nucleotide renatured repeated human DNA clones. *J Mol Biol*, **151**, 17-33.

Delrue, M.A., Chateil, J.F., Arveiler, B. and Lacombe, D. (2003) Costello syndrome and neurological abnormalities. *Am J Med Genet*, **123A**, 301-305.

Derynck, R., Akhurst, R.J. and Balmain, A. (2001) TGF-beta signaling in tumor suppression and cancer progression. *Nat Genet*, **29**, 117-129.

Di Rocco, M., Gatti, R., Gandullia, P., Barabino, A., Picco, P. and Borrone, C. (1993) Report on two patients with Costello syndrome and sialuria. *Am J Med Genet*, **47**, 1135-1140.

Ellis, D.L., Kafka, S.P., Chow, J.C., Nanney, L.B., Inman, W.H., McCadden, M.E. and King, L.E., Jr. (1987) Melanoma, growth factors, acanthosis nigricans, the sign of Leser-Trelat, and multiple acrochordons. A possible role for alpha-transforming growth factor in cutaneous paraneoplastic syndromes. *N Engl J Med*, **317**, 1582-1587.

Eming, S.A., Yarmush, M.L., Krueger, G.G. and Morgan, J.R. (1999) Regulation of the spatial organization of mesenchymal connective tissue: effects of cell-associated versus released isoforms of platelet-derived growth factor. *Am J Pathol*, **154**, 281-289.

Eriksson, M., Brown, W.T., Gordon, L.B., Glynn, M.W., Singer, J., Scott, L., Erdos, M.R., Robbins, C.M., Moses, T.Y., Berglund, P., Dutra, A., Pak, E., Durkin, S., Csoka, A.B., Boehnke, M., Glover, T.W. and Collins, F.S. (2003) Recurrent de novo point mutations in lamin A cause Hutchinson-Gilford progeria syndrome. *Nature*, **423**, 293-298.

Fahsold, R., Habash, T., Trautmann, U., Haustein, A. and Pfeiffer, R.A. (1995) Familial reciprocal translocation t(17;19) (q11.2;q13.2) associated with neurofibromatosis type 1, including one patient with non-Hodgkin lymphoma and an additional t(14;20) in B lymphocytes. *Hum Genet*, **96**, 65-69.

Fantes, J., Redeker, B., Breen, M., Boyle, S., Brown, J., Fletcher, J., Jones, S., Bickmore, W., Fukushima, Y., Mannens, M. and et al. (1995) Aniridia-associated cytogenetic rearrangements suggest that a position effect may cause the mutant phenotype. *Hum Mol Genet*, **4**, 415-422.

Feng, G.S. (1999) Shp-2 tyrosine phosphatase: signaling one cell or many. *Exp Cell Res*, **253**, 47-54.

Feng, G.S., Hui, C.C. and Pawson, T. (1993) SH2-containing phosphotyrosine phosphatase as a target of protein-tyrosine kinases. *Science*, **259**, 1607-1611.

Field, S.L., Khachigian, L.M., Sleigh, M.J., Yang, G., Vandermark, S.E., Hogg, P.J. and Chesterman, C.N. (1996) Extracellular matrix is a source of mitogenically active platelet-derived growth factor. *J Cell Physiol*, **168**, 322-332.

Fitch, K.R., McGowan, K.A., van Raamsdonk, C.D., Fuchs, H., Lee, D., Puech, A., Herault, Y., Threadgill, D.W., Hrabe de Angelis, M. and Barsh, G.S. (2003) Genetics of dark skin in mice. *Genes Dev*, **17**, 214-228.

Floeth, M. and Bruckner-Tuderman, L. (1999) Digenic junctional epidermolysis bullosa: mutations in COL17A1 and LAMB3 genes. *Am J Hum Genet*, **65**, 1530-1537.

Flomen, R.H., Vatcheva, R., Gorman, P.A., Baptista, P.R., Groet, J., Barisic, I., Ligutic, I. and Nizetic, D. (1998) Construction and analysis of a sequence-ready map in 4q25: Rieger syndrome can be caused by haploinsufficiency of RIEG, but also by chromosome breaks approximately 90 kb upstream of this gene. *Genomics*, **47**, 409-413.

Fowler, K.J., Walker, F., Alexander, W., Hibbs, M.L., Nice, E.C., Bohmer, R.M., Mann, G.B., Thumwood, C., Maglitto, R., Danks, J.A. and et al. (1995) A mutation in the epidermal growth factor receptor in waved-2 mice has a profound effect on receptor biochemistry that results in impaired lactation. *Proc Natl Acad Sci U S A*, **92**, 1465-1469.

Fragale, A., Tartaglia, M., Wu, J. and Gelb, B.D. (2004) Noonan syndrome-associated SHP2/PTPN11 mutants cause EGF-dependent prolonged GAB1 binding and sustained ERK2/MAPK1 activation. *Hum Mutat*, **23**, 267-277.

Freeman, R.M., Jr., Plutzky, J. and Neel, B.G. (1992) Identification of a human src homology 2-containing protein-tyrosine-phosphatase: a putative homolog of Drosophila corkscrew. *Proc Natl Acad Sci U S A*, **89**, 11239-11243.

Fuhrman, S.A., Deininger, P.L., LaPorte, P., Friedmann, T. and Geiduschek, E.P. (1981) Analysis of transcription of the human Alu family ubiquitous repeating element by eukaryotic RNA polymerase III. *Nucleic Acids Res*, **9**, 6439-6456.

Gahl, W.A., Renlund, M. and Thoene, J.G. (1989) Lysosomal transport disorders: cystinosis and sialic acid storage disorders. In Scriver, C.R., Beaudet, A.L., Sly, W.S. and Valle, D. (eds) *The Metabolic Basis of Inherited Disease*. McGraw-Hill, New York.

Galili, N., Davis, R.J., Fredericks, W.J., Mukhopadhyay, S., Rauscher, F.J., 3rd, Emanuel, B.S., Rovera, G. and Barr, F.G. (1993) Fusion of a fork head domain gene to PAX3 in the solid tumour alveolar rhabdomyosarcoma. *Nat Genet*, **5**, 230-235.

Gessler, M., Simola, K.O. and Bruns, G.A. (1989) Cloning of breakpoints of a chromosome translocation identifies the AN2 locus. *Science*, **244**, 1575-1578.

Gluzman, Y. (1981) SV40-transformed simian cells support the replication of early SV40 mutants. *Cell*, **23**, 175-182.

Gotter, A.L., Shaikh, T.H., Budarf, M.L., Rhodes, C.H. and Emanuel, B.S. (2004) A palindrome-mediated mechanism distinguishes translocations involving LCR-B of chromosome 22q11.2. *Hum Mol Genet*, **13**, 103-115.

Gripp, K.W., Scott, C.I., Jr., Nicholson, L., McDonald-McGinn, D.M., Ozeran, J.D., Jones, M.C., Lin, A.E. and Zackai, E.H. (2002) Five additional Costello syndrome patients with rhabdomyosarcoma: proposal for a tumor screening protocol. *Am J Med Genet*, **108**, 80-87.

Haase, I. and Hunzelmann, N. (2002) Activation of epidermal growth factor receptor/ERK signaling correlates with suppressed differentiation in malignant acanthosis nigricans. *J Invest Dermatol*, **118**, 891-893.

Hanahan, D. (1983) Studies on transformation of Escherichia coli with plasmids. *J Mol Biol*, **166**, 557-580.

Hatamochi, A., Nagayama, H., Kuroda, K., Shinkai, H., Ishikiriyama, S., Kobayashi, M. and Kobayashi, K. (2000) Costello syndrome with decreased gene expression of elastin in cultured dermal fibroblasts. *Dermatology*, **201**, 366-369.

Hatamochi, A., Wada, T., Takeda, K., Ueki, H., Kawano, S., Terada, K. and Morita, T. (1991) Collagen metabolism in cutis laxa fibroblasts: increased collagenase gene expression associated with unaltered expression of type I and type III collagen. *J Invest Dermatol*, **97**, 483-487.

Heldin, C.H. and Westermark, B. (1999) Mechanism of action and *in vivo* role of platelet-derived growth factor. *Physiol Rev*, **79**, 1283-1316.

Hellström, M., Kalen, M., Lindahl, P., Abramsson, A. and Betsholtz, C. (1999) Role of PDGF-B and PDGFR-beta in recruitment of vascular smooth muscle cells and pericytes during embryonic blood vessel formation in the mouse. *Development*, **126**, 3047-3055.

Hennekam, R.C. (2003) Costello syndrome: an overview. *Am J Med Genet*, **117C**, 42-48.

Hibi, M. and Hirano, T. (2000) Gab-family adapter molecules in signal transduction of cytokine and growth factor receptors, and T and B cell antigen receptors. *Leuk Lymphoma*, **37**, 299-307.

Hiltunen, M., Helisalmi, S., Mannermaa, A., Alafuzoff, I., Koivisto, A.M., Lehtovirta, M., Pirskanen, M., Sulkava, R., Verkkoniemi, A. and Soininen, H. (2000) Identification of a novel 4.6-kb genomic deletion in presenilin-1 gene which results in exclusion of exon 9 in a Finnish early onset Alzheimer's disease family: an Alu core sequence-stimulated recombination? *Eur J Hum Genet*, **8**, 259-266.

Hinek, A., Braun, K.R., Liu, K., Wang, Y. and Wight, T.N. (2004) Retrovirally mediated overexpression of versican v3 reverses impaired elastogenesis and heightened proliferation exhibited by fibroblasts from Costello syndrome and Hurler disease patients. *Am J Pathol*, **164**, 119-131.

Hinek, A., Mecham, R.P., Keeley, F. and Rabinovitch, M. (1991) Impaired elastin fiber assembly related to reduced 67-kD elastin-binding protein in fetal lamb ductus arteriosus and in cultured aortic smooth muscle cells treated with chondroitin sulfate. *J Clin Invest*, **88**, 2083-2094.

Hinek, A., Molossi, S. and Rabinovitch, M. (1996) Functional interplay between interleukin-1 receptor and elastin binding protein regulates fibronectin production in coronary artery smooth muscle cells. *Exp Cell Res*, **225**, 122-131.

Hinek, A. and Rabinovitch, M. (1994) 67-kD elastin-binding protein is a protective "companion" of extracellular insoluble elastin and intracellular tropoelastin. *J Cell Biol*, **126**, 563-574.

Hinek, A., Smith, A.C., Cutiongco, E.M., Callahan, J.W., Gripp, K.W. and Weksberg, R. (2000) Decreased elastin deposition and high proliferation of fibroblasts from Costello syndrome are related to functional deficiency in the 67-kD elastin-binding protein. *Am J Hum Genet*, **66**, 859-872.

Hinek, A. and Wilson, S.E. (2000) Impaired elastogenesis in Hurler disease: dermatan sulfate accumulation linked to deficiency in elastin-binding protein and elastic fiber assembly. *Am J Pathol*, **156**, 925-938.

Hogg, P.J., Hotchkiss, K.A., Jimenez, B.M., Stathakis, P. and Chesterman, C.N. (1997) Interaction of platelet-derived growth factor with thrombospondin 1. *Biochem J*, **326 ( Pt 3)**, 709-716.

Horwitz, A.L. (1979) The mucopolysaccaridoses: clinical and biochemical correlations. *Am J Ment Defic*, **84**, 113-123.

Hovnanian, A., Rochat, A., Bodemer, C., Petit, E., Rivers, C.A., Prost, C., Fraitag, S., Christiano, A.M., Uitto, J., Lathrop, M., Barrandon, Y. and de Prost, Y. (1997) Characterization of 18 new mutations in COL7A1 in recessive dystrophic epidermolysis bullosa provides evidence for distinct molecular mechanisms underlying defective anchoring fibril formation. *Am J Hum Genet*, **61**, 599-610.

Hutchinson, G.B., Andrew, S.E., McDonald, H., Goldberg, Y.P., Graham, R., Rommens, J.M. and Hayden, M.R. (1993) An Alu element retroposition in two families with Huntington disease defines a new active Alu subfamily. *Nucleic Acids Res*, **21**, 3379-3383.

IHGSC (International Human Genome Sequencing Consortium). (2001) Initial sequencing and analysis of the human genome. *Nature*, **409**, 860-921.

Inui, M., Nishi, N., Yasumoto, A., Takenaka, I., Miyanaka, H., Matsumoto, K., Nakamura, T. and Wada, F. (1996) Enhanced gene expression of transforming growth factor-alpha and c-met in rat urinary bladder cancer. *Urol Res*, **24**, 55-60.

Ioan, D.M. and Fryns, J.P. (2002) Costello syndrome in two siblings and minor manifestations in their mother. Further evidence for autosomal dominant inheritance? *Genet Couns*, **13**, 353-356.

Ion, A., Tartaglia, M., Song, X., Kalidas, K., van der Burgt, I., Shaw, A.C., Ming, J.E., Zampino, G., Zackai, E.H., Dean, J.C., Somer, M., Parenti, G., Crosby, A.H., Patton, M.A., Gelb, B.D. and Jeffery, S. (2002) Absence of PTPN11 mutations in 28 cases of cardiofaciocutaneous (CFC) syndrome. *Hum Genet*, **111**, 421-427.

Jakobs, S., Subramaniam, V., Schonle, A., Jovin, T.M. and Hell, S.W. (2000) EFGP and DsRed expressing cultures of Escherichia coli imaged by confocal, two-photon and fluorescence lifetime microscopy. *FEBS Lett*, **479**, 131-135.

Jurka, J. and Klonowski, P. (1996) Integration of retroposable elements in mammals: selection of target sites. *J Mol Evol*, **43**, 685-689.

Kaji, M., Kurokawa, K., Hasegawa, T., Oguro, K., Saito, A., Fukuda, T., Ito, M. and Sugie, H. (2002) A case of Costello syndrome and glycogen storage disease type III. *J Med Genet*, **39**, E8.

Kalscheuer, V.M., Tao, J., Donnelly, A., Hollway, G., Schwinger, E., Kubart, S., Menzel, C., Hoeltzenbein, M., Tommerup, N., Eyre, H., Harbord, M., Haan, E., Sutherland, G.R., Ropers, H.H. and Gecz, J. (2003) Disruption of the serine/threonine kinase 9 gene causes severe X-linked infantile spasms and mental retardation. *Am J Hum Genet*, **72**, 1401-1411.

Kamoda, T., Matsui, A. and Ochiai, N. (2003) Osteofibrous dysplasia in a Japanese boy with Costello syndrome. *Clin Dysmorphol*, **12**, 211-212.

Kaufman, R.J., Murtha, P. and Davies, M.V. (1987) Translational efficiency of polycistronic mRNAs and their utilization to express heterologous genes in mammalian cells. *Embo J*, **6**, 187-193.

Kelly, J.L., Sanchez, A., Brown, G.S., Chesterman, C.N. and Sleigh, M.J. (1993) Accumulation of PDGF B and cell-binding forms of PDGF A in the extracellular matrix. *J Cell Biol*, **121**, 1153-1163.

Kerr, B., Eden, O.B., Dandamudi, R., Shannon, N., Quarrell, O., Emmerson, A., Ladusans, E., Gerrard, M. and Donnai, D. (1998) Costello syndrome: two cases with embryonal rhabdomyosarcoma. *J Med Genet*, **35**, 1036-1039.

Kerr, B., Mucchielli, M.L., Sigaudy, S., Fabre, M., Saunier, P., Voelckel, M.A., Howard, E., Elles, R., Eden, T.O., Black, G.C. and Philip, N. (2003) Is the locus for Costello syndrome on 11p? *J Med Genet*, **40**, 469-471.

Kimura, T., Suzuki, H., Ohashi, T., Asano, K., Kiyota, H. and Eto, Y. (2001) The incidence of thanatophoric dysplasia mutations in FGFR3 gene is higher in low-grade or superficial bladder carcinomas. *Cancer*, **92**, 2555-2561.

Kleinjan, D.J. and van Heyningen, V. (1998) Position effect in human genetic disease. *Hum Mol Genet*, **7**, 1611-1618.

Koyama, S., Ikeda, K., Sato, M., Shibahara, K., Yuhara, K., Fukutomi, H., Fukunaga, K., Kanazawa, N., Yuzawa, K., Fukao, K., Iijima, T., Kikuchi, M., Tomiya, T. and Fujiwara, K. (1997) Transforming growth factor-alpha (TGF alpha)-producing gastric carcinoma with acanthosis nigricans: an endocrine effect of TGF alpha in the pathogenesis of cutaneous paraneoplastic syndrome and epithelial hyperplasia of the esophagus. *J Gastroenterol*, **32**, 71-77.

Kozak, M. (1996) Interpreting cDNA sequences: some insights from studies on translation. *Mamm Genome*, **7**, 563-574.

Krebs, I., Weis, I., Hudler, M., Rommens, J.M., Roth, H., Scherer, S.W., Tsui, L.C., Fuchtbauer, E.M., Grzeschik, K.H., Tsuji, K. and Kunz, J. (1997) Translocation breakpoint maps 5 kb 3' from TWIST in a patient affected with Saethre-Chotzen syndrome. *Hum Mol Genet*, **6**, 1079-1086.

Kutsche, K., Yntema, H., Brandt, A., Jantke, I., Nothwang, H.G., Orth, U., Boavida, M.G., David, D., Chelly, J., Fryns, J.P., Moraine, C., Ropers, H.H., Hamel, B.C., van Bokhoven, H. and Gal, A. (2000) Mutations in ARHGEF6, encoding a guanine nucleotide exchange factor for Rho GTPases, in patients with X-linked mental retardation. *Nat Genet*, **26**, 247-250.

Laemmli, U.K. (1970) Cleavage of structural proteins during the assembly of the head of bacteriophage T4. *Nature*, **227**, 680-685.

LaRochelle, W.J., Jeffers, M., McDonald, W.F., Chillakuru, R.A., Giese, N.A., Lokker, N.A., Sullivan, C., Boldog, F.L., Yang, M., Vernet, C., Burgess, C.E., Fernandes, E., Deegler, L.L., Rittman, B., Shimkets, J., Shimkets, R.A., Rothberg, J.M. and Lichenstein, H.S. (2001) PDGF-D, a new protease-activated growth factor. *Nat Cell Biol*, **3**, 517-521.

LaRochelle, W.J., May-Siroff, M., Robbins, K.C. and Aaronson, S.A. (1991) A novel mechanism regulating growth factor association with the cell surface: identification of a PDGF retention domain. *Genes Dev*, **5**, 1191-1199.

Lauf, U., Lopez, P. and Falk, M.M. (2001) Expression of fluorescently tagged connexins: a novel approach to rescue function of oligomeric DsRed-tagged proteins. *FEBS Lett*, **498**, 11-15.

Le Saux, O., Urban, Z., Tschuch, C., Csiszar, K., Bacchelli, B., Quaglino, D., Pasquali-Ronchetti, I., Pope, F.M., Richards, A., Terry, S., Bercovitch, L., de Paepe, A. and Boyd, C.D. (2000) Mutations in a gene encoding an ABC transporter cause pseudoxanthoma elasticum. *Nat Genet*, **25**, 223-227.

Lemire, J.M., Merrilees, M.J., Braun, K.R. and Wight, T.N. (2002) Overexpression of the V3 variant of versican alters arterial smooth muscle cell adhesion, migration, and proliferation *in vitro*. *J Cell Physiol*, **190**, 38-45.

Levéen, P., Pekny, M., Gebre-Medhin, S., Swolin, B., Larsson, E. and Betsholtz, C. (1994) Mice deficient for PDGF B show renal, cardiovascular, and hematological abnormalities. *Genes Dev*, **8**, 1875-1887.

Li, X., Ponten, A., Aase, K., Karlsson, L., Abramsson, A., Uutela, M., Backstrom, G., Hellstrom, M., Bostrom, H., Li, H., Soriano, P., Betsholtz, C., Heldin, C.H., Alitalo, K., Ostman, A. and Eriksson, U. (2000) PDGF-C is a new protease-activated ligand for the PDGF alpha-receptor. *Nat Cell Biol*, **2**, 302-309.

Lin, A.E., Grossfeld, P.D., Hamilton, R.M., Smoot, L., Gripp, K.W., Proud, V., Weksberg, R., Wheeler, P., Picker, J., Irons, M., Zackai, E., Marino, B., Scott, C.I., Jr. and Nicholson, L. (2002) Further delineation of cardiac abnormalities in Costello syndrome. *Am J Med Genet*, **111**, 115-129.

Lindahl, P., Hellstrom, M., Kalen, M., Karlsson, L., Pekny, M., Pekna, M., Soriano, P. and Betsholtz, C. (1998) Paracrine PDGF-B/PDGF-Rbeta signaling controls mesangial cell development in kidney glomeruli. *Development*, **125**, 3313-3322.

Lindahl, P., Johansson, B.R., Leveen, P. and Betsholtz, C. (1997) Pericyte loss and microaneurysm formation in PDGF-B-deficient mice. *Science*, **277**, 242-245.

Luetteke, N.C., Phillips, H.K., Qiu, T.H., Copeland, N.G., Earp, H.S., Jenkins, N.A. and Lee, D.C. (1994) The mouse waved-2 phenotype results from a point mutation in the EGF receptor tyrosine kinase. *Genes Dev*, **8**, 399-413.

Lurie, I.W. (1994) Genetics of the Costello syndrome. *Am J Med Genet*, **52**, 358-359.

Maccari, F., Gheduzzi, D. and Volpi, N. (2003) Anomalous structure of urinary glycosaminoglycans in patients with pseudoxanthoma elasticum. *Clin Chem*, **49**, 380-388.

Mancini, G.M., van Diggelen, O.P., Kleijer, W.J., Di Rocco, M., Farina, V., Yuksel-Apak, M., Kayserili, H. and Halley, D.J. (2003) Studies on the pathogenesis of Costello syndrome. *J Med Genet*, **40**, e37.

Mancini, G.M.S. (1991) *Lysosomal membrane transport: physiological and pathological events* (Thesis). Erasmus University, Rotterdam.

Mangasarian, K., Li, Y., Mansukhani, A. and Basilico, C. (1997) Mutation associated with Crouzon syndrome causes ligand-independent dimerization and activation of FGF receptor-2. *J Cell Physiol*, **172**, 117-125.

Maróti, Z., Kutsche, K., Sutajova, M., Gal, A., Nothwang, H.G., Czeizel, A.E., Tímár, L. and Sólyom, E. (2002) Refinement and delineation of the breakpoint regions of a chromosome 1;22 translocation in a patient with Costello syndrome. *Am J Med Genet*, **109**, 234-237.

Maroun, C.R., Naujokas, M.A., Holgado-Madruga, M., Wong, A.J. and Park, M. (2000) The tyrosine phosphatase SHP-2 is required for sustained activation of extracellular signal-regulated kinase and epithelial morphogenesis downstream from the met receptor tyrosine kinase. *Mol Cell Biol*, **20**, 8513-8525.

Massagué, J. (1998) TGF-beta signal transduction. *Annu Rev Biochem*, **67**, 753-791.

Matz, M.V., Fradkov, A.F., Labas, Y.A., Savitsky, A.P., Zaraisky, A.G., Markelov, M.L. and Lukyanov, S.A. (1999) Fluorescent proteins from nonbioluminescent Anthozoa species. *Nat Biotechnol*, **17**, 969-973.

McMullan, T.W., Crolla, J.A., Gregory, S.G., Carter, N.P., Cooper, R.A., Howell, G.R. and Robinson, D.O. (2002) A candidate gene for congenital bilateral isolated ptosis identified by molecular analysis of a de novo balanced translocation. *Hum Genet*, **110**, 244-250.

Merrilees, M.J., Lemire, J.M., Fischer, J.W., Kinsella, M.G., Braun, K.R., Clowes, A.W. and Wight, T.N. (2002) Retrovirally mediated overexpression of versican v3 by arterial smooth muscle cells induces tropoelastin synthesis and elastic fiber formation *in vitro* and in neointima after vascular injury. *Circ Res*, **90**, 481-487.

Miettinen, P.J., Berger, J.E., Meneses, J., Phung, Y., Pedersen, R.A., Werb, Z. and Derynck, R. (1995) Epithelial immaturity and multiorgan failure in mice lacking epidermal growth factor receptor. *Nature*, **376**, 337-341.

Mignone, F., Gissi, C., Liuni, S. and Pesole, G. (2002) Untranslated regions of mRNAs. *Genome Biol*, **3**, REVIEWS0004.

Mori, M., Yamagata, T., Mori, Y., Nokubi, M., Saito, K., Fukushima, Y. and Momoi, M.Y. (1996) Elastic fiber degeneration in Costello syndrome. *Am J Med Genet*, **61**, 304-309.

Mullis, K.B. and Faloona, F.A. (1987) Specific synthesis of DNA *in vitro* via a polymerase-catalyzed chain reaction. *Methods Enzymol*, **155**, 335-350.

Nothwang, H.G., Kim, H.G., Aoki, J., Geisterfer, M., Kubart, S., Wegner, R.D., van Moers, A., Ashworth, L.K., Haaf, T., Bell, J., Arai, H., Tommerup, N., Ropers, H.H. and Wirth, J. (2001) Functional hemizygosity of PAFAH1B3 due to a PAFAH1B3-CLK2 fusion gene in a female with mental retardation, ataxia and atrophy of the brain. *Hum Mol Genet*, **10**, 797-806.

Ohlsson, R., Falck, P., Hellstrom, M., Lindahl, P., Bostrom, H., Franklin, G., Ahrlund-Richter, L., Pollard, J., Soriano, P. and Betsholtz, C. (1999) PDGFB regulates the development of the labyrinthine layer of the mouse fetal placenta. *Dev Biol*, **212**, 124-136.

Ohtani, T. and Furukawa, F. (2002) Pseudoxanthoma elasticum. *J Dermatol*, **29**, 615-620.

Olsen, D.R., Fazio, M.J., Shamban, A.T., Rosenbloom, J. and Uitto, J. (1988) Cutis laxa: reduced elastin gene expression in skin fibroblast cultures as determined by hybridizations with a homologous cDNA and an exon 1-specific oligonucleotide. *J Biol Chem*, **263**, 6465-6467.

Orita, M., Iwahana, H., Kanazawa, H., Hayashi, K. and Sekiya, T. (1989) Detection of polymorphisms of human DNA by gel electrophoresis as single-strand conformation polymorphisms. *Proc Natl Acad Sci U S A*, **86**, 2766-2770.

Östman, A., Andersson, M., Betsholtz, C., Westermark, B. and Heldin, C.H. (1991) Identification of a cell retention signal in the B-chain of platelet-derived growth factor and in the long splice version of the A-chain. *Cell Regul*, **2**, 503-512.

Östman, A. and Heldin, C.H. (2001) Involvement of platelet-derived growth factor in disease: development of specific antagonists. *Adv Cancer Res*, **80**, 1-38.

Östman, A., Rall, L., Hammacher, A., Wormstead, M.A., Coit, D., Valenzuela, P., Betsholtz, C., Westermark, B. and Heldin, C.H. (1988) Synthesis and assembly of a functionally active recombinant platelet-derived growth factor AB heterodimer. *J Biol Chem*, **263**, 16202-16208.

Östman, A., Thyberg, J., Westermark, B. and Heldin, C.H. (1992) PDGF-AA and PDGF-BB biosynthesis: proprotein processing in the Golgi complex and lysosomal degradation of PDGF-BB retained intracellularly. *J Cell Biol*, **118**, 509-519.

Passi, A., Albertini, R., Baccarani Contri, M., de Luca, G., de Paepe, A., Pallavicini, G., Pasquali Ronchetti, I. and Tiozzo, R. (1996) Proteoglycan alterations in skin fibroblast cultures from patients affected with pseudoxanthoma elasticum. *Cell Biochem Funct*, **14**, 111-120.

Pekny, M., Ostman, A., Hermansson, A., Nister, M., Heldin, C.H. and Westermark, B. (1994) Differences in binding to the solid substratum and extracellular matrix may explain isoform-specific paracrine effects of platelet-derived growth factor. *Growth Factors*, **10**, 77-87.

Pollard, T.D. and Earnshaw, W.C. (2002) *Cell Biology*. Elsevier Science, USA.

Pollock, R.A. and Richardson, W.D. (1992) The alternative-splice isoforms of the PDGF A-chain differ in their ability to associate with the extracellular matrix and to bind heparin *in vitro*. *Growth Factors*, **7**, 267-277.

Prasher, D.C., Eckenrode, V.K., Ward, W.W., Prendergast, F.G. and Cormier, M.J. (1992) Primary structure of the Aequorea victoria green-fluorescent protein. *Gene*, **111**, 229-233.

Prigent, S.A. and Lemoine, N.R. (1992) The type 1 (EGFR-related) family of growth factor receptors and their ligands. *Prog Growth Factor Res*, **4**, 1-24.

Proud, V.K., Owen, W., Creswick, H.A., Proud, L.M. and Stone, C.A. (2001) Benign and malignant tumors characterize Costello syndrome. *XXII DW Smith Workshop*.

Puck, T.T. (1965) Cell turnover in mammalian tissues: use of cell depletion measurements to calculate x-ray reproductive survival curves *in vivo*. *Proc Natl Acad Sci U S A*, **54**, 1797-1803.

Pulkkinen, L. and Uitto, J. (1999) Mutation analysis and molecular genetics of epidermolysis bullosa. *Matrix Biol*, **18**, 29-42.

Quaglino, D., Boraldi, F., Barbieri, D., Croce, A., Tiozzo, R. and Pasquali Ronchetti, I. (2000) Abnormal phenotype of *in vitro* dermal fibroblasts from patients with Pseudoxanthoma elasticum (PXE). *Biochim Biophys Acta*, **1501**, 51-62.

Raines, E.W., Lane, T.F., Iruela-Arispe, M.L., Ross, R. and Sage, E.H. (1992) The extracellular glycoprotein SPARC interacts with platelet-derived growth factor (PDGF)-AB and -BB and inhibits the binding of PDGF to its receptors. *Proc Natl Acad Sci U S A*, **89**, 1281-1285.

Raines, E.W. and Ross, R. (1992) Compartmentalization of PDGF on extracellular binding sites dependent on exon-6-encoded sequences. *J Cell Biol*, **116**, 533-543.

Reardon, W., Winter, R.M., Rutland, P., Pulleyn, L.J., Jones, B.M. and Malcolm, S. (1994) Mutations in the fibroblast growth factor receptor 2 gene cause Crouzon syndrome. *Nat Genet*, **8**, 98-103.

Ringpfeil, F., Lebwohl, M.G., Christiano, A.M. and Uitto, J. (2000) Pseudoxanthoma elasticum: mutations in the MRP6 gene encoding a transmembrane ATP-binding cassette (ABC) transporter. *Proc Natl Acad Sci U S A*, **97**, 6001-6006.

Robertson, S.C., Meyer, A.N., Hart, K.C., Galvin, B.D., Webster, M.K. and Donoghue, D.J. (1998) Activating mutations in the extracellular domain of the fibroblast growth factor receptor 2 function by disruption of the disulfide bond in the third immunoglobulin-like domain. *Proc Natl Acad Sci U S A*, **95**, 4567-4572.

Rose, C.S. and Malcolm, S. (1997) A TWIST in development. *Trends Genet*, **13**, 384-387.

Rose, C.S., Patel, P., Reardon, W., Malcolm, S. and Winter, R.M. (1997) The TWIST gene, although not disrupted in Saethre-Chotzen patients with apparently balanced translocations of 7p21, is mutated in familial and sporadic cases. *Hum Mol Genet*, **6**, 1369-1373.

Rosenkranz, S. and Kazlauskas, A. (1999) Evidence for distinct signaling properties and biological responses induced by the PDGF receptor alpha and beta subtypes. *Growth Factors*, **16**, 201-216.

Rüdiger, N.S., Gregersen, N. and Kielland-Brandt, M.C. (1995) One short well conserved region of Alu-sequences is involved in human gene rearrangements and has homology with prokaryotic chi. *Nucleic Acids Res*, **23**, 256-260.

Sambrook, J. and Russell, D.W. (2001) *Moleculary Cloning - A Laboratory Manual*. Cold Spring Harbor Laboratory Press, New York.

Sanger, F., Nicklen, S. and Coulson, A.R. (1977) DNA sequencing with chain-terminating inhibitors. *Proc Natl Acad Sci U S A*, **74**, 5463-5467.

Saxton, T.M., Ciruna, B.G., Holmyard, D., Kulkarni, S., Harpal, K., Rossant, J. and Pawson, T. (2000) The SH2 tyrosine phosphatase shp2 is required for mammalian limb development. *Nat Genet*, **24**, 420-423.

Saxton, T.M., Henkemeyer, M., Gasca, S., Shen, R., Rossi, D.J., Shalaby, F., Feng, G.S. and Pawson, T. (1997) Abnormal mesoderm patterning in mouse embryos mutant for the SH2 tyrosine phosphatase Shp-2. *Embo J*, **16**, 2352-2364.

Say, B., Gucsavas, M., Morgan, H. and York, C. (1993) The Costello syndrome. *Am J Med Genet*, **47**, 163-165.

Schuler, G.D., Boguski, M.S., Stewart, E.A., Stein, L.D., Gyapay, G., Rice, K., White, R.E., Rodriguez-Tome, P., Aggarwal, A., Bajorek, E., Bentolila, S., Birren, B.B., Butler, A., Castle, A.B., Chiannilkulchai, N., Chu, A., Clee, C., Cowles, S., Day, P.J., Dibling, T., Drouot, N., Dunham, I., Duprat, S., East, C., Hudson, T.J. and et al. (1996) A gene map of the human genome. *Science*, **274**, 540-546.

Schwartz, R.A. (1994) Acanthosis nigricans. *J Am Acad Dermatol*, **31**, 1-19; quiz 20-12.

Selypes, A., Solyom, E. and Takacs, S. (1992) A new chromosomal translocation t/1;22/ /q25;q12/ in a 17-month-old girl. *Acta Paediatr Hung*, **32**, 3-10.

Sephel, G.C., Byers, P.H., Holbrook, K.A. and Davidson, J.M. (1989) Heterogeneity of elastin expression in cutis laxa fibroblast strains. *J Invest Dermatol*, **93**, 147-153.

Sibilia, M., Fleischmann, A., Behrens, A., Stingl, L., Carroll, J., Watt, F.M., Schlessinger, J. and Wagner, E.F. (2000) The EGF receptor provides an essential survival signal for SOS-dependent skin tumor development. *Cell*, **102**, 211-220.

Sibilia, M., Wagner, B., Hoebertz, A., Elliott, C., Marino, S., Jochum, W. and Wagner, E.F. (2003) Mice humanised for the EGF receptor display hypomorphic phenotypes in skin, bone and heart. *Development*, **130**, 4515-4525.

Sibilia, M. and Wagner, E.F. (1995) Strain-dependent epithelial defects in mice lacking the EGF receptor. *Science*, **269**, 234-238.

Siwik, E.S., Zahka, K.G., Wiesner, G.L. and Limwongse, C. (1998) Cardiac disease in Costello syndrome. *Pediatrics*, **101**, 706-709.

Söling, A., Simm, A. and Rainov, N. (2002) Intracellular localization of Herpes simplex virus type 1 thymidine kinase fused to different fluorescent proteins depends on choice of fluorescent tag. *FEBS Lett*, **527**, 153-158.

Soriano, P. (1994) Abnormal kidney development and hematological disorders in PDGF beta-receptor mutant mice. *Genes Dev*, **8**, 1888-1896.

Soriano, P. (1997) The PDGF alpha receptor is required for neural crest cell development and for normal patterning of the somites. *Development*, **124**, 2691-2700.

Stankiewicz, P. and Lupski, J.R. (2002) Genome architecture, rearrangements and genomic disorders. *Trends Genet*, **18**, 74-82.

Stephens, J.C., Schneider, J.A., Tanguay, D.A., Choi, J., Acharya, T., Stanley, S.E., Jiang, R., Messer, C.J., Chew, A., Han, J.H., Duan, J., Carr, J.L., Lee, M.S., Koshy, B., Kumar, A.M., Zhang, G., Newell, W.R., Windemuth, A., Xu, C., Kalbfleisch, T.S., Shaner, S.L., Arnold, K., Schulz, V., Drysdale, C.M., Nandabalan, K., Judson, R.S., Ruano, G. and Vovis, G.F. (2001) Haplotype variation and linkage disequilibrium in 313 human genes. *Science*, **293**, 489-493.

Suri, M. and Garrett, C. (1998) Costello syndrome with acoustic neuroma and cataract. Is the Costello locus linked to neurofibromatosis type 2 on 22q? *Clin Dysmorphol*, **7**, 149-151.

Takahashi-Tezuka, M., Yoshida, Y., Fukada, T., Ohtani, T., Yamanaka, Y., Nishida, K., Nakajima, K., Hibi, M. and Hirano, T. (1998) Gab1 acts as an adapter molecule linking the cytokine receptor gp130 to ERK mitogen-activated protein kinase. *Mol Cell Biol*, **18**, 4109-4117.

Tandoi, C., Botta, A., Fini, G., Sangiuolo, F., Novelli, G., Ricci, R., Zampino, G., Anichini, C. and Dallapiccola, B. (2001) Exclusion of the elastin gene in the pathogenesis of Costello syndrome. *Am J Med Genet*, **98**, 286-287.

Tang, T.L., Freeman, R.M., Jr., O'Reilly, A.M., Neel, B.G. and Sokol, S.Y. (1995) The SH2-containing protein-tyrosine phosphatase SH-PTP2 is required upstream of MAP kinase for early Xenopus development. *Cell*, **80**, 473-483.

Tartaglia, M., Cotter, P.D., Zampino, G., Gelb, B.D. and Rauen, K.A. (2003) Exclusion of PTPN11 mutations in Costello syndrome: further evidence for distinct genetic etiologies for Noonan, cardio-facio-cutaneous and Costello syndromes. *Clin Genet*, **63**, 423-426.

Tartaglia, M., Kalidas, K., Shaw, A., Song, X., Musat, D.L., van der Burgt, I., Brunner, H.G., Bertola, D.R., Crosby, A., Ion, A., Kucherlapati, R.S., Jeffery, S., Patton, M.A. and Gelb, B.D. (2002) PTPN11 mutations in Noonan syndrome: molecular spectrum, genotype-phenotype correlation, and phenotypic heterogeneity. *Am J Hum Genet*, **70**, 1555-1563.

Tartaglia, M., Mehler, E.L., Goldberg, R., Zampino, G., Brunner, H.G., Kremer, H., van der Burgt, I., Crosby, A.H., Ion, A., Jeffery, S., Kalidas, K., Patton, M.A., Kucherlapati, R.S. and Gelb, B.D. (2001) Mutations in PTPN11, encoding the protein tyrosine phosphatase SHP-2, cause Noonan syndrome. *Nat Genet*, **29**, 465-468.

Thogersen, V.B., Jorgensen, P.E., Sorensen, B.S., Bross, P., Orntoft, T., Wolf, H. and Nexo, E. (1999) Expression of transforming growth factor alpha and epidermal growth factor receptor in human bladder cancer. *Scand J Clin Lab Invest*, **59**, 267-277.

Threadgill, D.W., Dlugosz, A.A., Hansen, L.A., Tennenbaum, T., Lichti, U., Yee, D., LaMantia, C., Mourton, T., Herrup, K., Harris, R.C. and et al. (1995) Targeted disruption of mouse EGF receptor: effect of genetic background on mutant phenotype. *Science*, **269**, 230-234.

Torley, D., Bellus, G.A. and Munro, C.S. (2002) Genes, growth factors and acanthosis nigricans. *Br J Dermatol*, **147**, 1096-1101.

Tröger, B., Kutsche, K., Bolz, H., Luttgen, S., Gal, A., Almassy, Z., Caliebe, A., Freisinger, P., Hobbiebrunken, E., Morlot, M., Stefanova, M., Streubel, B., Wieczorek, D. and Meinecke, P. (2003) No mutation in the gene for Noonan syndrome, PTPN11, in 18 patients with Costello syndrome. *Am J Med Genet*, **121A**, 82-84.

Urbán, Z. and Boyd, C.D. (2000) Elastic-fiber pathologies: primary defects in assembly-and secondary disorders in transport and delivery. *Am J Hum Genet*, **67**, 4-7.

van Eeghen, A.M., van Gelderen, I. and Hennekam, R.C. (1999) Costello syndrome: report and review. *Am J Med Genet*, **82**, 187-193.

Varon, R., Gooding, R., Steglich, C., Marns, L., Tang, H., Angelicheva, D., Yong, K.K., Ambrugger, P., Reinhold, A., Morar, B., Baas, F., Kwa, M., Tournev, I., Guerguelcheva, V., Kremensky, I., Lochmuller, H., Mullner-Eidenbock, A., Merlini, L., Neumann, L., Burger, J., Walter, M., Swoboda, K., Thomas, P.K., von Moers, A., Risch, N. and Kalaydjieva, L. (2003) Partial deficiency of the C-terminal-domain phosphatase of RNA polymerase II is associated with congenital cataracts facial dysmorphism neuropathy syndrome. *Nat Genet*, **35**, 185-189.

Vogel, W., Lammers, R., Huang, J. and Ullrich, A. (1993) Activation of a phosphotyrosine phosphatase by tyrosine phosphorylation. *Science*, **259**, 1611-1614.

Vortkamp, A., Gessler, M. and Grzeschik, K.H. (1991) GLI3 zinc-finger gene interrupted by translocations in Greig syndrome families. *Nature*, **352**, 539-540.

Waite, K.A. and Eng, C. (2003) From developmental disorder to heritable cancer: it's all in the BMP/TGF-beta family. *Nat Rev Genet*, **4**, 763-773.

Wang, J., Coltrera, M.D. and Gown, A.M. (1994) Cell proliferation in human soft tissue tumors correlates with platelet-derived growth factor B chain expression: an immunohistochemical and in situ hybridization study. *Cancer Res*, **54**, 560-564.

Wilkie, A.O., Slaney, S.F., Oldridge, M., Poole, M.D., Ashworth, G.J., Hockley, A.D., Hayward, R.D., David, D.J., Pulleyn, L.J., Rutland, P. and et al. (1995) Apert syndrome results from localized mutations of FGFR2 and is allelic with Crouzon syndrome. *Nat Genet*, **9**, 165-172.

Willis, I.M. (1993) RNA polymerase III. Genes, factors and transcriptional specificity. *Eur J Biochem*, **212**, 1-11.

Wirth, J., Wagner, T., Meyer, J., Pfeiffer, R.A., Tietze, H.U., Schempp, W. and Scherer, G. (1996) Translocation breakpoints in three patients with campomelic dysplasia and autosomal sex reversal map more than 130 kb from SOX9. *Hum Genet*, **97**, 186-193.

Yanushevich, Y.G., Staroverov, D.B., Savitsky, A.P., Fradkov, A.F., Gurskaya, N.G., Bulina, M.E., Lukyanov, K.A. and Lukyanov, S.A. (2002) A strategy for the generation of non-aggregating mutants of Anthozoa fluorescent proteins. *FEBS Lett*, **511**, 11-14.

Zampino, G., Mastroiacovo, P., Ricci, R., Zollino, M., Segni, G., Martini-Neri, M.E. and Neri, G. (1993) Costello syndrome: further clinical delineation, natural history, genetic definition, and nosology. *Am J Med Genet*, **47**, 176-183.

Zucman-Rossi, J., Legoix, P., Victor, J.M., Lopez, B. and Thomas, G. (1998) Chromosome translocation based on illegitimate recombination in human tumors. *Proc Natl Acad Sci U S A*, **95**, 11786-11791.

# List of Publications

## Original Articles

Maróti, Z., Kutsche, K., **Sutajova, M.**, Gal, A., Nothwang, H.G., Czeizel, A.E., Tímár, L. and Sólyom, E. (2002) Refinement and delineation of the breakpoint regions of a chromosome 1;22 translocation in a patient with Costello syndrome. *Am J Med Genet*, **109**, 234-237.

Martinez-Garay, I., Jablonka, S., **Sutajova, M.**, Steuernagel, P., Gal, A. and Kutsche, K. (2002) A new gene family *(FAM9)* of low-copy repeats in Xp22.3 expressed exclusively in testis: implications for recombinations in this region. *Genomics*, **80**, 259-267.

*The majority of the data presented in my Ph.D. thesis are summarized in:*

**Šutajová, M.**, Neukirchen, U., Meinecke, P., Czeizel, A.E., Tímár, L., Sólyom, E., Gal, A. and Kutsche, K. (2004) Disruption of the *PDGFB* gene in a 1;22 translocation patient does not cause Costello syndrome. *Genomics*, **83**, 883-892.

## Abstracts – Posters

**Sutajova, M.**, Neukirchen, U., Czeizel, E., Timar, L., Gal, A. and Kutsche, K. (2002) Molecular characterization of a chromosome 1;22 translocation in a patient with Costello syndrome: implication for the genes of the *PDGF* and *PDGFR* families in the trait. *13th Annual Meeting of the German Society of Human Genetics*, September 29 - October 2, 2002, Leipzig, Germany.

Martínez-Garay, I., **Sutajova, M.**, Steuernagel, P., Gal, A. and Kutsche K. (2002) Three members of a new gene family of low copy repeats in Xp22.3 expressed exclusively in testis: implications for recombinations in this region. *13th Annual Meeting of the German Society of Human Genetics*, September 29 - October 2, 2002, Leipzig, Germany.

**Sutajova, M.**, Neukirchen, U., Gal, A. and Kutsche K. (2003) Disruption of the *PDGFB* gene in a patient with a chromosome 1;22 translocation and presumed Costello syndrome: accumulation of aberrant PDGFB fusion proteins in the extracellular matrix. *14th Annual Meeting of the German Society of Human Genetics*, October 1-4, 2003, Marburg, Germany.

Kutsche, K., **Sutajova, M.**, Cichy, R., Albrecht, B. and Gillessen-Kaesbach, G. (2004) No mutation in the *LMNA* gene in four patients with Hallermann-Streiff syndrome. *European Human Genetics Conference*, June 12-15, 2004, Munich, Germany.

## Abstracts – Talks

**Sutajova, M.** and Kutsche, K. (2000) Characterization of a novel gene family in Xp22.3 with homology to the synaptonemal complex protein 3 (SCP3). *20. Treffen der Norddeutschen Humangenetiker*, 4.11.2000, Rostock.

Kutsche, K., **Sutajova, M.** and Gal, A. (2001) Das Costello-Syndrom: ein klinischer Überblick und erste Ansätze zur Identifizierung des ursächlichen Gendefektes. *21. Treffen der Norddeutschen Humangenetiker*, 3.11.2001, Greifswald.

# Affidavit

I hereby declare that I have done the present work by myself, not used other than the stated sources and aids and that any used statement from literature is noted as well.

I further confirm that this dissertation is not submitted to any other institution to open the dissertation procedure.

Hamburg, 28th of April 2004

……

Markéta Šutajová

# Eidesstattliche Erklärung

Hiermit erkläre ich an Eides statt, dass ich meine Dissertation allein und selbstständig angefertigt habe, anderen Werken wörtlich oder inhaltlich entnommene Stellen als solche kenntlich gemacht und keine anderen als die angegebenen Hilfsmittel benutzt habe.

Ferner versichere ich, dass ich noch keine Promotionsversuche an anderen Universitäten unternommen habe.

Hamburg, 28th of April 2004

……

Markéta Šutajová

# Acknowledgement

First and foremost I would like to thank Dr. Kerstin Kutsche for her excellent supervision, support and ongoing interest during the whole period of my thesis. I thank her for all ideas and enthusiasm she brought into our discussions about the project.

This study has been performed at the Institute of Human Genetics at the University Hospital Hamburg-Eppendorf. I thank Prof. Dr. Andreas Gal, the head of the institute, for providing excellent facilities for this research work and for his engaged support during the project.

I am very grateful to Prof. Dr. Wolfgang W. Deppert for his external supervision and interest throughout my whole thesis.

I thank all current and former members of the research group for a pleasant working atmosphere and their help. My special thanks go to Karoline Kruse, Ramona Cichy, and students of the BTA School of Hamburg for help with mutation screening as well as to Ursula Neukirchen who performed mutation screening of the *PDGFRB* gene for her medical thesis. I thank all co-workers of the institute for their help I ever needed.

My parents, my sister Petra, and all my friends I thank for the support and patience they have with me. My special thanks go to Martina and Alena for their continual friendship.

Tato práce je věnována Gerritovi a naší holčičce.

# Curriculum Vitae

## Personal Data

| | |
|---|---|
| Name: | Markéta Šutajová |
| Address: | Nienstedtener Straße 26, 22609 Hamburg |
| Date of Birth: | 18th of December 1973 |
| Birthplace: | Trutnov, Czech Republic |
| Nationality: | Czech |

## Graduation

| | |
|---|---|
| since January 2001 | Ph.D. thesis at the Institute of Human Genetics, UKE, Hamburg<br>Working group of Dr. Kerstin Kutsche<br>Fellowship from the Graduiertenkolleg 336 „Molekulare Endokrinologie - Molekularer Stoffwechsel“<br>Topic of Ph.D. thesis: Molecular characterization of a chromosome 1;22 translocation in a patient with a phenotype resembling Costello syndrome |

## Education

| | |
|---|---|
| 1998 | Diploma in Biochemistry |
| October 1996 - June 1998 | University of Pardubice, CR<br>Faculty of Chemical Technology<br>Specialization: Analysis of Biological Materials<br>Topic of diploma work: Immobilization of the enzyme galactose oxidase to the hydrazide derivative of bead cellulose |
| September 1993 - September 1996 | University of Pardubice, CR<br>Faculty of Chemical Technology<br>Specialization: Clinical Biology and Chemistry |
| May 1992 | School-leaving exam at grammar school in Trutnov, CR |

## Work experience

| | |
|---|---|
| September 2000 - December 2000 | Guest scientist at the Institute of Human Genetics, UKE, Hamburg<br>Working group of Dr. Kerstin Kutsche |
| September 1998 - January 2001 | Employee in the Laboratory of Molecular Genetics Institute of Biology and Medical Genetics 2nd Medical Faculty Charles University and University Hospital Motol in Prague, CR |
| December 1992 - June 1993 | Au-pair in London, UK |